The Role of Damaged DNA Binding Protein 2 in Colon Cancer

BY

Shuo Huang
B.S., Zhejiang University, 2010

THESIS

Submitted as partial fulfillment of the requirements
for the degree of Doctor of Philosophy in Biochemistry and Molecular Genetics
in the Graduate College of the
University of Illinois at Chicago, 2017

Chicago, Illinois

Defense Committee:

Pradip Raychaudhuri, Chair and Advisor
Bradley Merrill
Nissim Hay
Angela Tyner
Lijun Rong, Microbiology and Immunology

AKNOWLEDGEMENTS

I sincerely thank my thesis advisor Dr. Raychaudhuri for his exceptional support and constant encouragement during the years of PhD study.

I would like to thank my thesis committee—Dr. Merrill, Dr. Hay, Dr. Tyner and Dr. Rong for their unwavering support and assistance. They provided guidance in all areas that helped me accomplish my research goals and enjoy myself in the process.

I also want to acknowledge my colleagues for their help and encouragement throughout the years.

I am thanking my whole family for the outstanding support, especially my dear husband, Yuanbo Liu.

TABLE OF CONTENTS

CHAPTER **PAGE**

TABLE OF CONTENTS (continued)

CHAPTER **PAGE**

LIST OF FIGURES

FIGURE **PAGE**

LIST OF FIGURES (continued)

FIGURE **PAGE**

LIST OF TABLES

TABLE **PAGE**

LIST OF ABBREVIATIONS

APC	Adenomatous polyposis coli
TGF	Transforming growth factor
FZD	Frizzled receptor
LRP	Lipoprotein receptor-related protein
GSK3	Glycogen synthase kinase 3
TCF/LEF	T-cell factor/lymphoid enhancer factor
GI	Gastrointestinal
ISC	Intestinal stem cells
TA	Transit-amplifying
CBC	Crypt base columnar cells
RSPO	R-spondin
LGR5	G protein-coupled receptor 5
RNF43	Ring finger protein 43
ZNRF3	Zinc and Ring Finger 3
DDB2	Damaged DNA binding protein 2
NER	Nuclear excision repair
UV	Ultra Violet
XP	Xeroderma pigmentosum
EMT	Epithelial to mesenchymal transition
ChIP	Chromatin Immunoprecipitation
AOM/DSS	Azoxymethane/Dextran Sulfate
3C	Chromatin Conformation Capture

SUMMARY

Deregulation of the Wnt/β-catenin signaling pathway plays causal roles in the development of colon cancer. However, the complex regulatory network of the Wnt/β-catenin signaling in colorectal cells is not fully understood. I discovered that DDB2 is critical for β-catenin-mediated activation of RNF43, an E3 ubiquitin ligase that controls Wnt-signaling by removing the Wnt-receptors from cell surface. Also, in human hyperplastic colonic foci there is a strong correlation between reduced expression of DDB2 and RNF43. Mechanistically, DDB2 recruits EZH2 and β-catenin at an upstream site in the *Rnf43* gene, allowing a functional interaction with distant TCF4/β-catenin binding sites in the intron of *Rnf43*. This new activity of DDB2 is required for RNF43 function as a negative feedback regulator of Wnt-signaling. Moreover, DDB2 knock-out mice exhibit increased susceptibility to colon tumor development, and that coincides with abolished expression of RNF43, and higher abundance of the Wnt-receptors expressing cells with consequent greater activation of the downstream Wnt-pathway. Together, the results described in my thesis demonstrate that DDB2 is both a partner and a regulator of Wnt-signaling, and that it plays an important role in suppression of colon cancer development.

1. INTRODUCTION

1.1 Molecular genetics in colon cancer development

Colon cancer is the second most commonly diagnosed cancer and the second leading cause of cancer-related death among men and women in the United States (Markowitz, Dawson et al. 2002). In the United States in the year of 2017, there are estimated to be 135,430 newly diagnosed colon and rectal cancer cases, and 50,260 deaths (Siegel, Miller et al. 2017). The majority of new cases of sporadic colorectal cancer occur in people aged 65 years or older; whereas, the rare inherited forms of colorectal cancer are mostly diagnosed in people younger than 50 years old (Wolpin and Mayer 2008, Siegel, Miller et al. 2017).

Over the past decades, the studies of familial hereditary form of colon cancer syndromes have helped to uncover some of the critical mutations that initiate the tumorigenesis. Several oncogenes and tumor-suppressor genes are found to be mutated in colon cancer cases. For instance, germ-line inactivation of *Apc* gene ,which encodes the adenomatous polyposis coli (APC) protein causes the inherited familial adenomatous polyposis (FAP) syndrome, in which hundreds to thousands of adenoma polyps develop in the colon and rectum of the patients in their early adulthood, and the lifetime risk of colon cancer in untreated FAP patients approaches 100% (Markowitz, Dawson et al. 2002, Fearon 2011, Dienstmann and Tabernero 2016). APC protein functions as a negative regulator of Wnt/β-catenin signaling by mediating the degradation of β-catenin, and thereby suppressing β-catenin mediated transcriptional activity (Clevers 2006). Thus loss-of-function mutations in APC result in the abnormal hyper-activation of Wnt signaling in colonic tissue, and therefore initiation of tumorigenesis. Also, germ-line mutations in

components of the DNA Mismatch Repair (MMR) complex often lead to hereditary non-polyposis colon cancer (HNPCC) (Markowitz, Dawson et al. 2002, Fearon 2011). Carriers of the autosomal dominant mutations in the MMR genes have an approximately 80% risk of developing colon cancer, and an increased risk of gastric and endometrial cancers (van den Brink and Offerhaus 2007, Fearon 2011). The impaired MMR results in the condition of genetic hypermutability, which is typically detected by microsatellite instability (MSI) (Fearon 2011). MSI is observed also in more than 15% of apparently sporadic colon cancer (Markowitz, Dawson et al. 2002, Fearon 2011). Alterations in MSH2 (~60%) and MLH1 (~30%) are the most frequent mutations in HNPCC families (Markowitz, Dawson et al. 2002).

The studies of somatic genetics of sporadic colon cancer revealed that alterations of several signaling pathways contribute to colon cancer initiation, development and progression (Fearon 2011). Activation of the Wnt signaling pathway is believed as the earliest event for colon adenoma formation (Clevers 2004, Krausova and Korinek 2014). In addition to the role of APC mutation in FAP and variant syndromes, it plays an even more prominent role in sporadic colon cancer (Clevers 2006, Clevers and Nusse 2012). Nearly 80% of sporadic colorectal adenomas and adenocarcinomas have somatic loss-of-function mutations of APC (Fearon 2011, Clevers and Nusse 2012). Alternatively, some colon cancer patients harbor activating mutations of β-catenin (Fearon 2011). RAS mutations, majorly in K-ras, are detected in 50% of large adenomas and colon cancers (Markowitz, Dawson et al. 2002). Besides, mutations inactivating the TGF-β signaling arise in approximately 30% of colon cancers and are temporally coincident with the progression of colon adenomas to carcinomas (Fearon 2011). TGF-β signaling is inactivated by somatic mutations in the TGFβ-RII kinase domain (15% of cases) or in SMAD4 (15% of cases)

Figure 1: Schematic of colon cancer development and progression.

The schematic shows the steps in development of sporadically occurring cancer in a normal colon epithelium. Progression from normal epithelium to colorectal cancer requires an accumulation of mutations in particular genes that affect the balance between proliferation and apoptosis. However, not all colorectal tumors exhibit all the mutations shown in the figure.

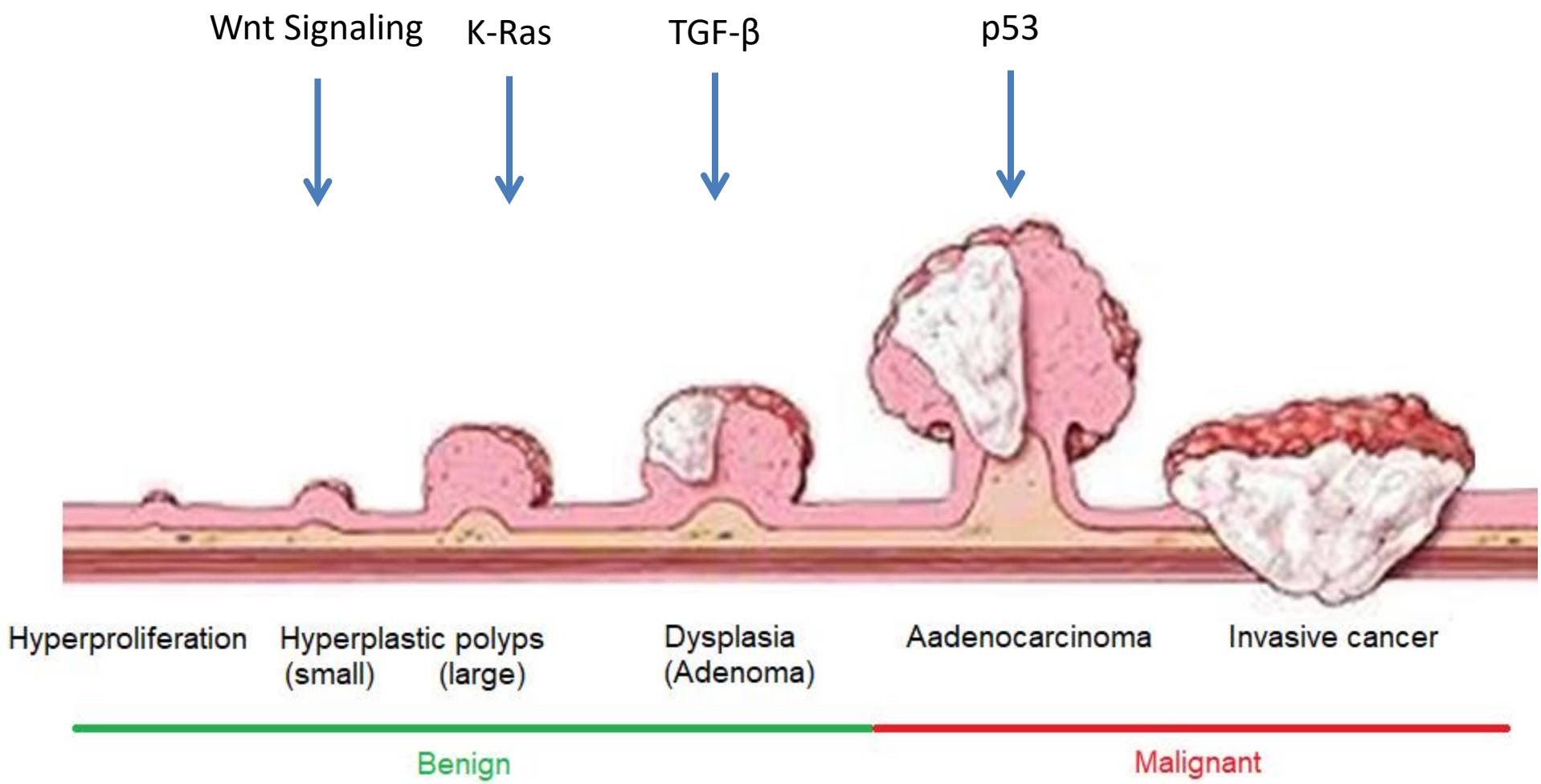
Wnt Signaling
K-Ras
TGF-β
p53
Hyperproliferation
Hyperplastic polyps
(small)
(large)
Dysplasia
(Adenoma)
Aadenocarcinoma
Invasive cancer
Benign
Malignant

or SMAD2 (5% of cases), which are the transcription factors downstream of TGF-β pathway (Markowitz, Dawson et al. 2002, Fearon 2011). Mutational inactivation of p53 is also related to colon tumor progression. More than 50% of colon cancer cases bear mutations in p53 (Fearon 2011, Dienstmann and Tabernero 2016). Lastly, loss of Muc2 mucin expression, a frequent event in human colon adenomas and cancers, induces intestinal cancers in Muc2 knockout mice (Markowitz, Dawson et al. 2002, Taketo and Edelmann 2009).

1.2 Canonical Wnt signaling pathway in intestinal development and colon cancer

The canonical Wnt signaling pathway, also known as Wnt/β-catenin signaling, is one of three Wnt pathways which are all activated by binding Wnt-protein ligands to Frizzled family receptors and LRPs co-receptors (Nusse 2005, Clevers 2006). Wnt/β-catenin signaling is highly conserved among species (Nusse and Varmus 2012). At the core of the pathway is the tightly regulated protein β-catenin, encoded by *ctnnb1* gene. β-catenin variably exists in three distinct pools: (1) at cellular adherent junctions, where it associates with E-cadherin and maintains cell-cell interaction; (2) in the cytoplasm, where it is synthesized and degraded; and (3) in the nucleus, where it participates as a transcriptional co-activator (Nusse 2005, Clevers 2006, Cadigan and Waterman 2012, Clevers and Nusse 2012). When Wnt/β-catenin signaling is inactivated, the levels of cytoplasmic and nuclear β-catenin are controlled by a multiprotein destruction complex that targets β-catenin for degradation by the proteasomes (Nusse 2005, Clevers 2006).

That destruction complex, composed of the core proteins AXIN, APC, and two kinases-glycogen synthase kinase 3 (GSK3), and casein kinase 1 (CK1), phosphorylates the N-terminus of β-catenin. And the phosphorylated β-catenin is then recognized by the ubiquitin E3 ligase β-TrCP for ubiquitination and subsequent proteasomal degradation (Clevers and Nusse 2012). The binding of certain "canonical" Wnt ligands to cognate receptors of the FZDs and LRPs inhibits β-catenin phosphorylation, thereby allowing β-catenin to escape degradation, accumulate in the cytosol, and translocate to the nucleus (Cadigan and Waterman 2012, Clevers and Nusse 2012). In the nucleus, β-catenin interacts with the downstream transcription factors - members of the T-cell factor/lymphoid enhancer factor (TCF/LEF) family to transactivate target genes. There are over a hundred genes that have been identified as Wnt target genes, among which are genes critical for cell proliferation, including c-Myc and Cyclin D1 (Cadigan and Waterman 2012).

Wnt/β-catenin signaling was first identified for its role in carcinogenesis. In 1980s, int1-a novel proto-oncogene was identified in the Mouse Mammary Tumour Virus (MMTV) infected mouse breast cancer models, and later was renamed as Wnt1- the gene that encodes WNT1 ligand in Wnt/β-catenin signaling pathway (Nusse and Varmus 2012). Then knock-out of Wnt1 gene in mice by homologous gene targeting produced a developmental phenotype, which revealed its function in embryonic development (Nusse and Varmus 2012). The embryonic processes it controls include cell proliferation, cell differentiation, cell polarity, and cell migration (Clevers 2006). Besides embryonic

Figure 2: Schematic of Wnt/β-catenin signaling pathway.

In the absence of Wnt ligands, the destruction complex phosphorylates and degrades β-catenin. And the expression of Wnt target genes are repressed without nuclear β-catenin binding with TCF/LEF transcription factors (Left Panel). In the present of Wnt ligands, Wnt binds Fzd and LRP5/6 co-receptors. And LRP5/6 are phosphorylated and then be able to recruit the destruction complex components, leading to inactivation of the destruction complex, resulting in β catenin stabilization. Accumulated β-catenin proteins translocate into nucleus and bind with TCF/LEF transcription factors, which activates Wnt target genes expression (Right Panel).

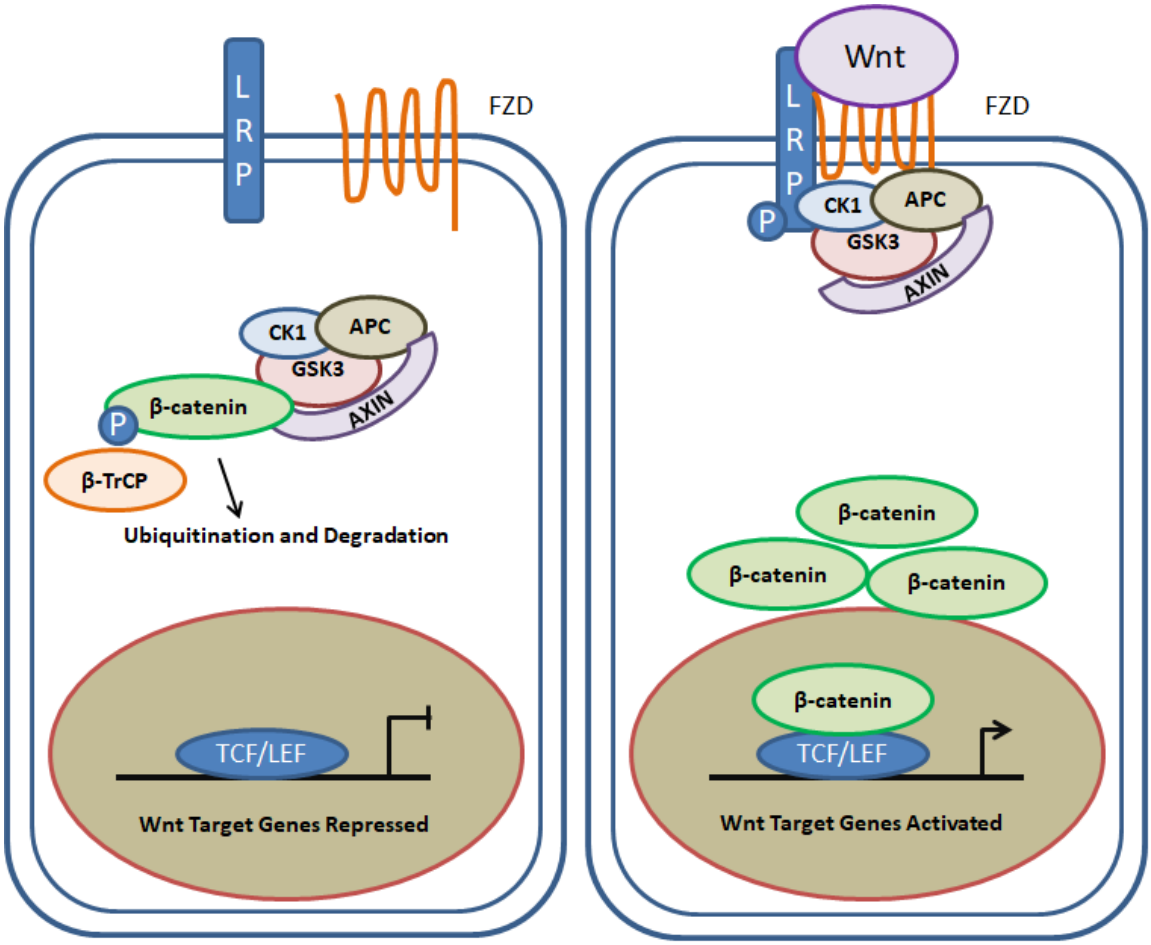
LRP
FZD
CK1
APC
GSK3
β-catenin
AXIN
P
β-TrCP
Ubiquitination and Degradation
TCF/LEF
Wnt Target Genes Repressed
Wnt
LRP
FZD
CK1
APC
GSK3
AXIN
P
β-catenin
β-catenin
β-catenin
β-catenin
TCF/LEF
Wnt Target Genes Activated

development, Wnt/β-catenin signaling also critically regulates cell renewal and tissue regeneration in adults, including adult bone marrow, skin and intestine tissues (Krausova and Korinek 2014). In gastrointestinal (GI) tract, the architecture of the small intestine and colon is designed to maximize the surface of the organ to resorb nutrients and water from food (Medema and Vermeulen 2011). In colonic tissue, a single-cell epithelial sheet penetrates into the underlying connective tissue of lamina propria to form tubular glands called crypts (Medema and Vermeulen 2011, Krausova and Korinek 2014). The epithelial lining represents one of the most intensively self-replenishing organs in mammals with a rate of entire renewal every 3–5 days along the crypt axis (Medema and Vermeulen 2011, Fujii and Sato 2014). The homeostasis is sustained by crypt resident multi-potent intestinal stem cells (ISCs) (Medema and Vermeulen 2011). They give rise to a pool of highly proliferative progenitors called transit-amplifying (TA) cells (Erwin, Jarboe et al. 2006, Drost, van Jaarsveld et al. 2015). These cells undergo several rounds of cell divisions and commence differentiation towards all intestinal lineages as they migrate upwards the crypt length to the crypt orifice (Drost, van Jaarsveld et al. 2015). Numerous studies conducted both *in vivo* and *in vitro* have firmly established the role of Wnt signaling in the preservation of ISCs proliferation and pluripotency (Krausova and Korinek 2014). Self-renewal, proliferation and differentiation are coordinated along a Wnt gradient in the intestinal crypt (Taipale and Beachy 2001, Clevers 2006, Krausova and Korinek 2014). Recent studies demonstrated that stem-cell membranes constitute a reservoir for Wnt proteins, and 'plasma membrane dilution' through cell division shape the epithelial Wnt3 gradient (Drost, van Jaarsveld et al. 2015, Farin, Jordens et al. 2016). Moreover, expression of the ISC markers Ascl2, EphB2, Bmi1, Lgr5 and Tert is

governed by the Wnt/β-catenin pathway (Krausova and Korinek 2014). And the strength of the Wnt cascade is restrained in crypt base columnar cells (CBC) -the actively dividing stem cells, by a negative feedback-loop mechanism that involve upregulation of the β-catenin negative regulator Axin2 and expression of Frizzled (Wnt-receptor) specific ubiquitin ligases RNF43 and ZNRF3 (Hao, Xie et al. 2012, Koo, Spit et al. 2012, Krausova and Korinek 2014).

Given the critical role of Wnt/β-catenin signaling in maintaining the stem cells in the crypts, it is not surprising that Wnt/β-catenin pathway mutations are frequently observed in colon cancer. Dysregulation of signaling is traditionally attributed to mutations in APC, β-catenin, Axin or TCF4 that lead to constitutive hyperactivation of the pathway (Clevers 2004, Clevers 2006, Clevers and Nusse 2012). Accumulating data suggest that somatic mutations in Wnt/β-catenin pathway are an early and perhaps the earliest event in the development of most adenomas (Fearon 2011, Clevers and Nusse 2012). First, it has been shown that APC or β-catenin mutations have nearly the same frequency in very small adenomas as in much more advanced adenomas and adenocarcinomas, in contrast to the situation for some other somatically mutations in colon tumors (Fearon 2011). Second, somatic mutations in APC or β-catenin are found even in the earliest hyperplastic lesions (Fearon 2011). Despite these genetic lesions that cause cell-autonomous and intracellular stimulation of Wnt/β-catenin signaling, activation of the pathway through Frizzled (FZD) seven-transmembrane Wnt-receptors also is important in colon cancer. Blocking Wnt ligand secretion reduces β-catenin activity in colon cancer cells harboring APC truncating or β-catenin-stabilizing mutations (Voloshanenko, Erdmann et al. 2013, Jung, Jun et al.

2015). Blocking Wnt ligand secretion was also recently shown to be effective in treating colon cancer patient-derived xenografts (Madan, Ke et al. 2016).

1.3 R-spondin/LGR/RNF43 regulatory module

As discussed above, the Wnt/β-catenin signaling pathway is tightly regulated to restrain the stem cell niche in intestinal crypts. A feedback-loop mechanism, which involves the secreted R-spondin (RSPO) ligands, the seven-transmembrane receptor Lgr4,5,6, and the ubiquitin E3 ligases RNF43 and ZNRF3, has been identified recently to play a role in controlling stem cell activity by regulating surface expression of Wnt receptors (Jin and Yoon 2012, Chen, Chen et al. 2013, de Lau, Peng et al. 2014).

The four human R-spondin proteins (RSPO1-RSPO4) are secreted agonists and activators of Wnt signaling (Jin and Yoon 2012, Chen, Chen et al. 2013). All four RSPOs have similar structures with two cysteine-rich furin-like repeats (FU-like CR) in N-terminus, and a C-terminal thrombospondin type1 repeat (TSR) domain (Jin and Yoon 2012, Chen, Chen et al. 2013, Carmon, Gong et al. 2014). The FU-like CR domains are necessary to activate Wnt/β-catenin pathway (Seshagiri, Stawiski et al. 2012, Planas-Paz, Orsini et al. 2016). The functional connection between RSPOs and the Wnt/β-catenin pathway was demonstrated by the discovery of RSPO2 while screening for Wnt/β-catenin signaling activators in Xenopus (Jin and Yoon 2012). Although it has been more than ten years since the RSPO proteins was found to act as positive Wnt/β-catenin signaling regulators and exhibit ligand properties, the receptors of RSPOs were identified more recently. The

LRP5/6 receptors were first found to be required for activation of canonical Wnt signaling pathway by RSPOs (Jin and Yoon 2012) .Later on, in several Wnt-dependent stem cell compartments such as the intestine and hair follicles, the gene encoding leucine-rich repeat containing G protein-coupled receptor 5 (LGR5) was identified as a Wnt/β-catenin signaling target (Haegebarth and Clevers 2009, Chai, Xia et al. 2011) and later validated as a stem cells marker (Takeda, Kinoshita et al. 2011, Leushacke and Barker 2012) . And interestingly, the RSPO1 protein showed a strong mitogenic activity on $LGR5^+$ cells of the intestinal crypts and hair follicles (Carmon, Gong et al. 2011). Subsequent studies conclusively determined that LGR4/5/6, members of the Rhodopsin G-protein coupled receptor (GPCR) family, are the receptors for RSPOs (Carmon, Gong et al. 2011, Gong, Carmon et al. 2012) . All four RSPOs are bound to all three LGRs with high affinity, and this leads to increased phosphorylation of the co-receptor LRP5/6 and stabilization of β-catenin, but does not affect G-protein signaling (Chen, Chen et al. 2013). More interestingly, RSPOs -triggered Wnt/β-catenin signaling requires Clathrin, suggesting that receptor internalization plays a mechanistic role in RSPO signaling (Seshagiri, Stawiski et al. 2012, Chen, Chen et al. 2013, Carmon, Gong et al. 2014, de Lau, Peng et al. 2014, Malinauskas and Jones 2014).

In 2012, two groups independently discovered Ring finger protein 43 (RNF43) and its functional homolog Zinc and Ring Finger 3 (ZNRF3), which are members of a family of ubiquitin E3 ligases, to target specifically on FZD receptors and LRPs, inhibiting Wnt signaling activity by ubiquitination and consequent clearance of Wnt receptors from the cell membrane (Hao, Xie et al. 2012, Koo, Spit et al. 2012). Furthermore, RSPOs have

been shown to reduce RNF43/ZNRF3 activity through direct interactions that generate ternary complexes comprising RNF43/ZNRF3, RSPOs and LGR4/5/6 (de Lau, Peng et al. 2014, Hao, Jiang et al. 2016, Planas-Paz, Orsini et al. 2016). Current model suggests that RSPOs act to prevent the degradation of LRPs and FZDs from the cell surface (de Lau, Peng et al. 2014, Hao, Jiang et al. 2016). With the binding of RSPOs ligands, more LRPs and FZD receptors are present on the membrane, which allows the Wnt ligands to generate much stronger signals. Intriguingly, RNF43 and ZNRF3 themselves are Wnt target genes, which allows them to function as negative feedback regulators of Wnt receptor expression (de Lau, Peng et al. 2014, Zebisch and Jones 2015, Hao, Jiang et al. 2016). Both RNF43 and ZNRF3 are found to be enriched in $Lgr5^{+}$ stem cells in normal colonic crypts, as well as in colon cancer cells, due to the hyperactivation of Wnt/β-catenin signaling (Koo, Spit et al. 2012, de Lau, Peng et al. 2014, Jiang, Charlat et al. 2015).

Although RNF43 and ZNRF3 are highly functional homologous, they are not totally redundant to each other. RNF43 and ZNRF3 mRNA are differentially expressing in tissues and cell lines suggesting divergent transcription regulation machinery of these two genes besides Wnt/β-catenin pathway (Hao, Xie et al. 2012, Koo, Spit et al. 2012). Structurally, only dimers of ZNRF3/RSPO1 were observed, but not RNF43/ RSPO1 (Chen, Chen et al. 2013, Zebisch, Xu et al. 2013). And RSPOs binding enhances dimerization of ZNRF3 but not of RNF43 (Chen, Chen et al. 2013, Zebisch, Xu et al. 2013), which indicates a difference of the organization of the complex. Moreover, a recent study suggests that RNF43 can translocate into nucleus and sequester TCF4 to

Figure 3: Schematic of the modulation of surface Wnt receptor density by R-spondin/LGR/RNF43.

Cell surface FZD is ubiquitinated and cleared by E3 ubiquitin ligases RNF43/ZNRF3 for dampening the signaling (Upper Panel). R-spondin (RSPO) enhances Wnt/β-catenin signaling pathway by binding to RNF43/ZNRF3 and LGRs, triggering internalization of ternary complex consisting RNF43/ZNRF3 thereby increasing surface receptor density (Lower Panel).

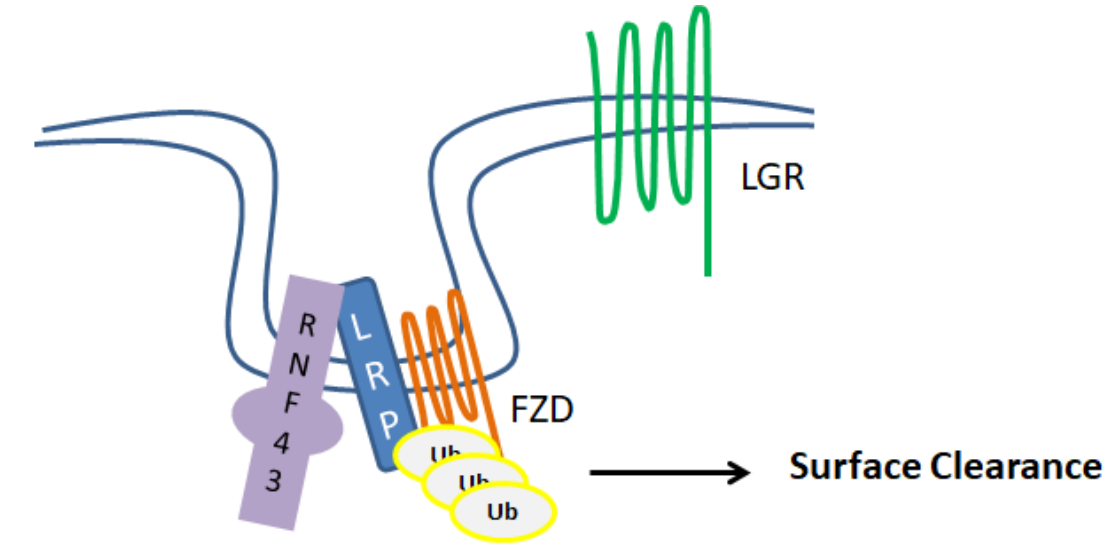
LGR
RNF43
LRP
FZD
Ub
Ub
Ub
Surface Clearance

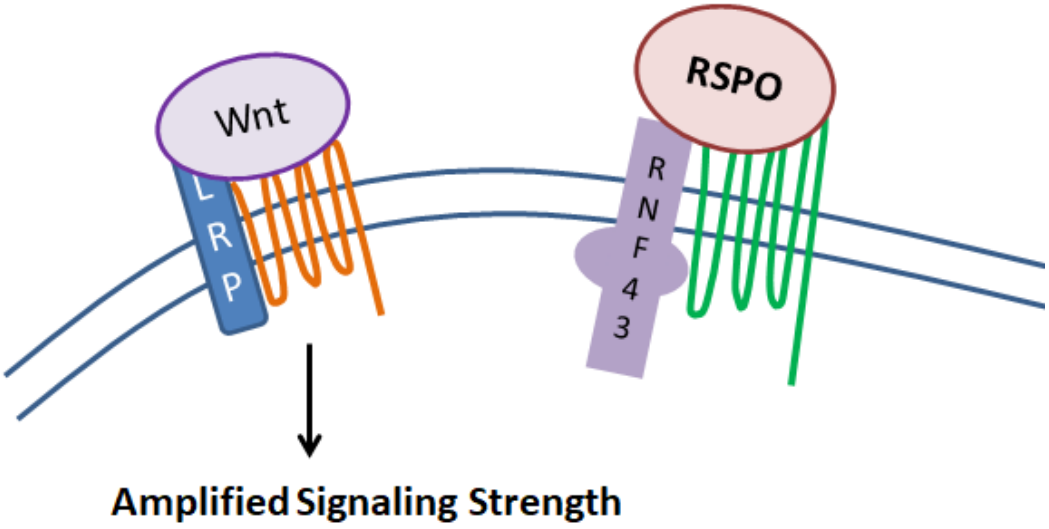
Wnt
LRP
RSPO
RNF43
Amplified Signaling Strength

the nuclear membrane, which also suppresses downstream Wnt/β-catenin pathway (Loregger, Grandl et al. 2015).

Because of the up-regulated expression of RNF43 in colon cancer, it was first characterized as an oncoprotein that could promote cell growth *in vitro* (Yagyu, Furukawa et al. 2004, Miyamoto, Sakurai et al. 2008, Sugiura, Yamaguchi et al. 2008, Shinada, Tsukiyama et al. 2011). But several lines of recent evidence have shown that RNF43 suppresses tumor growth by inhibiting Wnt/β-catenin signaling (Hao, Xie et al. 2012, Koo, Spit et al. 2012, Ryland, Hunter et al. 2013, Carmon, Gong et al. 2014, Jiang, Charlat et al. 2015, Loregger, Grandl et al. 2015, Niu, Qin et al. 2015, Xie, Xing et al. 2015, Bond, McKeone et al. 2016, Min, Hwang et al. 2016, Planas-Paz, Orsini et al. 2016). Loss of expression of RNF43 and ZNRF3 is predicted to result in hyper-responsiveness to endogenous Wnt signals (Hao, Xie et al. 2012, Koo, Spit et al. 2012, Giannakis, Hodis et al. 2014, Jiang, Charlat et al. 2015). Consistently, simultaneous deletion of these two Wnt modulators induces formation of adenomas in the intestinal epithelium consisting entirely of stem cells and their niche (Hao, Xie et al. 2012, Koo, Spit et al. 2012). Indeed, somatic mutations in *Rnf43* are seen in over 18% of colorectal adenocarcinomas and endometrial carcinomas (Bond, McKeone et al. 2016, Dienstmann and Tabernero 2016, Matsushita, Yamamoto et al. 2017, Steinhart, Pavlovic et al. 2017, Wang, Fu et al. 2017), as well as in a variety of human tumor types (Ryland, Hunter et al. 2013, Giannakis, Hodis et al. 2014, Planas-Paz, Orsini et al. 2016, Sekine, Yamashita et al. 2016), but mutations in ZNRF3 are much less frequent in cancers (Bond, McKeone et al. 2016).

1.4 DDB2 is a DNA damage repair protein

Damaged DNA binding protein 2 (DDB2), encoded by the XPE gene, is a DNA damage repair protein participating in the early steps of nuclear excision repair (NER) (Itoh, Nichols et al. 2001, Nag, Bondar et al. 2001, Fitch, Cross et al. 2003, Fitch, Nakajima et al. 2003). NER is a DNA repair mechanism for the removal of structurally and chemically diverse lesions. These lesions include ultraviolet-induced cyclobutane pyrimidine dimers (CPD) and 6-4 pyrimidine-pyrimidone photoproducts (6-4PP), and a variety of bulky adducts induced by carcinogens (Dijk, Typas et al. 2014, Waters, van Eijk et al. 2015). NER can be divided into two sub-pathways: global genomic NER (GG-NER) and transcription coupled NER (TC-NER). These two sub-pathways recognize DNA damage in different manners, but share the same process for the subsequent repair, and ligation (Dijk, Typas et al. 2014, Waters, van Eijk et al. 2015).

DDB2 is typically involved in the recognition stage of GG-NER (Hwang, Ford et al. 1999). GG-NER repairs damage in both transcribed and untranscribed DNA strands in active and inactive genes throughout the genome (Dijk, Typas et al. 2014). And DDB2 is one of the “damage sensing” protein in this pathway (Hwang, Ford et al. 1999, Fitch, Nakajima et al. 2003). DDB2 works together with DDB1 in the heterodimer DDB complex, and is capable of binding tightly with 6–4PP and CPD (Dualan, Brody et al. 1995, Zolezzi and Linn 2000, Itoh, Nichols et al. 2001). On the other hand, another damage recognition factor XPC recognizes a wide variety of lesions that

thermodynamically destabilize DNA duplexes (Li, Wang et al. 2006). *In vitro*, DDB binds to pyrimidine dimers including isomers of CPD and 6-4PP with the highest reported affinity and specificity of all NER proteins (Dualan, Brody et al. 1995, Itoh, Mori et al. 1999). XPC, by contrast, has substantially lower affinity and specificity for UV lesions (Fitch, Nakajima et al. 2003, Wang, Zhu et al. 2004). *In vivo*, DDB2 localizes ahead of XPC to CPD and 6-4PP lesions (Zolezzi and Linn 2000, Fitch, Nakajima et al. 2003). In the absence of DDB2, XPC still recognizes 6-4PP, although with substantially delayed kinetics (Fitch, Nakajima et al. 2003). In DDB2-deficient cells, CPDs are poorly recognized by XPC, and the CPD repair is largely abolished, while 6-4PP repair is affected to a lesser extent (Fitch, Nakajima et al. 2003, Wang, Zhu et al. 2004).

.

The DDB1 subunit associates tightly with the CUL4-RBX1 complex and forms a cullin family ubiquitin ligase (Nag, Bondar et al. 2001, El-Mahdy, Zhu et al. 2006). Following UV exposure, the DDB1–DDB2–CUL4A–RBX1 complex localizes to the site of damage and ubiquitinates XPC and DDB2 (El-Mahdy, Zhu et al. 2006, Li, Wang et al. 2006, Sugasawa 2016). Poly-ubiquitination of DDB2 reduces its affinity for damage while XPC remains unaffected, and this is thought to facilitate the handover of the lesion to XPC (El-Mahdy, Zhu et al. 2006, Dijk, Typas et al. 2014, Waters, van Eijk et al. 2015). Additional DDB-CUL4 substrates include histones H2A, H3, and H4 around the site of damage (Waters, van Eijk et al. 2015). H3 and H4 ubiquitination has been shown to loosen nucleosome binding in vitro, providing a pathway to assemble the NER repairosome in the otherwise inaccessible chromatin environment (Dijk, Typas et al. 2014, Waters, van Eijk et al. 2015).

Figure 4: Schematic of the initiation of global genomic nucleotide excision repair (GG-NER).

GG- NER repairs damage in both transcribed and untranscribed DNA strands in active and inactive genes throughout the genome. This process is not dependent on transcription. This pathway employs several "damage sensing" proteins including the UV-DDB complex, which recruits Cul4-Roc1 and XPC that constantly scan the genome and recognize helix distortions.

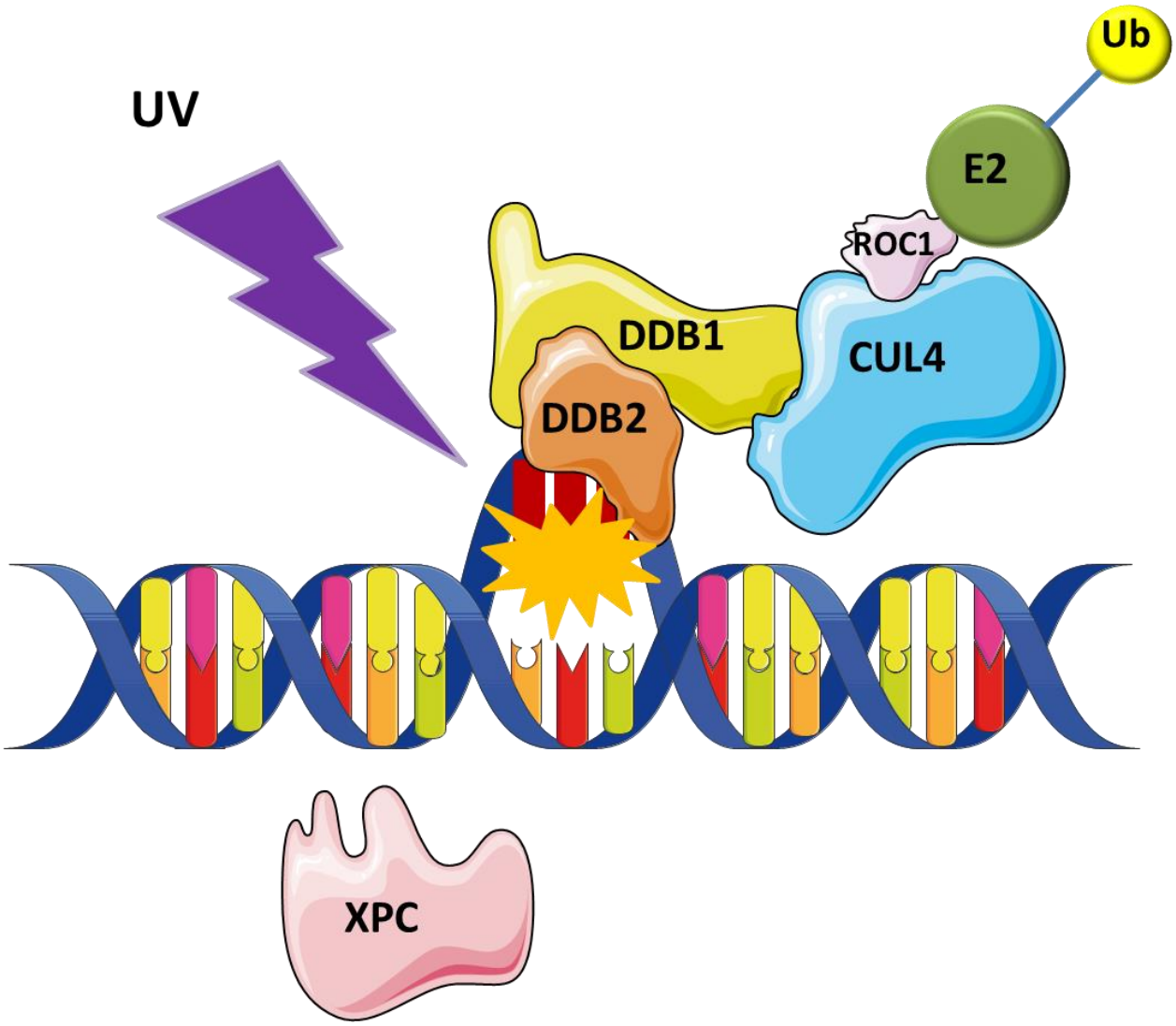
Ub
UV
E2
ROC1
DDB1
CUL4
DDB2
XPC

Mutations in NER pathway are associated with rare autosomal recessive syndromes such as xeroderma pigmentosum (XP) characterized by heightened UV sensitivity, neurological abnormalities, and an increased propensity to develop skin neoplasms (Itoh, Nichols et al. 2001). Particularly, mutations in DDB2 gene cause XPE- a mild form of xeroderma pigmentosum (Itoh, Nichols et al. 2001, Matakidou, Eisen et al. 2006). Patients in the XPE group have mild dermatological manifestations and are usually neurologically unaffected (Itoh, Nichols et al. 2001).

1.5 DDB2 is a transcription factor

Several DNA repair proteins are multi-functional proteins. For instance, XPB (ERCC3) protein, a key repair protein in NER that assists in unwinding the DNA double helix after damage is initially recognized, also plays a role in normal basal transcription as a component of transcription factor IIH (Weeda, Rossignol et al. 1997, Lin and Gralla 2005). Also, the Ku proteins, a dimeric protein complex that binds to DNA double-strand break ends and is required for the non-homologous end joining (NHEJ) pathway of DNA repair, is involved in transcription regulation (Featherstone and Jackson 1999, Tuteja and Tuteja 2000) as well as in telomere maintenance (Fisher and Zakian 2005).

In the past decades, function of DDB2 other than DNA repair has been studied. And it was found to possess transcriptional regulatory activity. DDB2 interacts with

transcription factor E2F1 and, in conjunction with DDB1, enhances the transcriptional activity of E2F1 in reporter assays (Hayes, Shiyanov et al. 1998). DDB2 has been reported to transcriptionally repress the expression of manganese superoxide dismutase (MnSOD) in breast cancer cells (Minig, Kattan et al. 2009). In that story, the binding of DDB2 was shown to be associated with the loss of acetylated H3 histones and the decrease in the binding of Sp1 but not AP-2α transcription factors to the SOD2 proximal promoter (Minig, Kattan et al. 2009). DDB2 also represses NEDD4L, an E3 ligase for Smad2/Smad3, in ovarian cancer cells to enhance TGF-β signaling transduction and increases the responsiveness of ovarian cancer cells to TGF-β-induced growth inhibition (Zhao, Cui et al. 2015). And the repression of NEDD4L by DDB2 was shown to involve PRC2 complex on the H3K27Me3 of the NEDD4L gene (Zhao, Cui et al. 2015). On the other hand, DDB2 also possesses transcriptional stimulatory activity. It binds to the promoter of the NFKBIA gene, which encodes an NF-kB inhibitor IκBα, to activate its expression and attenuate NF-kB activity, and that has been linked to regulation of invasiveness of breast cancer cells (Ennen, Klotz et al. 2013). That study also identified a DNA-element (TCCCCTTA) specifically recognized by DDB2 in the NFKBIA gene (Ennen, Klotz et al. 2013). A similar DDB2-cognate element is also found in NEDD4L that is repressed by DDB2 (Zhao, Cui et al. 2015). And our lab recently observed that DDB2 stimulates expression of SEMA3A in colon cancer cells, and that involves an interaction with the XRCC5/6 proteins (Fantini, Huang et al. 2017).

1.6 DDB2 is a tumor suppressor

DDB2, which is activated by p53 in human but not in mouse (Tan and Chu 2002), has been identified as a tumor suppressor in human cell lines and mice models. Studies in human cancer cell lines, including breast cancer cells, ovarian cancer cells and colon cancer cells, suggest that DDB2 inhibits tumor cell growth and invasiveness (Ennen, Klotz et al. 2013, Roy, Bommi et al. 2013, Roy, Elangovan et al. 2013, Han, Zhao et al. 2014, Qiao, Guo et al. 2015, Zhao, Cui et al. 2015). Moreover, *in vivo* studies in DDB2-/- mice models revealed a more comprehensive role of DDB2 in tumor suppression (Zolezzi and Linn 2000, Itoh, Cado et al. 2004, Itoh, Iwashita et al. 2007). The study, which exposed DDB2-deficient mice to UV light, demonstrated that DDB2 gene disruption leads to increased skin tumor incidence due to decreased p53-mediated apoptosis after UV-irradiation exposure (Itoh, Cado et al. 2004). Interestingly, without UV exposure, DDB2-/- mice exhibit shortened lifespans compared with wild-type littermates, and develop spontaneous tumors at a high rate between the ages of 16 and 24 months, which is not seen in other XP-deficient mice (Yoon, Chakrabortty et al. 2005). The spontaneous tumors developed in DDB2 deficient mice affect numerous organs including lung, mammary gland, lymph nodes, bone marrow, etc. (Yoon, Chakrabortty et al. 2005). The observations indicate that, in addition to DNA repair, other functions of DDB2 are significant in its tumor suppression role.

Previously, our lab showed that DDB2 plays a significant role in suppressing colon cancer metastasis (Roy, Bommi et al. 2013). The protein level of DDB2 decreases in

metastatic colon cancer, and that coincides also with loss of cell surface E-cadherin expression (Roy, Bommi et al. 2013). Depletion of DDB2 in an orthotopic mouse model for colon cancer causes a strong increase in metastasis of the colon cancer cells to the liver(Roy, Bommi et al. 2013). Reciprocally, expression of DDB2 suppresses metastatic potential of colon cancer cells harboring mutations in the Wnt-pathway (Ilyas, Tomlinson et al. 1997). The metastasis suppressor function of DDB2, at least partly, correlates with suppression of epithelial to mesenchymal (EMT)-like changes of the colon cancer cells. For example, expression of DDB2 in SW620 cells, mesenchymal type, changes the morphology to epithelial type. Conversely, depletion of DDB2 in SW480, epithelial type, changes the morphology of those cells to mesenchymal-like (Roy, Bommi et al. 2013).

1.7 Thesis project

Given the previously demonstrated role of DDB2 as a transcription factor, I sought to investigate genes that are regulated by DDB2. A high through-put RNA-seq analysis in HCT 116 colon cancer cells revealed *Rnf43* as a putative DDB2 target gene. In my thesis project, I identified a novel regulatory mechanism in which DDB2 works together with Wnt/β-catenin signaling and activates the expression of RNF43. In my study, I utilized techniques including Chromatin Immunoprecipitation (ChIP), Co-Immunoprecipittaion (Co-IP) and Chromatin Conformation Capture (3C) to demonstrate a transcription regulatory complex involving DDB2 bound to an *Rnf43* gene cis-rgulatory element, which links the upstream regulatory region to the intron area TCF-binding sites in the

Rnf43 gene. The transcription regulatory complex consists of DDB2, EZH2, β-catenin and TCF4. DDB2 directly binds with -2,900 bps upstream of *Rnf43* transcription start site (TSS), and recruits EZH2. In the intron area, the Wnt signaling downstream transcription factor TCF4 recruits β-catenin onto the TCF binding elements. EZH2 associates with β-catenin, which brings interaction between two cis-regulatory elements and forms a chromatin looping structure. I have shown that the looping structure led by the transcription regulatory complex is essential for the activation of RNF43. The molecular mechanism of RNF43 activation allowed me to characterize DDB2 as a novel partner of the Wnt/ β-catenin pathway.

Given the important role of RNF43 in the negative feedback-loop regulation of Wnt/ β-catenin signaling, I sought to investigate whether DDB2 regulates Wnt/ β-catenin signaling through RNF43. A ubiquitin assay indicated that DDB2 is required for the RNF43-mediated ubiquitination of FZD5. Meanwhile, immune-fluorescent staining showed that DDB2 also induced sequestration of TCF4 to nuclear membrane through RNF43. Moreover, DDB2-deficiency was shown to up-regulate Wnt/ β-catenin signaling activity in colon cancer cells. These observations suggested that DDB2 modulates Wnt/ β-catenin signaling pathway through RNF43 *in vitro.*

In addition to *in vitro* studies summarized above, I also studied how DDB2 regulates Wnt/ β-catenin signaling pathway in mouse colon tumor models. Wild-type mice and DDB2-/- mice were subjected to Azoxymethane (AOM)/Dextran Sulfate (DSS) chemical

carcinogenesis protocol for the colonic tumor development. I observed more tumor incidences and accelerated tumor development in the DDB2-/- mice, coinciding with increased abundance of the Wnt receptors and higher Wnt/ β-catenin signaling activity. Moreover, the immunostaining in human patient tissue microarray indicated a correlation between DDB2 and RNF43 expression in colonic tissues. And interestingly, the expression of both proteins decreased in early hyperplastic stage, in which Wnt/ β-catenin signaling is thought to begin altered.

In summary, I identified DDB2 as a novel partner as well as a regulator of Wnt/ β-catenin signaling pathway in colon cancer development.

2. MATERIALS AND METHODS

2.1 Plasmid, siRNA and Antibodies

pCDNA-V5-mFZD5 was a kind gift from Dr. Hans Clevers. TCF4-DN in pLX303 was a gift from Dr. William Hahn (Addgene plasmid # 42592). Two distinct DsiRNA-DDB2, two DsiRNA-EZH2 and non-targeting DsiRNA-Control were purchased from IDT DNA pre-designed library. Complete sequences are listed in Table 1. ON-TARGET plus PAF siRNA smartpool and non-targeting siRNA smartpool were purchased from Dharmacon. Antibodies used in this study include DDB2 (Western Blotting: 5416, Cell Signaling; Chromatin Immunoprecipitation: sc-25368, Santa Cruz; co-Immunoprecipitation: ab181136, Abcam), EZH2 (Western Blotting: 5246, Cell Signaling; Chromatin Immunoprecipitation: 39875, Active Motif), β-catenin (8480, Cell Signaling), RNF43 (orb140091, Biorbyt), EED (sc-28701, Santa Cruz), SUZ12 (3737, Cell Signaling), TCF4 (2569, Cell Signaling), V5 tag (R960-25, Invitrogen), T7 tag (69522, EMD Millipore), α-Tubulin (T9026, Sigma-Aldrich) and LRP5/6 (bs-2905R, BIOSS). HRP-conjugated secondary antibodies were purchased from BioRad.

2.2 Cell culture, Transfection and Stable Cell Lines

HCT116 cells and HT-29 cells were grown in DMEM medium containing 10% Fetal Bovine Serum and 1% Penicillin-Streptomycin at 37°C and 5% CO_2. SW480 and SW620 were grown in RPMI medium containing 10% Fetal Bovine Serum and 1% Penicillin-

Streptomycin at 37°C and 5% CO_2. Cell transfection experiments were conducted using Lipofectamine2000 (Thermo Fisher Scientific) and following manufacturer's recommendations. For transient expression of plasmids, cells were harvested 36hrs after transfection. For transient knockdown, cells were harvested 72h after siRNA transfection. Two distinct siRNAs targeting different regions of the gene were used to eliminate off-target effect. HCT116 cells stably expressing shRNA targeting DDB2 were described before. HCT116 cells stably expressing FLAG-HA-tagged DDB2 were established using a retroviral vector. And HCT116 cells stably expressing dn-TCF4 were established using a lentiviral vector and selected by Blasticidin.

2.3 CHIR99021, Deoxycholic Acid (DCA) and Recombinant Wnt3A Treatment

HCT 116 cells were treated with CHIR99021 (Stemgent) at 3.3μM for 16 hours in serum-free medium. HT-29 cells were treated with CHIR99021 at 6.7μM for 24 hours in serum-free medium. And HCT 116 cells and HT-29 cells were treated with DCA (Sigma-Aldrich) at 10μM for 2hours in serum-free medium. HT-29 cells were treated with recombinant human Wnt3A protein (R&D system) at 300ng/ml for 24 hours after 24 hours serum starvation.

2.4 Protein Extraction, Immunoblotting and Co-immunoprecipitations

For immunoblotting, total cell were lysated with RIPA buffer (50 mM Tris-HCl pH 7.4, 150 mM NaCl, 1% NP-40, 0.1% SDS, 1 mM EDTA and 0.5% sodium deoxycholate) supplemented with protease inhibitor cocktail, and cleared by centrifugation at 16,000g for 15 min at 4°C. Cell lysates were then boiled in 1 x Laemmli buffer for 5 min at 95°C. Samples were separated on 8% SDS-PAGE gel and western blotting was performed using standard procedures and the antibodies listed above diluted in 5% BSA (Sigma) in TBS supplemented with 0.1% Tween 20 (Thermo Fisher Scientific).

Nuclear extracts preparation and co-immunoprecipitation using anti-FLAG M2 agarose bead slurry were performed as decribed before (Fantini, Huang et al. 2017). For endogenous DDB2 pull down, nuclear extracts were rotated for 5h at 4°C with 10 ug anti-DDB2 monoclonal antibody. Protein G–Sepharose beads were added and samples were further rocked for 1h. After 3 washes with IP buffer, beads were eluted in 50 mM Tris-HCl, 500 mM NaCl, 0.1% SDS and 1 mM PMSF. Co-immunoprecipitates were analyzed by standard western blotting.

2.5 Chromatin Immunoprecipitation (ChIP)

Chromatin Immunoprecipitation experiments were performed as described before (Roy, Bommi et al. 2013). Anti-DDB2, anti-T7 tag, anti-EZH2, anti-β-Catenin and anti-TCF4

antibodies were used for immunoprecipitation. De-crosslinked chromatin was analyzed by qPCR using the primers described in Table 2. *Rnf43* Intron2-A, Intron2-B and c-Myc primers were described in. Axin2 Intron1 primers were purchased from Cell Signaling.

2.6 Gene Editing with CRISPR/Cas9 System

The deletion of target sequences in HT-29 cells was performed by the Genome Editing Core, University of Illinois at Chicago. Briefly, HT-29 cells were transfected with plasmids encoding Cas9 and guide RNAs (sgRNAs) that target the 132bps (Short Del) and 416bps (Long Del) fragments respectively. Clones were screened by PCR, and then confirmed by Sanger genomic DNA sequencing. The PCR results are included in Figure 7.

2.7 RNA Extraction and qPCR

Total RNA was extracted using TRIzol (Thermo Fisher Scientific) following manufacturer's instructions. cDNA was synthesized using iScript cDNA Synthesis Kit (BioRad) and quantitative PCR was performed using iTaq universal SYBR Green supermix (BioRad) and a CFX96 system (BioRad). Oligonucleotides used as primers are described in Table 3.

2.8 Ubiquitination Assay

HT-29 cells were transfected with V5-tagged FZD5 vectors and His-tagged ubiquitin, as indicated, and either siRNA-Control or siRNA-DDB2. Also the parental, short del and long del HT-29 cells were used in the assay. The major procedure and material were described before (Koo, Spit et al. 2012). Briefly, the HT-29 cells were washed and collected in ice-cold PBS with N-ethylmaleimide (Sigma). Then the cells were lysed in lysis buffer consist of 10 mM Tris–HCl, 100 mM phosphate buffer, 6 M guanidinium pH 8.0, 20 mM imidazole, and 10 mM β-mercaptoethanol, followed by sonication. Then the lysates were centrifuged, and the supernatants were incubated with nickel-nitrilotriacetic acid–agarose beads (Qiagen) for 3 hours at room temperature. Beads were then washed with lysis buffer with 0.2% Triton X-100, followed by sequential washes with buffers 1, 2 and 3 (Buffer 1: 10 mM Tris–HCl pH 8.0, 8 M urea, 100 mM phosphate buffer pH 8.0, 10 mM β-mercaptoethanol and 0.2% Triton X-100; Buffer 2: 10 mM Tris–HCl pH 6.3, 8 M urea, 100 mM phosphate buffer pH 6.3, 10 mM β-mercaptoethanol and 0.2% Triton X-100; Buffer 3: 10 mM Tris–HCl pH 6.3, 8 M urea, 100 mM phosphate buffer pH 6.3, 10 mM β-mercaptoethanol and 0.1% Triton X-100). After washes, the His-tagged proteins were eluted in two beads volumes of elution buffer (10 mM Tris–HCl pH 7.0, 6.2 M urea, 100 mM phosphate buffer and 200 mM imidazole and 1x Laemmli buffer). For western blotting, anti-V5, anti-DDB2, anti-RNF43and anti-α-Tubulin antibodies were used.

2.9 Chromatin Conformation Capture (3C) Assay

The protocol used for the assay was adapted from the protocol developed by Dekker and coworkers (Dekker, Marti-Renom et al. 2013). Single cell suspension of ~$1x10^7$ HCT 116 cells expressing shControl vs. shDDB2, and empty vector vs. dn-TCF4 were diluted in 18 ml of DMEM medium. The cells were cross-linked with 2% formaldehyde for 10 minutes at room temperature, followed by 5 minutes incubation with 0.125M glycine for quenching the reaction. The cells were collected by 10 minutes centrifugation at 800xg at 4^{o}C. Then the cell pellet was washed twice with ice-cold PBS and lysed with 5ml of ice-cold lysis buffer (10mM Tris-HCl pH 8.0, 0.2% NP-40, 10mM NaCl supplemented by protease inhibitor cocktail) using Dounce homogenizer. The nuclei were centrifuged at 5,000 rpm and washed three times with 500 µl 1x NEBuffer 3.1. Then the nuclei were re-suspended in 0.5ml 1.2x NEBuffer 3.1 with 0.3% final concentration of SDS, and incubated for 1 hour at 37^{o}C. Then 1.8% final concentration of TritonX-100 was added and the nuclei were incubated for 1 hour at 37^{o}C, to quench the effect of SDS. To digest the nuclei, 400 units of BglII (NEB) were added to the samples, and the samples were incubated overnight at 37^{o}C with rotation. The restriction enzyme was then inactivated by adding SDS (1.3% final concentration) and incubating for 20 minutes at 65^{o}C. To ligate the nuclei, the samples were then incubated with 7ml of 1x ligation buffer (NEB) containing 1% TritonX-100 for 1 hour at 37^{o}C. 4,000 units of T4 DNA ligase (NEB) were added and the samples were then incubated for 4 hours at 16^{o}C. After ligation, the samples were reverse cross-linked by overnight incubation at 65^{o}C with 300µg Proteinase K, followed by RNAse treatment for 30 minutes at 37^{o}C. Finally the DNA fragments were extracted by standard phenol/chloroform protocol and precipitated by ethanol. To

generate control templates for the standard curve, regular PCR was used to amplify the regions spanning each BglII site of interest as described before from HCT 116 cells. A set of PCR products was mixed in equimolar amounts. The mixture was then digested with 400 units of BglII overnight at 37^{o}C and re-ligated by T4 DNA ligase. DNA was phenol chloroform extracted and ethanol precipitated. The sample purity and concentration were assessed by SybGreen qPCR. The 3C analysis quantifies ligation products generated by ligation of two fragments of the locus. And the highly specific *Taqman* real-time PCR was performed to quantify the relative crosslinking frequencies of 3C samples. The primers and probes for the *Taqman* PCR were designed using the PrimerQuest Tool from IDT. And the location of each primer is marked in Figure 9C. 100ng 3C template from each sample is used per PCR. Standard curves were performed in each run using serial dilutions of the control template. The relative crosslinking frequencies were normalized to *gapdh* gene. Oligonucleotides used as primers and probes are described in Table 4.

2.10 Immunofluorescent Staining

SW620 and HT-29 cells were grown on coverslips in 24-well plates till the cells were ready for staining. The cells were fixed in ice-cold acetone for 10 min at 4C, followed by 3 times washing with PBS. After washes, the cells were incubated with blocking and permeabilization solution (5% goat serum, 0.5% TritonX-100 in PBS) for 30 min at room temperature and then TCF4 primary antibody (Cell Signaling) for overnight at 4C (1:200 dilution in blocking solution). The goat anti-rabbit Alexa Fluor 594 (Abcam) were used

as secondary antibody (1:500 dilution). After washes, the cells were incubated with DAPI for 2 minutes, and then mounted in Vectashield Mounting Medium for Fluorescence. The fluorescent staining was visualized using a ZEISS LSM 700 confocal microscope.

2.11 Animals and Tissues

The DDB2 whole body knock-out (DDB2-/-) mouse line was described previously. In the AOM/DSS colon carcinogenesis model, 6 weeks old male DDB2+/+ and DDB2-/- mice were given a single I.P. injection of AOM (10 mg/kg). One week after AOM injection, animals received 2% DSS in their drinking water for 7 days. 12 DDB2+/+ mice and 14 DDB2-/- mice were sacrificed at 15 weeks. For immunohistochemistry, colorectal tissues were fixed in 10% buffered formalin and embedded in paraffin. RNA extracts were prepared from colorectal tissues using TRIzol and RNeasy Mini Kit (QIAGEN).

2.12 Immunohistochemistry

Immunohistochemistry of paraffin-embedded tissue samples was performed using Avidin/Biotin Blocking Kit, Vectastain ABC Kit and DAB Substrate Kit (Vector Laboratories) according to manufacturer's instructions. DDB2 antibody was diluted 1:250 for human samples; RNF43 antibody was diluted 1:200 for mouse samples and 1:50 for human samples; LRP5/6 antibody was diluted 1:300 in 3% goat serum in TBS

buffer. Nuclei were counter stained with hematoxylin. Controls were performed with normal rabbit IgG.

2.13 Whole Exome Sequencing (WES)

The WES was performed in tumor samples from six AOM/DSS treated male mice. Two samples (BDM_31WT and BDM_33WT) were isolated from the distal colon of two wild-type mice, and four samples (BDM_29KO, BDM_39KO, BDM_41KO, BDM_42KO) were isolated from the distal colon of four DDB2 -/- mice. The raw data were aligned to reference mouse genome mm10 and the in-house C57BL/6 background was filtered.

2.14 Human Colorectal specimen

All the human samples for tissue arrays were collected from Department of Pathology, University of Illinois at Chicago. The tissue microarrays (TMA) were prepared by the Research Histology Core in UIC. The adequacy, quality, and structural integrity of the paraffin-embedded tissue blocks were assessed and verified prior to inclusion in the study. Colon resection cases provided sample tissue for construction of tissue arrays. The tissue arrays were designed and constructed based on prescribed practices. Hematoxylin and eosin-stained adjacent tissue sections were reviewed and used to identify areas of normal,

hyperplastic, dysplastic and carcinomatous colonic tissue. Cores from archived normal colon specimens provided non-disease controls. Donor core tissues 0.6 mm diameter were obtained from corresponding regions in the donor paraffin block and embedded in a recipient block. A duplicate donor core tissue from each lesion was sampled across a patient's colonic resection. The donor cores from all subjects were embedded in a tissue microarray (TMA) recipient block. Each of the tissue microarray cores was histologically examined to document and record tissue-sampling adequacy and diagnoses. All tissue samples were de-identified, containing no patient demographic information. Total 24 patients were analyzed by immunohistochemistry.

2.15 Statistical analyses

All statistical analyses were performed using GraphPad Prism 6 software. Unpaired, two-tailed Student *t*-tests and Mann-Whitney *U*-tests were used to analyze statistical significance. SD was indicated in the figure, and sample volume was indicated in the figure legends. Two-tailed, paired *t*-tests were used to analyze human TMA staining positivity. And the Spearman rank coefficient was used as a statistical measure of correlation between DDB2 expression and RNF43 expression in each patient. Unless otherwise indicated, all the experiments were performed at least three times.

Table 1: Sequences of DsiRNA

Genes	DsiRNA # 1 (5'-3')	DsiRNA #2 (5'-3')
DDB2	AGUUUAACCCUCUCAAUACCAACCA UGGUUGGUAUUGAGAGGGUUAAACUUC	AGGUUAUCUUGGAACUAAAUGACTT AAGUCAUUUAGUUCCAAGAUAACCUUG
EZH2	GAGGAUCACCGAGAUGAUAAAGAAA UUUCUUUAUCAUCUCGGUGAUCCUCCA	UAAUGCAGUAUGGUACAUUUUUCAA UUGAAAAAUGUACCAUACUGCAUUAUU

Table 2: Primers for ChIP assays

Regions	Forward Primer (5'-3')	Reverse Primer (5'-3')
5'UTR	CACTTTGTCAGCAGGTAGAGAGCG	TCCCAGAGAGAGAGAAGGCAGTATC
P1	GCAGCCATTTAGTAGAAGCTATGCC	AACTGGACATCCAAGACATCCTTC
P2	GAAAAGCGACCTGTGTGGTCC	TGGAAATTGGGTCTCCTCTTCAC
P3	TGGATCTCCTGCTATCCTTACACG	TCAGACCCTACTGGCTAATTCACAG
P4	TGCCGTTAGGGATAAGGACAATTC	GTTTTGGAGTTACCCTCTAGGGTTG
P5	CTTGAGTTTCTCCAAGTCTCCAGG	CAAAGGAATGAAAAGACCTAGCCC
P6	TGGAGACCATCCTGGCTAACAC	TCTCGGCTCACTGCAAGCTC
P7	CTACAGGGGAAACAATGTTGAAGG	TTTCTGAACCGCTGCCATAAAC
P8	ATGGACAGAGCCCTTCCCAG	TGCACCCAACAGAGCATAGATG

Table 3: Primers for gene expression assays

Genes	Forward Primer (5'-3')	Reverse Primer (5'-3')
DDB2	CCAACCAGTTTTACGCCTCCTC	TGTCTCCTGTGACCACCATTCG
RNF43	TCCCCTTGAAAATGGACCCC	GCTTGACGATGCTGATGAATCC
AXIN2	AGCGATGAGTTTGCCTGTG	AATCGATCCGCTCCACTTT
GAPDH	GTGGTCTCCTCTGACTTCAAC	GGAAATGAGCTTGACAAAGTGG
18S rRNA	CTTAGAGGGACAAGTGGCG	ACGCTGAGCCAGTCAGTGTA
c-Myc	CACCGAGGAGAATGTCAAGAG	CTTGGACGGACAGGATGTATG
EZH2	GGAGACGATCCTGAAGAAAGAG	TCTTCTGCTGTGCCCTTATC
PAF	TGCTTGGTTCTTCCACCTCTGC	CCTTTTTGCCACTTGGGAGTTG
m-DDB2	TCAATGGAGGGAACAACCAGG	TAACCACCACTCTGCTCTTGGC
m-RNF43	ATGGACCCCACAGGAAAACTG	TGTCGTCATCACTGGCGTTG
m-Axin2	CTTTACACTCCTTGTTGGGTGACC	GGTATCCTTCAGGTTCATCTGCC
m-Cdx1	CACCTGGAGATTTCCCAAGA	GCTGGAAGAGGAGACAGGTG

Table 4: Primers and probes for 3C assay

Sets	Forward Primer (5'-3')	Reverse Primer (5'-3')	Probe
Set1	CCATGATGGCACAACTG	CTGATCAGAGATCTAATAACTAACC	/56-FAM/CTCCAGCGT/ZEN/GGGTAACACAAGACC/3IABkFQ/
Set2	CTACCTCAGCTATCCAAGCTATC	CTAATCAGAGGGACCACACAG	/56-FAM/ACTGCAGAT/ZEN/CAATACAGAGCTCACCC/3IABkFQ/
Set3	CTACCTCAGCTATCCAAGCTATC	TGTCATCCATTCCTCACTCTTT	/56-FAM/ATCTTCATC/ZEN/TGCTGGTGGACGTGG/3IABkFQ/
Set4	CTCTCATCTTGGCATGCAGTA	CCCAGTTGTAACCCTACTTTGA	/56-FAM/ACCTCAGCT/ZEN/ATCCAAGCTATCTTTGCAG/3IABkFQ/

3. RESULTS

3.1 DDB2 activates expression of Wnt-receptor regulator RNF43

The transcriptional regulatory function of DDB2 plays significant tumor suppressor roles in colon cancer metastasis. We showed that depletion of DDB2 causes colon cancer cells to undergo epithelial to mesenchymal transition along with an increase in their metastatic potential (Roy, Bommi et al. 2013). Since the Wnt/β-catenin pathway is important in the development and progression of colon cancer, we sought to investigate whether the regulatory mechanism of DDB2 interacts with the Wnt/β-catenin signaling pathway. We analyzed the Wnt/β-catenin pathway genes, and discovered a role of DDB2 in the activation of *Rnf43* that regulates Wnt/β-catenin signaling by removing the receptors from cell surface. We measured the mRNA expression level of *Rnf43* with or without DDB2 shRNA or siRNA in several colon cancer cell lines. In SW480, HT-29 and HCT116 cells, silencing of DDB2 resulted in a loss of the *Rnf43* transcript (Figure 5A and B). HCT116 cells express a frame-shift mutant *Rnf43*-mRNA, and the mutant protein was not detected by the antibody. The protein levels of RNF43 in HT-29 and SW480 were reduced upon treatment with siRNA-DDB2 (Figure 5C). Reciprocally, expression of DDB2 resulted in an increase in the level of *Rnf43*-mRNA. For example, HCT116, SW480 and SW620 cells were infected with adenovirus expressing DDB2 or LacZ. Quantitative RT-PCR assays of the RNAs from the infected samples showed that the *Rnf43* mRNA level was increased in cells infected with adenovirus expressing DDB2 (Figure 6A). Consistently, the protein level of RNF43 also increased in DDB2 overexpressing cells (Figure 6B). These results show that DDB2 is required for expression of *Rnf43* in colon cancer cells.

Figure 5: DDB2-defiency abolishes RNF43 expression in colon cancer cells.

(A) SW480 cells and HT-29 cells were transient transfected with DsiRNAs (siControl or siDDB2). Total RNA was analyzed using qRT-PCR for the mRNA level of *Rnf43* N=3, Error bars indicate SD. (B) Total mRNA, extracted from HCT 116 cells stably expressing shRNAs (shControl and shDDB2), was analyzed using qRT-PCR for the mRNA level of *Rnf43*. (C) Total levels of DDB2, RNF43 and α-Tubulin (Loading Control) proteins in SW 480, HT-29 and HCT 116 cell lines were analyzed by Western Blotting.

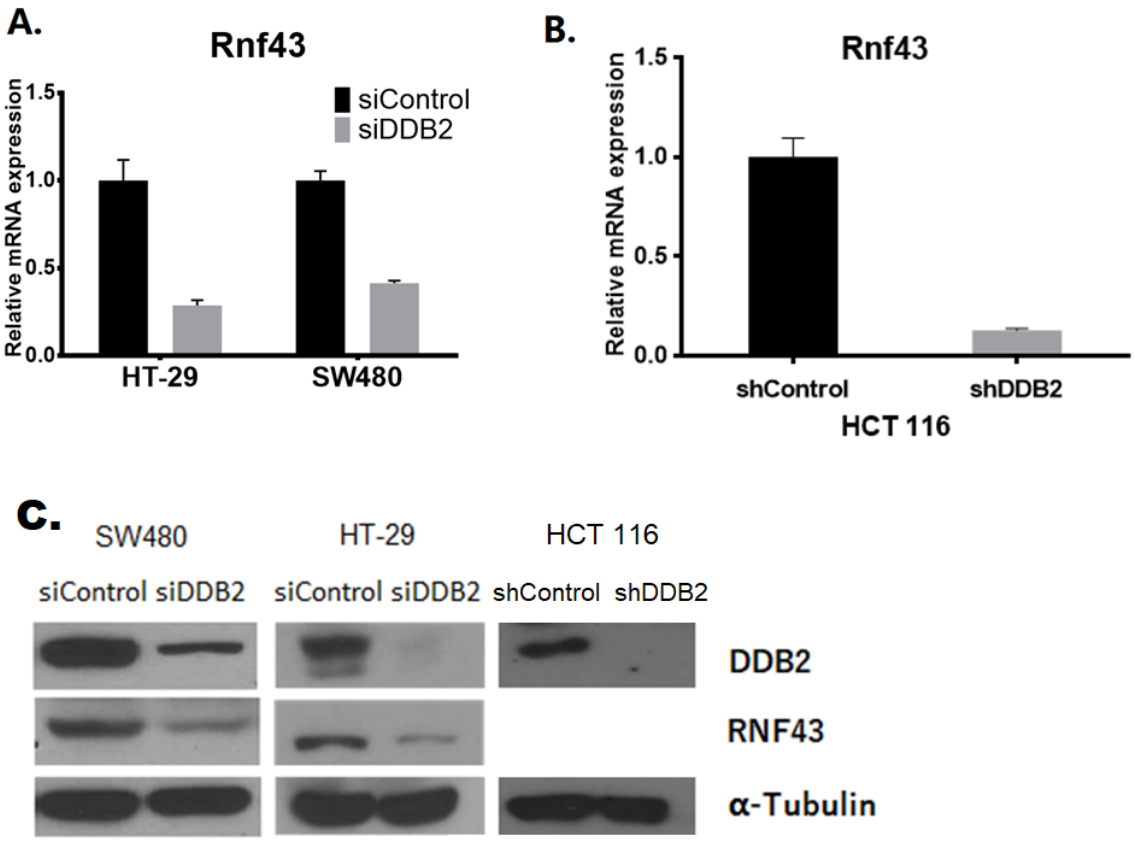
A.
Rnf43
siControl
siDDB2
Relative mRNA expression
1.5
1.0
0.5
0.0
HT-29
SW480
B.
Rnf43
Relative mRNA expression
1.5
1.0
0.5
0.0
shControl
shDDB2
HCT 116
C.
SW480
HT-29
HCT 116
siControl siDDB2
siControl siDDB2
shControl shDDB2
DDB2
RNF43
α-Tubulin

Figure 6: Overexpression of DDB2 stimulates RNF43 expression in colon cancer cells.

(A and B) The indicated cell lines were infected with adenovirus expressing either LacZ or T7 tagged DDB2 (T7-DDB2). qRT-PCR (A) was performed to analyze relative mRNA level of *Rnf43*expression (Normalized by *gapdh*). N=3, Error bars indicate SD. Western blotting (B) was performed to analyze the protein levels of DDB2, RNF43 and α-Tubulin.

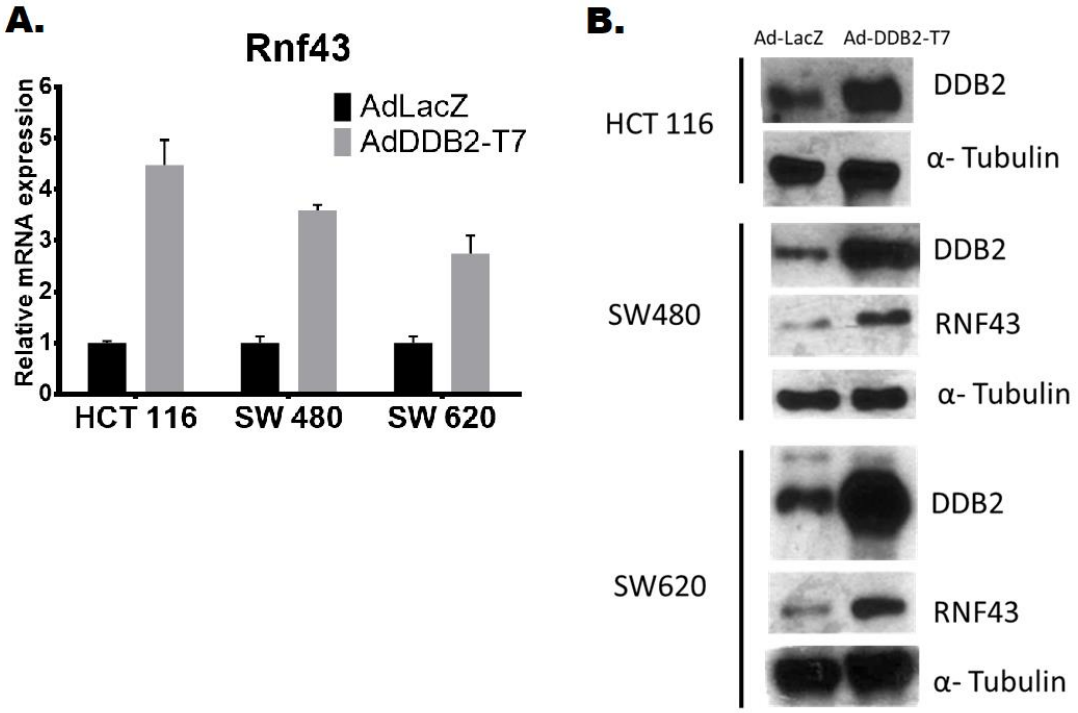
A.
Rnf43
AdLacZ
AdDDB2-T7
Relative mRNA expression
0
1
2
3
4
5
6
HCT 116
SW 480
SW 620
B.
Ad-LacZ
Ad-DDB2-T7
HCT 116
DDB2
α- Tubulin
SW480
DDB2
RNF43
α- Tubulin
SW620
DDB2
RNF43
α- Tubulin

Rnf43 is also a Wnt/β-catenin signaling target gene, and is activated by β-catenin (Koo, Spit et al. 2012). We sought to investigate whether the Wnt/β-catenin mediated activation of *Rnf43* also involves DDB2. We employed CHIR99021, a GSK3 inhibitor, to activate β-catenin in colon cancer cells in the presence and absence of DDB2-depletion. HCT116 (Figure 7A) and HT-29 cells (Figure 7B) were treated with CHIR99021 for 16 hours and 24 hours respectively. Quantitative RT-PCR was performed on total RNAs isolated from the CHIR99021 or vehicle treated cells to measure the mRNA level of DDB2, *Rnf43* and Axin2. Interestingly, CHIR99021 stimulated *Rnf43* mRNA expression in control cells but not in the cells with silenced DDB2. However Axin2, as another Wnt/β-catenin target gene, is stimulated in both control cells and DDB2 silenced cells following CHIR99021 treatment. Moreover, deoxycholic acid (DCA) that was shown to activate downstream Wnt-signaling (Pai, Tarnawski et al. 2004) exhibited similar effects on *Rnf43* and Axin2 expression (Figure 7C). These results suggest that DDB2 is required for the activation of *Rnf43*, but not Axin2, by Wnt/β-catenin signaling.

3.2 Reduced expression of RNF43 in human colonic hyperplasia correlates with reduced expression of DDB2

DDB2 is a p53-activated gene, and its expression in colon cancer is down regulated in high-grade metastatic colon cancer (Roy, Bommi et al. 2013). However, deregulation of Wnt/β-catenin is one of the earliest events during colon cancer development. Moreover, in our mouse studies, we observed increased susceptibility of the DDB2-deficient mice in

Figure 7: DDB2 is required for the activation of *Rnf43* mRNA expression by Wnt/β-catenin.

(A) HCT 116 cells stably expressing shRNAs (shControl or shDDB2) were treated with DMSO or CHIR99021 (3.3uM, 16 hrs). The mRNA levels of DDB2, *Rnf43* and Axin2 were analyzed using qRT-PCR (Normalized by 18S rRNA). N=3. All error bars indicate SD. (B) HT-29 cells expressing DsiRNAs (siControl or siDDB2) were treated with DMSO or CHIR99021 (6.7uM, 24 hrs). The mRNA levels of DDB2, *Rnf43* and Axin2 were measured and analyzed using qRT-PCR (Normalized by 18S rRNA). N=3. All error bars indicate SD. (C) Deoxycholic acid (DCA) was used to activate downstream Wnt signaling as an alternative to CHIR99021. HCT 116 cells stably expressing shControl or shDDB2 were treated with 10uM DCA for 1 hour. The relative mRNA levels of DDB2, RNF43 and Axin2 were analyzed using qRT-PCR. N=3. All error bars indicate SD.

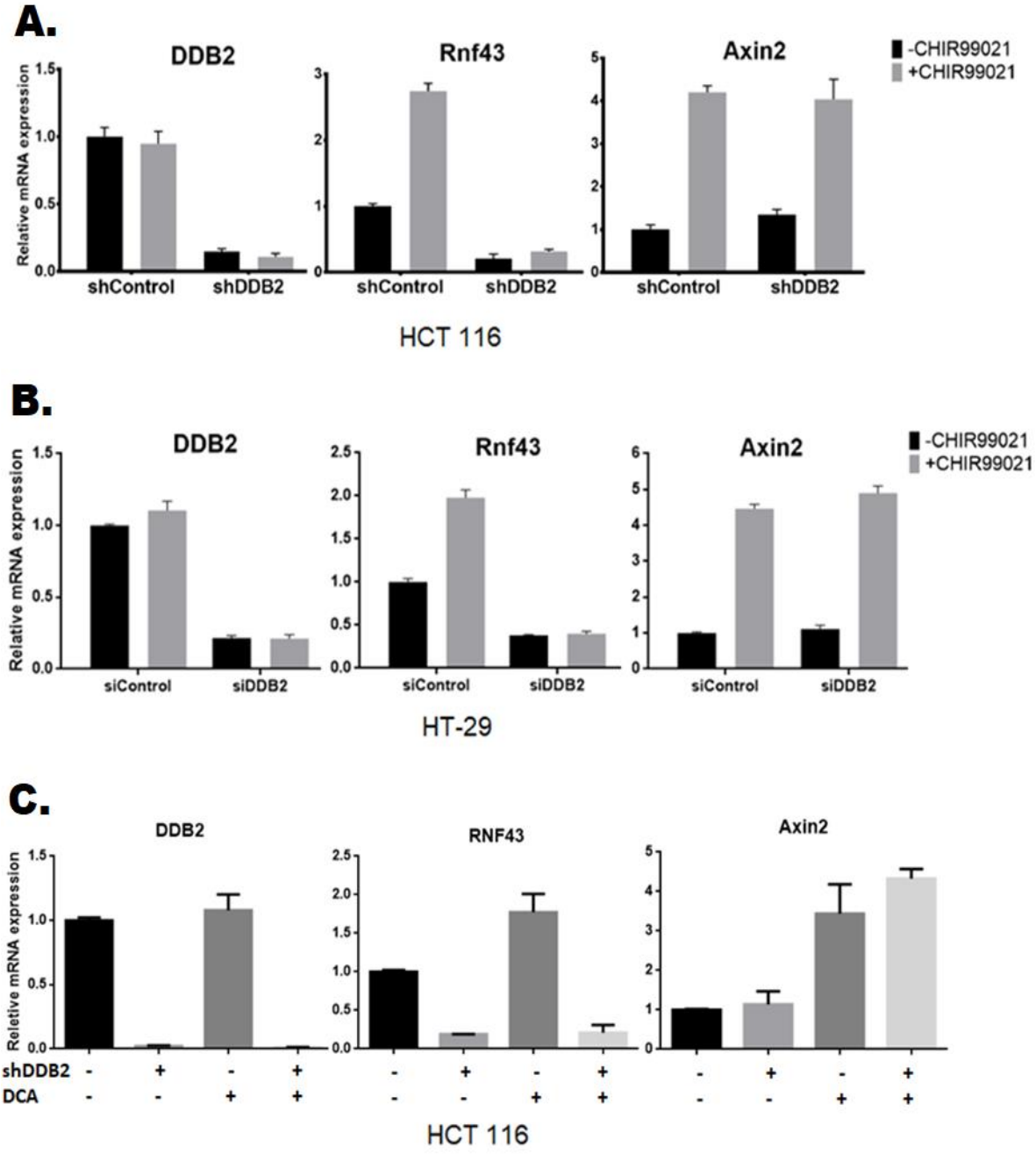
A.
DDB2
Rnf43
Axin2
-CHIR99021
+CHIR99021
Relative mRNA expression
shControl
shDDB2
HCT 116
B.
DDB2
Rnf43
Axin2
-CHIR99021
+CHIR99021
Relative mRNA expression
siControl
siDDB2
HT-29
C.
DDB2
RNF43
Axin2
Reletive mRNA expression
shDDB2
DCA
HCT 116

colon tumor development. Therefore, we analyzed human colonic specimens for the expression of DDB2 and RNF43 at the early stages of tumor development. We analyzed tissue microarray samples at different stages from 24 patients who eventually developed adenocarcinoma. Immunohistochemical staining of the samples indicated down regulation of both DDB2 and RNF43 expression in the hyperplastic foci in a high proportion of the samples (Figure 8A-C). To examine whether RNF43 and DDB2 expressions are correlated in tissue microarray, we performed Spearman correlation analysis for DDB2 and RNF43 expression. Samples from each patient were analyzed separately, to eliminate various backgrounds among different patients (Table 5). 16 out of 24 patients showed significantly correlated expressions of DDB2 and RNF43. The reduced expression of RNF43 in the early stage of foci development is interesting because often it is at that stage Wnt-signaling begins to get deregulated. We did not detect reductions in the low-grade adenocarcinoma samples. However, in Bittner Colon datasets (Oncomine), there were significant reductions of *Rnf43* in the high-grade samples (Figure 9) and that would be consistent with our previous observation on loss of DDB2 expression in high-grade samples (Roy, Bommi et al. 2013).

Figure 8: Expression of *Rnf43* in human colonic tissues correlates with DDB2.

(A and B) Immunohistochemical staining of RNF43 and DDB2 in adjacent normal, adjacent foci of hyperplasia, dysplasia and low-grade adenocarcinoma samples were quantified as positivity (=Number of Positive/Number of Total). Positivity of DDB2 (A) and RNF43 (B) were plotted. N of Adjacent normal = 47, N of Adjacent foci of hyperplasia= 42, N of Dysplasia = 18, N of Low-grade adenocarcinoma = 47. **** $P < 0.0001$ (C) Representative images of DDB2 expression and RNF43 expression from same patient. Scale bar =50 μm.

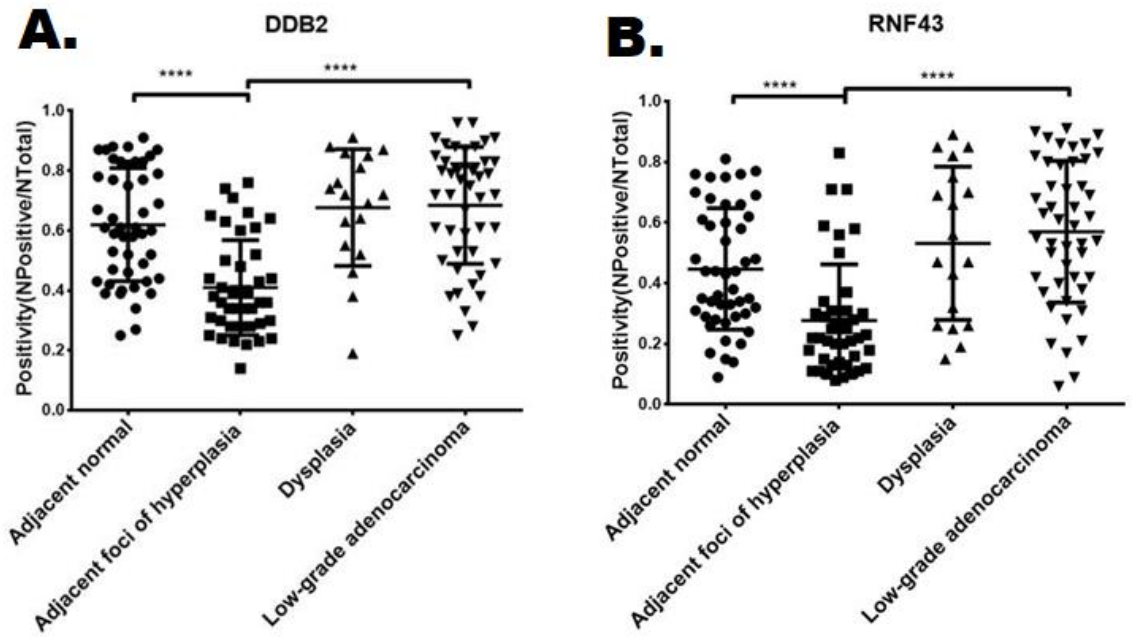
A.
DDB2
****
****
Positivity(NPositive/NTotal)
1.0
0.8
0.6
0.4
0.2
0.0
Adjacent normal
Adjacent foci of hyperplasia
Dysplasia
Low-grade adenocarcinoma
B.
RNF43
****
****
Positivity(NPositive/NTotal)
1.0
0.8
0.6
0.4
0.2
0.0
Adjacent normal
Adjacent foci of hyperplasia
Dysplasia
Low-grade adenocarcinoma

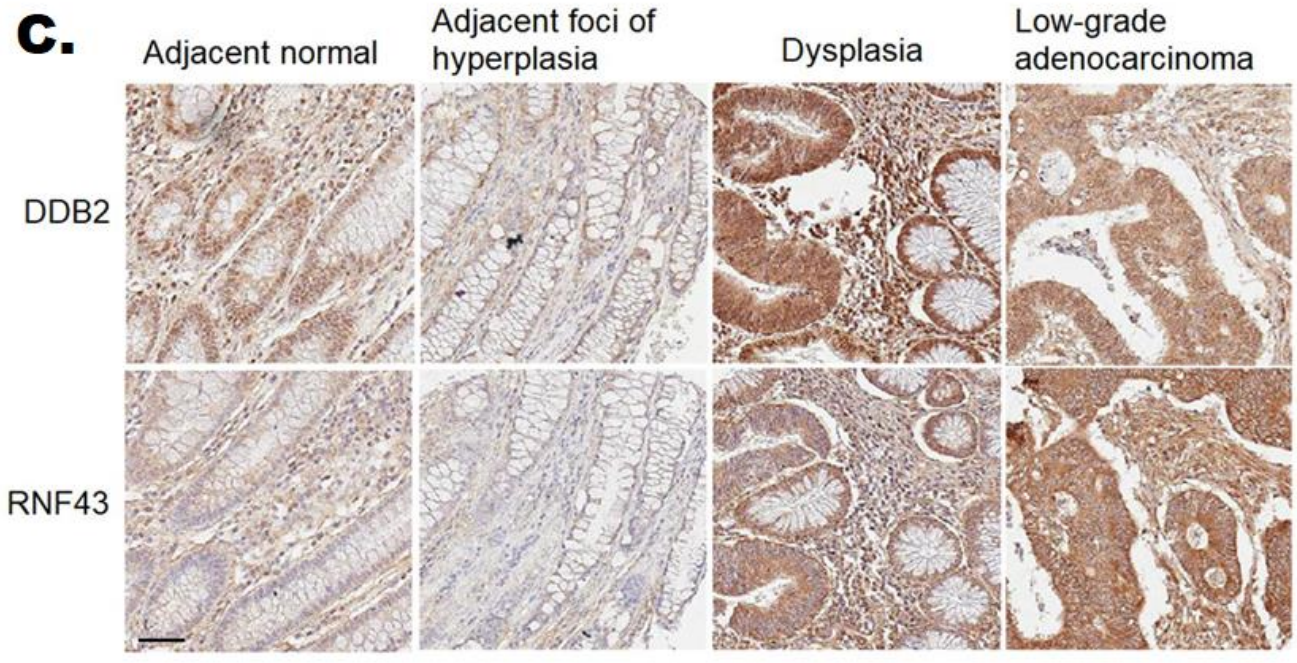
C.
Adjacent normal
Adjacent foci of hyperplasia
Dysplasia
Low-grade adenocarcinoma
DDB2
RNF43

Table 5. Correlation analysis of DDB2 and RNF43 expression in patient colonic samples

Patients	DDB2/RNF43			
	NO. of Pairs	Spearman r	p value	Significant
A	8	0.8095	0.0218	Yes
B	7	0.8929	0.0123	Yes
C	8	0.4192	0.3039	No
D	7	0.5364	0.223	No
E	8	0.7892	0.0237	Yes
F	8	0.7591	0.0347	Yes
G	8	0.81	0.0196	Yes
H	7	0.7928	0.0397	Yes
I	6	0.9856	0.0056	Yes
J	6	0.3714	0.4972	No
K	5	0.6	0.35	No
L	5	0.9	0.0833	No
M	6	0.5429	0.2972	No
N	6	0.9856	0.0056	Yes
O	6	0.6377	0.2	No
P	6	0.9429	0.0167	Yes
Q	6	0.8986	0.0278	Yes
R	6	0.9559	0.0111	Yes
S	6	0.6377	0.1944	No
T	6	0.9276	0.0222	Yes
U	6	0.971	0.0111	Yes
V	6	0.9429	0.0167	Yes
W	5	0.9747	0.0333	Yes
X	6	0.9856	0.0056	Yes
Total # of Significant Correlation				16 / 24

Figure 9: mRNA expression of RNF43 decreases from Grade 2 to Grade 3 in human patient colon adenocarcinoma samples.

Data of RNF 43 expression are obtained from Oncomine Bittner Colon Dataset. mRNA expression of RNF43 is plotted according to different grades of colon adenocarcinoma. Error bars indicate Min to Max, **** P< 0.0001.

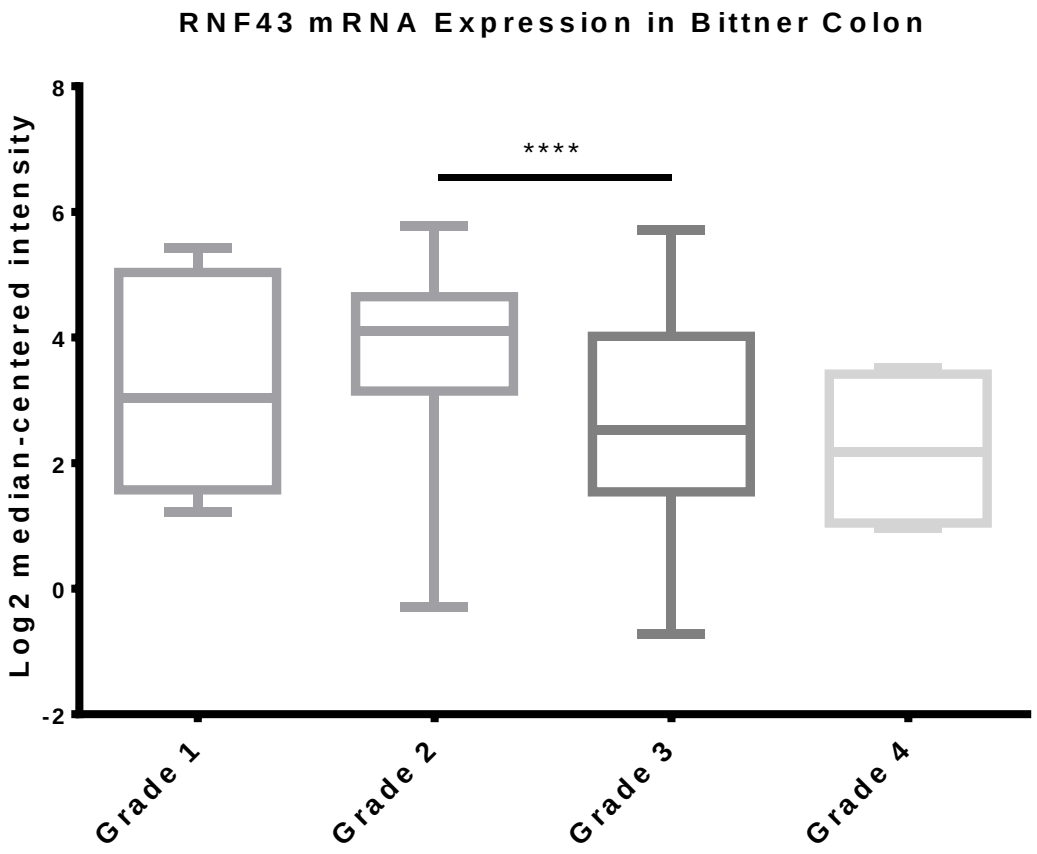
RNF43 mRNA Expression in Bittner Colon
Log2 median-centered intensity
8
6
4
2
0
-2
****
Grade 1
Grade 2
Grade 3
Grade 4

3.3 Association of DDB2 with the upstream regulatory region in *Rnf43* is critical for its activation by a GSK3-inhibitor

DDB2 associates with the promoter region of its target genes, including SOD2, NFKBIA and NEDD4L (Minig, Kattan et al. 2009, Ennen, Klotz et al. 2013, Zhao, Cui et al. 2015). To study whether DDB2 also associates with the *Rnf43* promoter, Chromatin immunoprecipitation (ChIP) assays were conducted in HCT116 cells. Nine pairs of primers were designed to cover 4,000 bps upstream of *Rnf43* transcription start site, and 500 bps in 5'UTR. The ChIP experiment results demonstrated interactions of DDB2 with two consecutive chromatin fragments, P2 and P3 (Figure 10A and B). Interaction with the P2 region was confirmed also in cells expressing T7-tagged DDB2. Chromatin-IP with T7-antibody specifically showed interaction in cells expressing T7-DDB2, but not in cells expressing LacZ (Figure 10C). DDB2-antibody, on the other hand, showed interactions in both LacZ and T7-DDB2 expressing cells.

Interestingly, a putative DDB2 binding element TCCCCTAA, which is one nucleotide different from the ones found in NFKBIA (Ennen, Klotz et al. 2013) or NEDD4L (Zhao, Cui et al. 2015), is located between the fragments P2 and P3. The available PAM motif in the region around that DDB2-cognate element and CRISPR/Cas9 genome editing technique allowed us to generate two HT-29 cell lines that harbor deletions of 132bp (between P2 and P3) and 416bp (partially overlapping with P2 and P3) (Figure 11A and B). Both deletions removed the putative DDB2 binding element (clone selection data are included in Figure 11C). Loss of DDB2 interactions was confirmed by ChIP experiments.

Figure 10: DDB2 binds to an upstream region in the *Rnf43* gene.

(A) The schematic representation of the human *Rnf43*upstream regulatory region. The thick truncated lines mark the regions covered by primer sets of interest. TSS: Transcription start site. (B) Chromatin-IP (ChIP) assays for binding of DDB2 with regulatory region upstream of the *Rnf43*gene. The ChIP assay was conducted to analyze the local enrichment of DDB2 across the upstream regulatory region and part of 5' UTR of *Rnf43*gene in HCT 116 cells. The relative fold enrichment was quantified by normalization to input. And the fold enrichment of IgG is set as 1 for all primer sets. N = 5, Error bars indicate SD. **: P <0.01. (C) ChIP assay was conducted to analyze the local enrichment of DDB2 and T7 tagged DDB2 at P2 region in HCT 116 cells expressing AdLacZ or AdDDB2-T7. The relative fold enrichment was quantified by normalization to input, and the fold enrichment of IgG is set as 1. N = 5, Error bars indicate SD.

A.

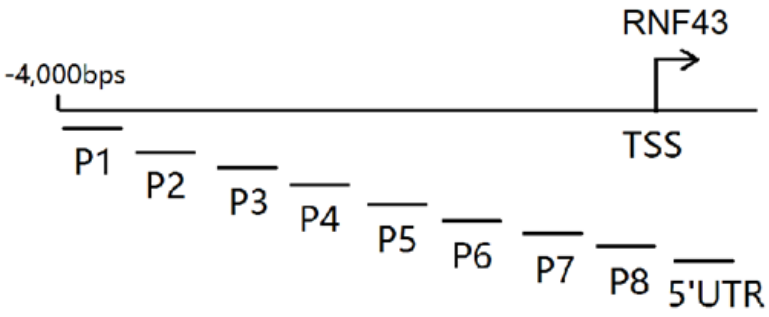
RNF43
-4,000bps
TSS
P1
P2
P3
P4
P5
P6
P7
P8
5'UTR

B.

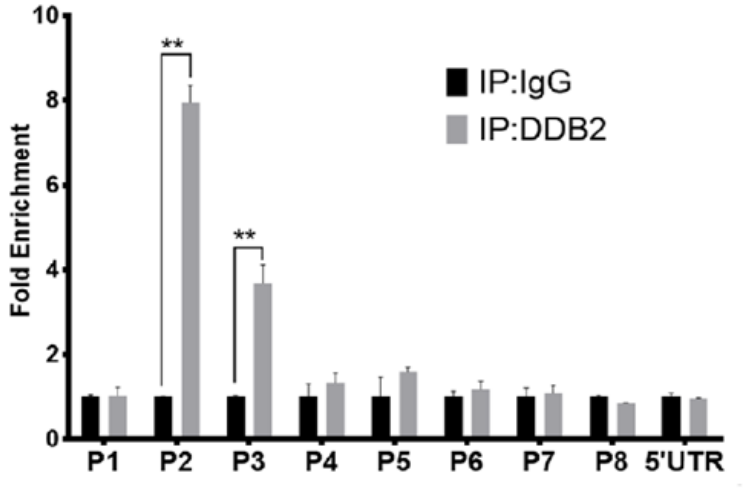
Fold Enrichment
10
8
6
4
2
0
**
**
IP:IgG
IP:DDB2
P1
P2
P3
P4
P5
P6
P7
P8
5'UTR

C.

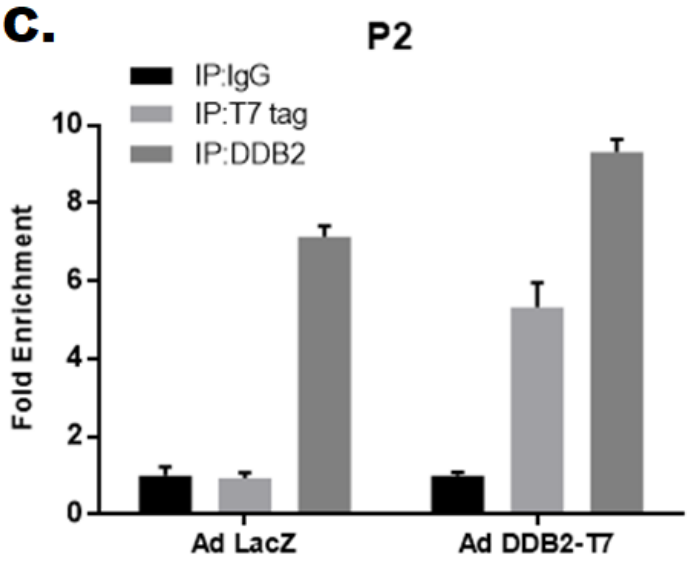
P2
IP:IgG
IP:T7 tag
IP:DDB2
Fold Enrichment
10
8
6
4
2
0
Ad LacZ
Ad DDB2-T7

Figure 11: Deletion of DDB2-binding region on *Rnf43* gene using CRISPR/Cas9 system.

(A and B) The schematic representation of the human *Rnf43*upstream regulatory region. The thick truncated lines mark the P2 and P3 regions. The white rectangle between P2 and P3 regions indicates the putative DDB2 binding element 'TCCCCTAA'. Dash lines indicate location of the sequences targeted by sgRNAs used in CRISPR/Cas9 genome editing. The orange arrowheads indicate the precise region where the Cas9 Nuclease cuts the genomic sequence. (C) PCR results showing one clone of short deletion cells (Short Del) and two clones of long deletion cells (Long Del #1 and #2) that were selected for the experiments. (D) Western blotting shows decreased expression of the RNF43 protein level in Short Del, Long Del #1 and Long Del #2 cells compared to the Parental HT-29 cells.

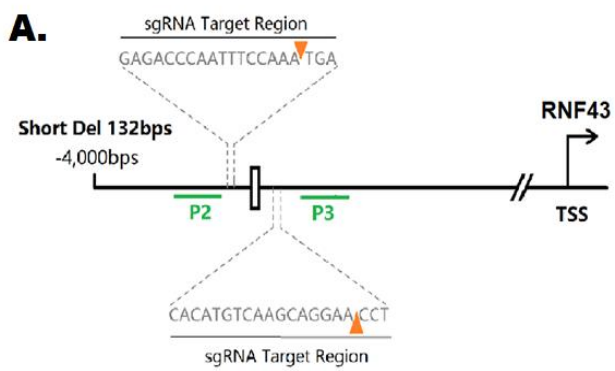
A.
sgRNA Target Region
GAGACCCAATTTCCAAATGA
Short Del 132bps
-4,000bps
RNF43
P2
P3
TSS
CACATGTCAAGCAGGAACCT
sgRNA Target Region

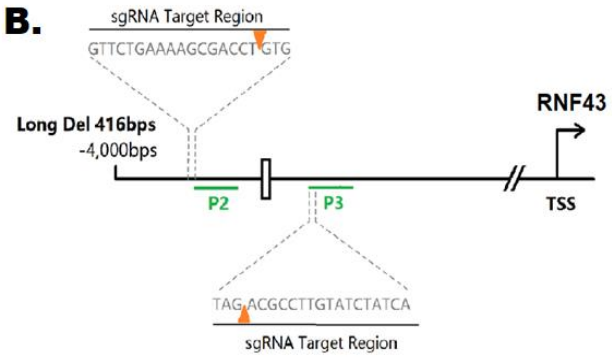
B.
sgRNA Target Region
GTTCTGAAAAGCGACCTGTG
Long Del 416bps
-4,000bps
RNF43
P2
P3
TSS
TAGACGCCTTGTATCTATCA
sgRNA Target Region

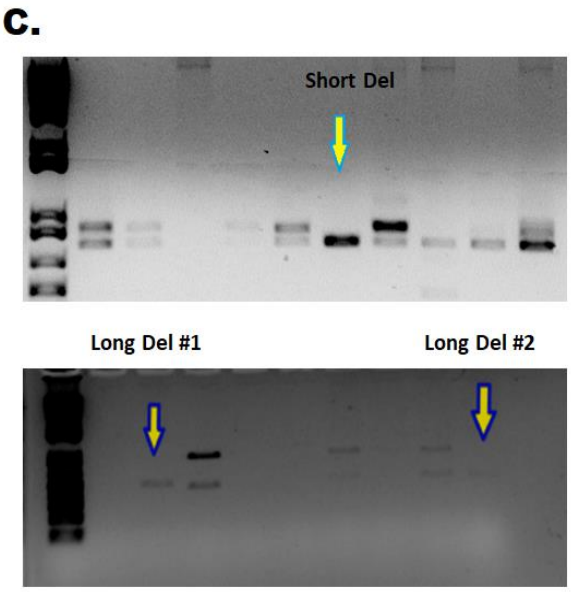
C.
Short Del
Long Del #1
Long Del #2

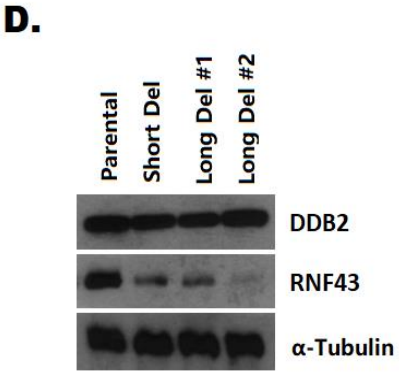
D.
Parental
Short Del
Long Del #1
Long Del #2
DDB2
RNF43
α-Tubulin

For example, ChIP experiment showed that DDB2 no longer associate with the P2 or P3 region in the 132bp-deleted HT-29 cells (Figure 12A and B). Next, we analyzed CHIR99021-induced expression of *Rnf43*-mRNA in undeleted and deleted (both 132bp and 416bp) HT-29 cells. As expected from our DDB2 knockdown experiments, deletion of the DDB2-interaction site resulted in a loss of basal expression of *Rnf43* in the HT-29 cells without impacting DDB2 expression (Figure 13A and B, and Figure 11D). More interestingly, CHIR99021 treatment, which activated expression of Axin2, failed to activate *Rnf43* expression in the deleted cells (Figure 13B and C). That was observed in both 132bp and 416bp deleted HT-29 cells. These results indicate that DDB2 supports Wnt/β-catenin activation of the *Rnf43* promoter by directly binding to the upstream region between P2 and P3.

3.4 DDB2 recruits β-catenin onto the upstream regulatory region in *Rnf43* through an interaction with EZH2

The 132bp region between P2 and P3 upstream chromatin fragments in the *Rnf43* gene lacks any recognizable TCF-binding element. Moreover, a ChIP experiment failed to detect a TCF4 interaction in that upstream region (Figure 14). Interestingly, one study identified cis-regulatory elements bound by TCF4 in the introns of *Rnf43* (Takahashi, Yamaguchi et al. 2014). We could confirm the interactions of TCF4 in those intronic regions by ChIP (Figure 14). However, those intronic cis-regulatory elements are

Figure 12: Deletion of DDB2-binding motif abolishes DDB2 enrichment on *Rnf43* upstream regulatory region.

(A and B) ChIP assay was performed to analyze the local enrichment of DDB2 in HT-29 Parental cells (A) and Short Del cells (B). The relative fold enrichment was quantified by normalization to input. And the fold enrichment of IgG is set as 1 for all primer sets.

A.

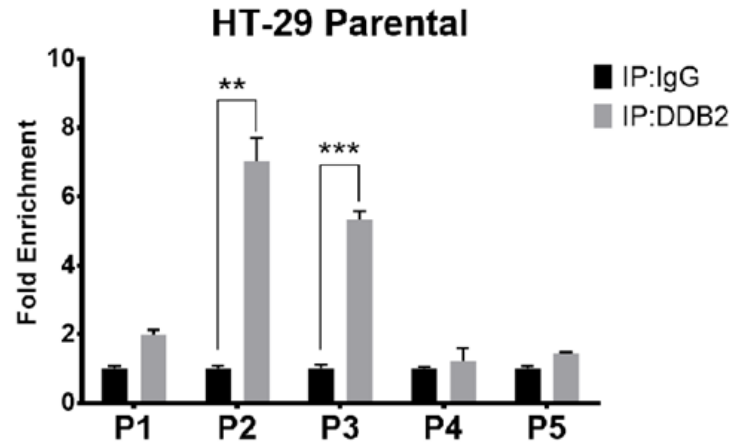
HT-29 Parental
Fold Enrichment
10
8
6
4
2
0
**
***
IP:IgG
IP:DDB2
P1
P2
P3
P4
P5

B.

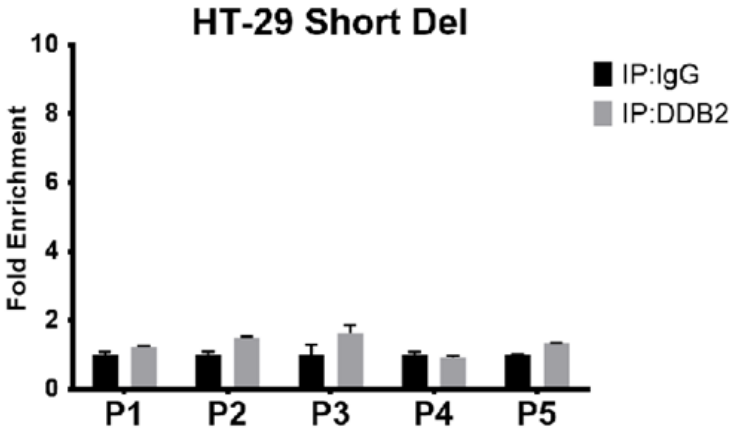
HT-29 Short Del
Fold Enrichment
10
8
6
4
2
0
IP:IgG
IP:DDB2
P1
P2
P3
P4
P5

Figure 13: Deletion of DDB2-binding motif inhibits *Rnf43* expression.

(A-C) Parental HT-29 cells, Short Del HT-29 cells and two clones of Long Del HT-29 cells were treated with DMSO or CHIR99021 (6.7 μM, 24 hrs). The mRNA levels of DDB2 (A), *Rnf43* (B) and Axin2 (C) were analyzed using qRT-PCR (Normalized by 18S rRNA). N = 3, Error bars indicate SD. **: P <0.01. ***: P <0.001

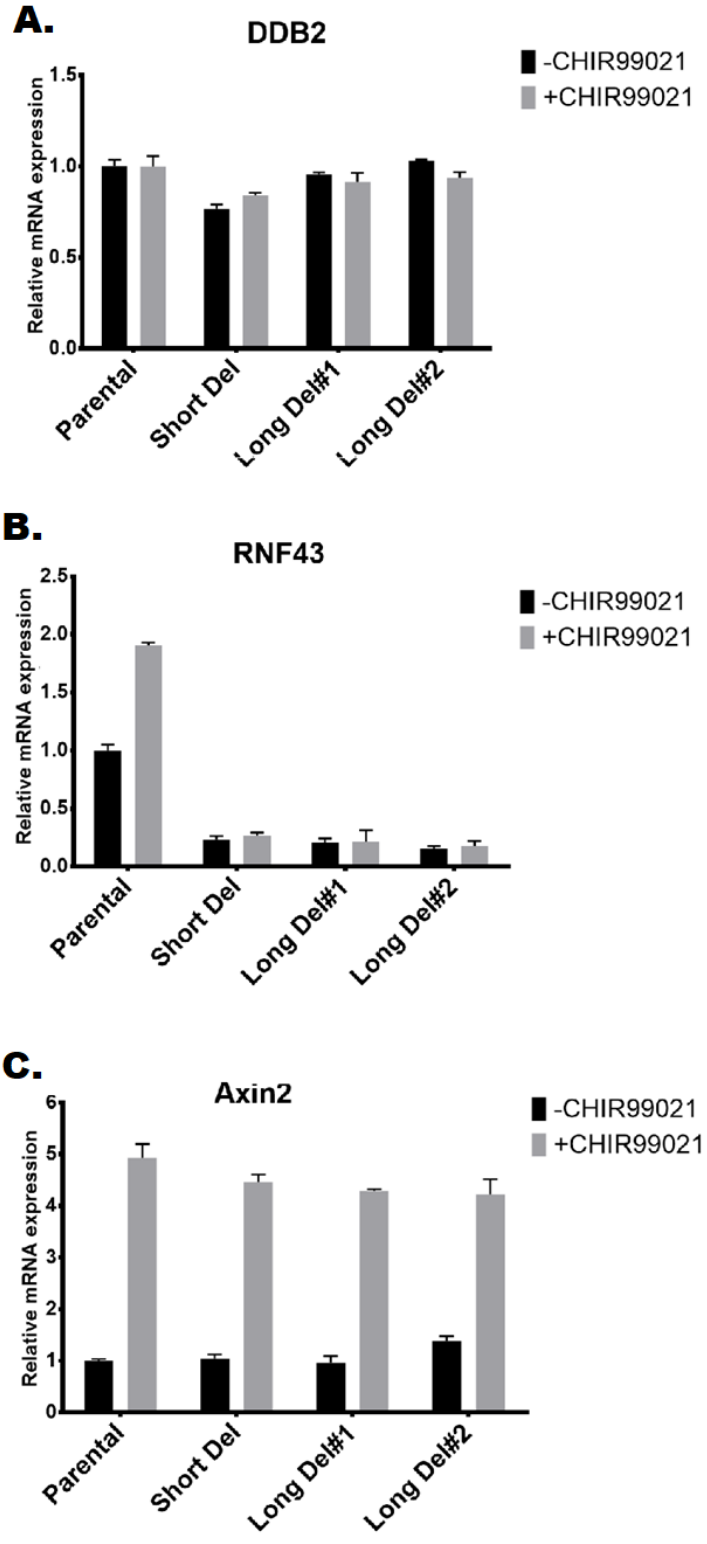
A.
DDB2
-CHIR99021
+CHIR99021
Relative mRNA expression
1.5
1.0
0.5
0.0
Parental
Short Del
Long Del#1
Long Del#2
B.
RNF43
-CHIR99021
+CHIR99021
Relative mRNA expression
2.5
2.0
1.5
1.0
0.5
0.0
Parental
Short Del
Long Del#1
Long Del#2
C.
Axin2
-CHIR99021
+CHIR99021
Relative mRNA expression
6
5
4
3
2
1
0
Parental
Short Del
Long Del#1
Long Del#2

Figure 14: Association of DDB2, TCF4 and β-catenin on *Rnf43* upstream region and intron regions.

The ChIP assay was conducted to analyze the local enrichment of DDB2, TCF4 and β-catenin at P1, P2, P3 regions, as well as Intron2-A and Intron2-B regions of *Rnf43* gene in HCT 116 cells. The relative fold enrichment was quantified by normalization to input. And the fold enrichment of IgG is set as 1 for all primer sets. N=3. All error bars indicate SD.

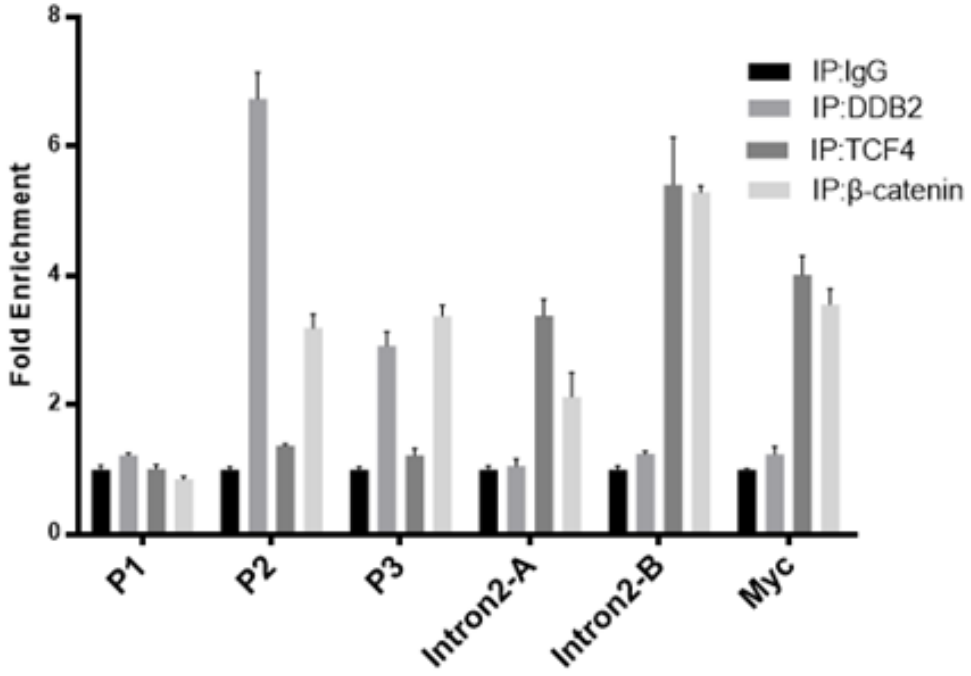
Fold Enrichment
8
6
4
2
0
IP:IgG
IP:DDB2
IP:TCF4
IP:β-catenin
P1
P2
P3
Intron2-A
Intron2-B
Myc

insufficient to activate *Rnf43*, because the DDB2-depleted cells or cells lacking the 132bp upstream sequence failed to respond to GSK3–inhibitor or DCA. Therefore, we investigated the role of DDB2 in the mechanism by which *Rnf43* responds to the GSK3–inhibitor CHIR99021, which functions by increasing nuclear β-catenin. We observed that DDB2 could associate with β-catenin. Immunoprecipitation of nuclear extracts from HCT116 cells that express Flag and HA tagged DDB2 with Flag-antibody resulted in co-precipitation of β-catenin (Figure 15A).

Next, we sought to determine whether β-catenin is recruited to the upstream region of *Rnf43* by DDB2. A ChIP assay was performed in HCT 116 cells expressing control-shRNA or DDB2-shRNA. Clearly, there were enrichments of the P2 and P3 regions in the chromatin-IPs with antibodies against DDB2 and β-catenin when control-shRNA cells were used (Figure 16A). However, in DDB2-shRNA cells, the bindings of both DDB2 and β-catenin were decreased in P2 and P3 regions (Figure 16B), indicating that DDB2 recruits β-catenin onto the P2/P3 regions in the *Rnf43* gene. A set of primers that amplifies the β-catenin binding region in the Axin2 promoter was used as a positive control, showing no effect of DDB2-depletion on β-catenin recruitment to the Axin2 promoter (Figure 16A and B). Furthermore, a ChIP assay was performed in HT-29 parental cells and HT-29 cells harboring deletion in the upstream DDB2-binding region with β-catenin antibody. Consistent with the DDB2/β-catenin interaction, enrichments of the P2 and P3 regions with β-catenin antibody were observed in the parental HT-29 cells, but not in the DDB2-binding site deleted cells (Figure 17A and B). Together, these

Figure 15: DDB2 interacts with β-catenin and EZH2 in nucleus.

(A) Nuclear extracts of HCT 116 cells expressing empty vector or Flag-HA-DDB2 were immunoprecipitated by ANTI-FLAG M2 affinity gel and analyzed by Western Blotting using DDB2 and total β-catenin antibodies. IP: Immunoprecipitation; IB: Immunoblotting. (B) Nuclear extracts of HCT 116 cells expressing empty vector or Flag-HA-DDB2 were immunoprecipitated by ANTI-FLAG M2 affinity gel and analyzed by Western Blotting using EZH2, EED and SUZ12 antibodies. IP: Immunoprecipitation; IB: Immunoblotting.

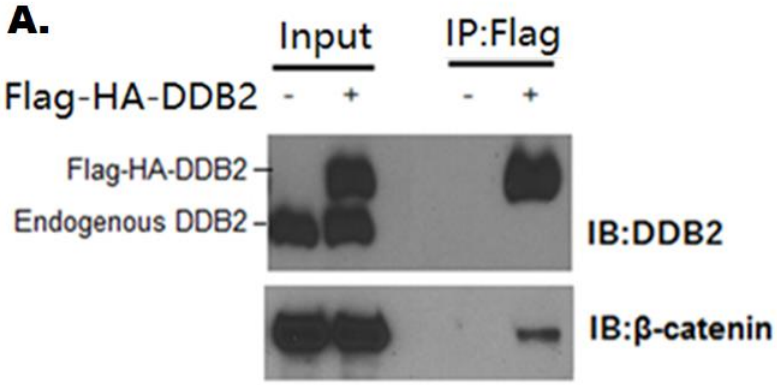
A.
Input
IP:Flag
Flag-HA-DDB2
- + - +
Flag-HA-DDB2
Endogenous DDB2
IB:DDB2
IB:β-catenin

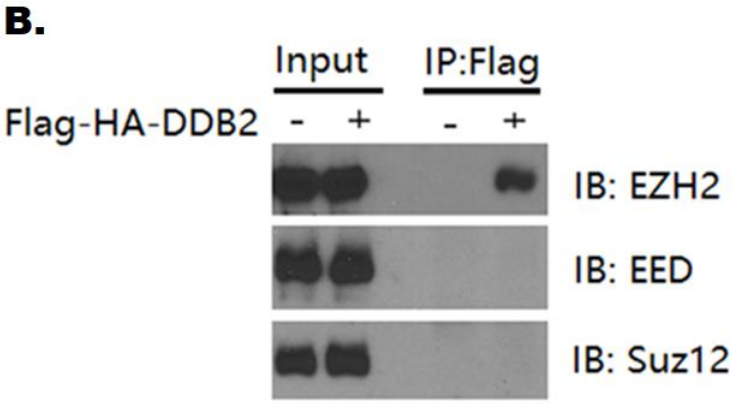
B.
Input
IP:Flag
Flag-HA-DDB2
- + - +
IB: EZH2
IB: EED
IB: Suz12

Figure 16: DDB2 recruits β-catenin onto *Rnf43* upstream regulatory region.

(A and B) ChIP assay was performed to analyze the local enrichment of DDB2 and β-catenin across the upstream regulatory region and part of 5' UTR of *Rnf43*gene in HCT 116 cells expressing either shControl (A) or shDDB2 (B). The relative fold enrichment was quantified by normalization to input. And the fold enrichment of IgG is set as 1 for all primer sets. A primer set which amplifies the TCF/ β-catenin binding site on Axin2 intron1 (Cell Signaling) is used as positive control for β-catenin immunoprecipitation.

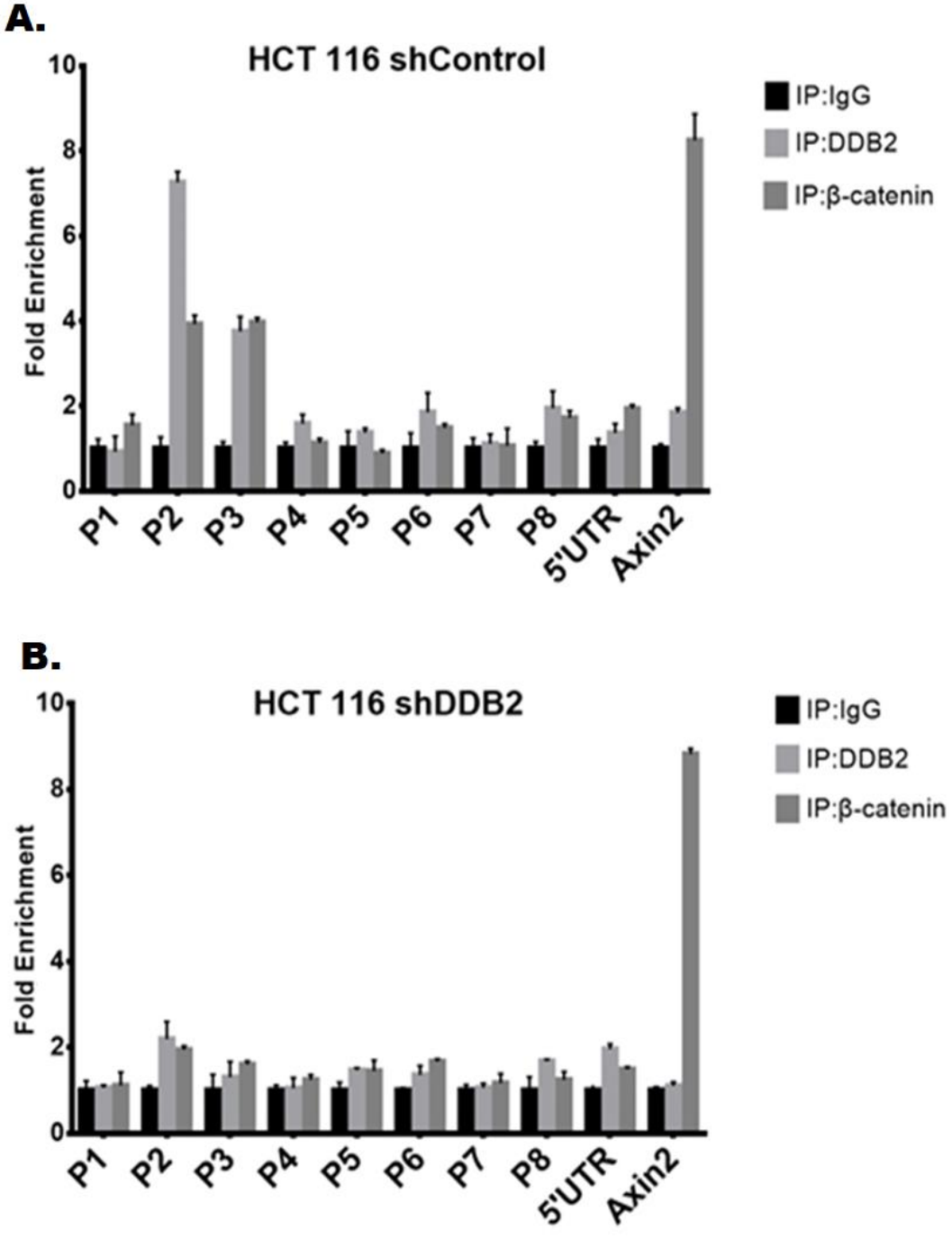
A.
HCT 116 shControl
Fold Enrichment
0
2
4
6
8
10
P1
P2
P3
P4
P5
P6
P7
P8
5'UTR
Axin2
IP:IgG
IP:DDB2
IP:β-catenin
B.
HCT 116 shDDB2
Fold Enrichment
0
2
4
6
8
10
P1
P2
P3
P4
P5
P6
P7
P8
5'UTR
Axin2
IP:IgG
IP:DDB2
IP:β-catenin

Figure 17: The recruitment of β-catenin onto *Rnf43* upstream regulatory region requires DDB2-binding motif.

(A and B) ChIP assay was performed to analyze the local enrichment of β-catenin from P1 to P5 regions of Rnf43gene in HT-29 Parental (A) and Short Del (B) cells. The relative fold enrichment was quantified by normalization to input. And the fold enrichment of IgG is set as 1 for all primer sets. A primer set which amplifies the TCF/ β-catenin binding site on c-Myc promoter is used as positive control. N = 3, Error bars indicate SD. **: P <0.01. ***: P <0.001

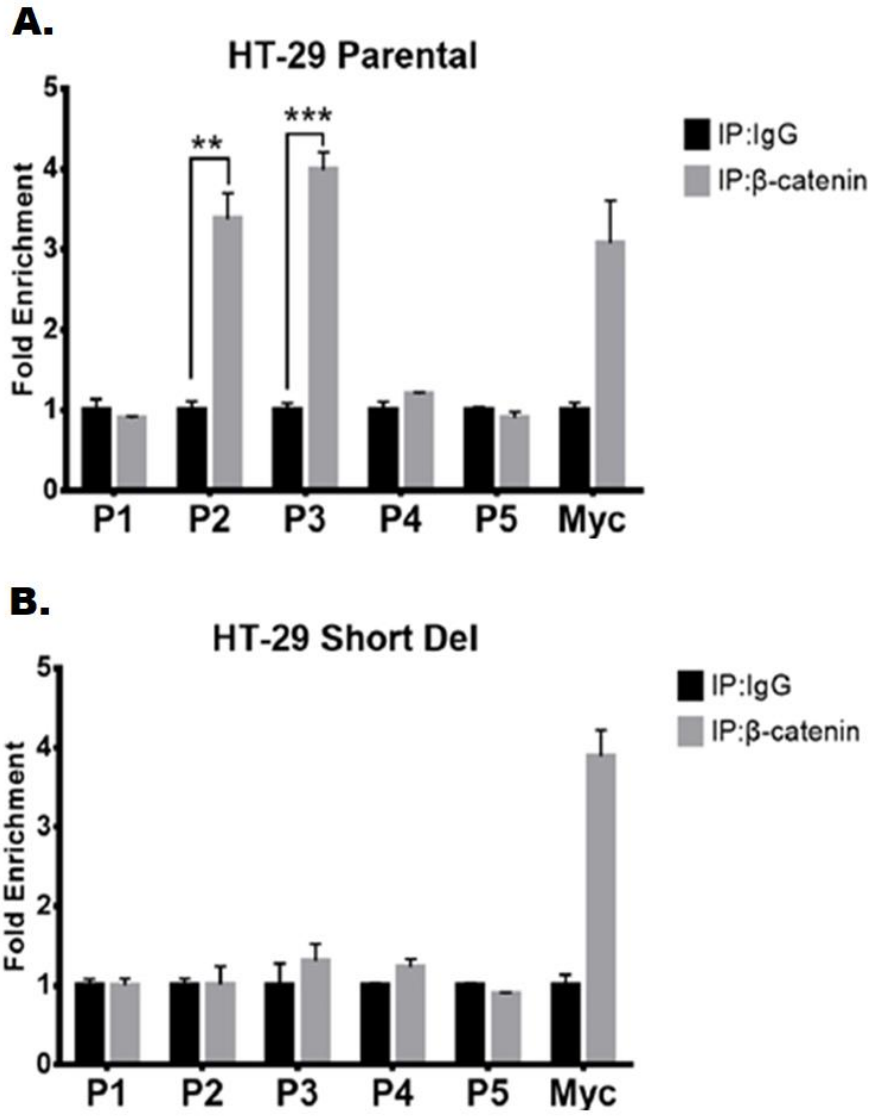
A.
HT-29 Parental
Fold Enrichment
0
1
2
3
4
5
**
***
P1
P2
P3
P4
P5
Myc
IP:IgG
IP:β-catenin
B.
HT-29 Short Del
Fold Enrichment
0
1
2
3
4
5
P1
P2
P3
P4
P5
Myc
IP:IgG
IP:β-catenin

results show that DDB2 recruits β-catenin onto the upstream P2/P3 regions in the *Rnf43* gene.

A previous study provided evidence for an interaction between β-catenin and EZH2, involving the PCNA-associated factor PAF (Jung, Jun et al. 2013). Moreover, a recent study demonstrated an interaction between DDB2 and EZH2 through the WD40 domain of DDB2 (Zhao, Cui et al. 2015). Intriguingly, a publicly available ChIP-seq dataset (UCSC Genome Browser) indicated interaction of EZH2 with the upstream sequences in the *Rnf43* gene around -2,900bp, which is the region between P2 and P3. Therefore, we tested whether EZH2 is a part of the DDB2 transcriptional complex. A co-immunoprecipitation experiment in HCT116 cells showed that DDB2 interacts with EZH2, but not with the other PRC2 components EED and Suz12 (Figure 15B). Next, we conducted ChIP assay to test whether EZH2 is recruited by DDB2 onto the upstream region of *Rnf43*. The P2 region was tested in HCT116 cells with control-shRNA and DDB2-shRNA. As the shown in Figure 18A, the enrichments of both DDB2 and EZH2 decrease significantly upon depletion of DDB2, indicating that EZH2 is recruited by DDB2. Next, we considered the possibility that the interaction of DDB2 with β-catenin might be mediated by EZH2. As shown in Figure 18B, indeed siRNA mediated knockdown of EZH2 resulted in a reduction of co-immunoprecipitation of β-catenin with DDB2. Moreover, depletion of EZH2 also resulted in a reduction of recruitment of β-catenin in the upstream regulatory region of *Rnf43*, between P2 and P3 (Figure 19A-C), and inhibition of *Rnf43* expression (Figure 20A-C). Together, these observations show that DDB2 recruits β-catenin onto the Rnf43regulatory region requiring EZH2.

Figure 18: EZH2 associates with *Rnf43* upstream regulatory region and mediates DDB2/β-catenin interaction.

(A) ChIP assay was conducted to analyze the local enrichment of DDB2 and EZH2 at P2 region in HCT 116 cells expressing shControl or shDDB2. The relative fold enrichment was quantified by normalization to input, and the fold enrichment of IgG is set as 1. N = 3, Error bars indicate SD. ***: P <0.001. (B) Nuclear extracts of HCT 116 cells transfected with siRNA-Control or siRNA-EZH2 were immunoprecipitated by normal Rabbit IgG or DDB2 antibodies. The results were analyzed by Western Blotting using DDB2, EZH2 and β-catenin antibodies. IP: Immunoprecipitation; IB: Immunoblotting.

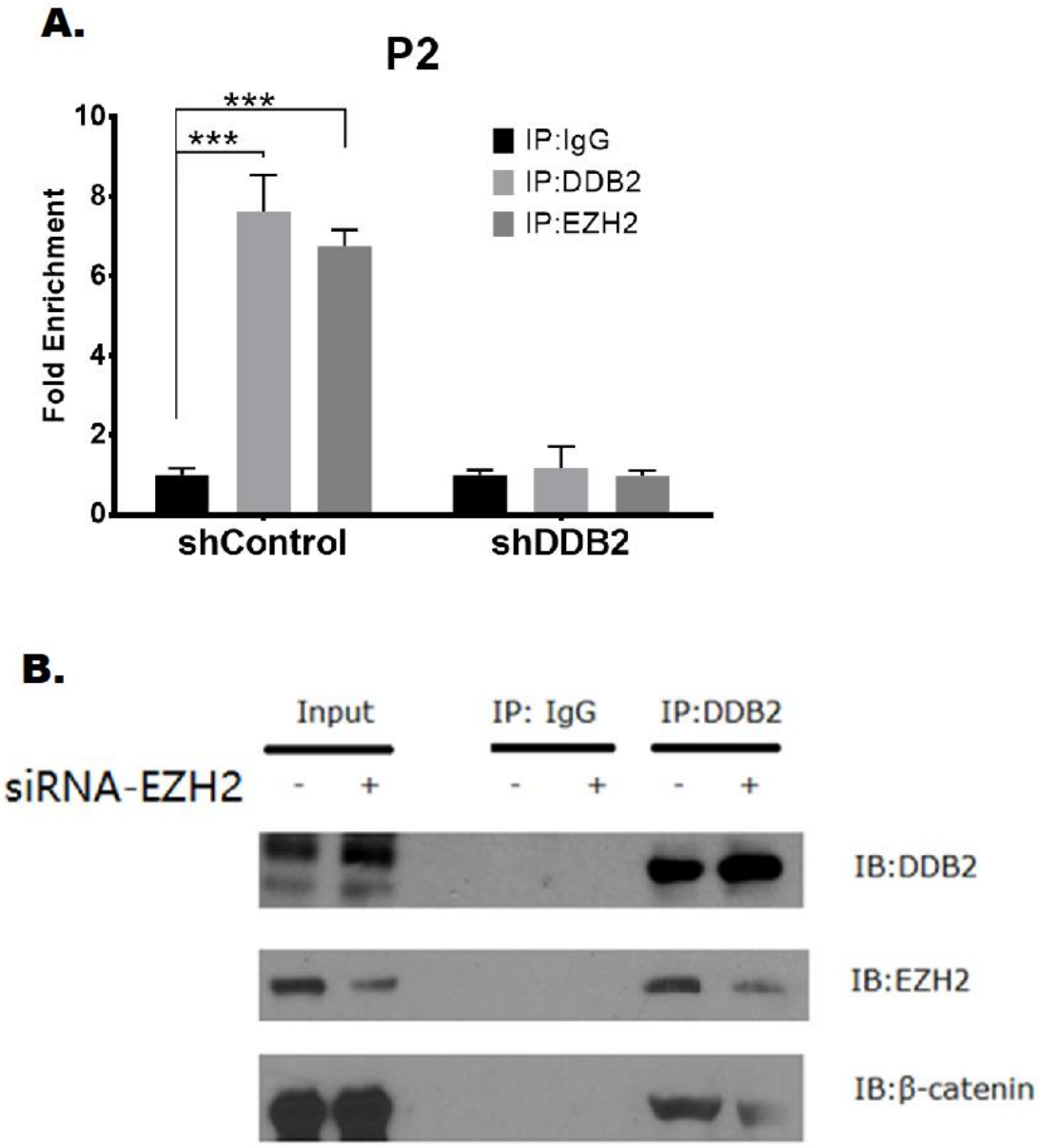
A.
P2
***
***
10
8
6
4
2
0
Fold Enrichment
IP:IgG
IP:DDB2
IP:EZH2
shControl
shDDB2
B.
Input
IP: IgG
IP:DDB2
siRNA-EZH2
- + - + - +
IB:DDB2
IB:EZH2
IB:β-catenin

Figure 19: EZH2 mediates DDB2/β-catenin interaction on *Rnf43* upstream regulatory region.

(A-C) EZH2 mediates DDB2- β-catenin interaction on P2 and P3 regions. The ChIP assays were conducted to analyze the enrichment of DDB2, EZH2 and β-catenin at P1(A), P2(B) and P3(C) regions in HCT 116 cells transfected with siRNA-Control or siRNA-EZH2. The relative fold enrichment was quantified by normalization to input, and the fold enrichment of IgG is set as 1. N = 3, Error bars indicate SD. *: P <0.05,**: P <0.01,***: P <0.001

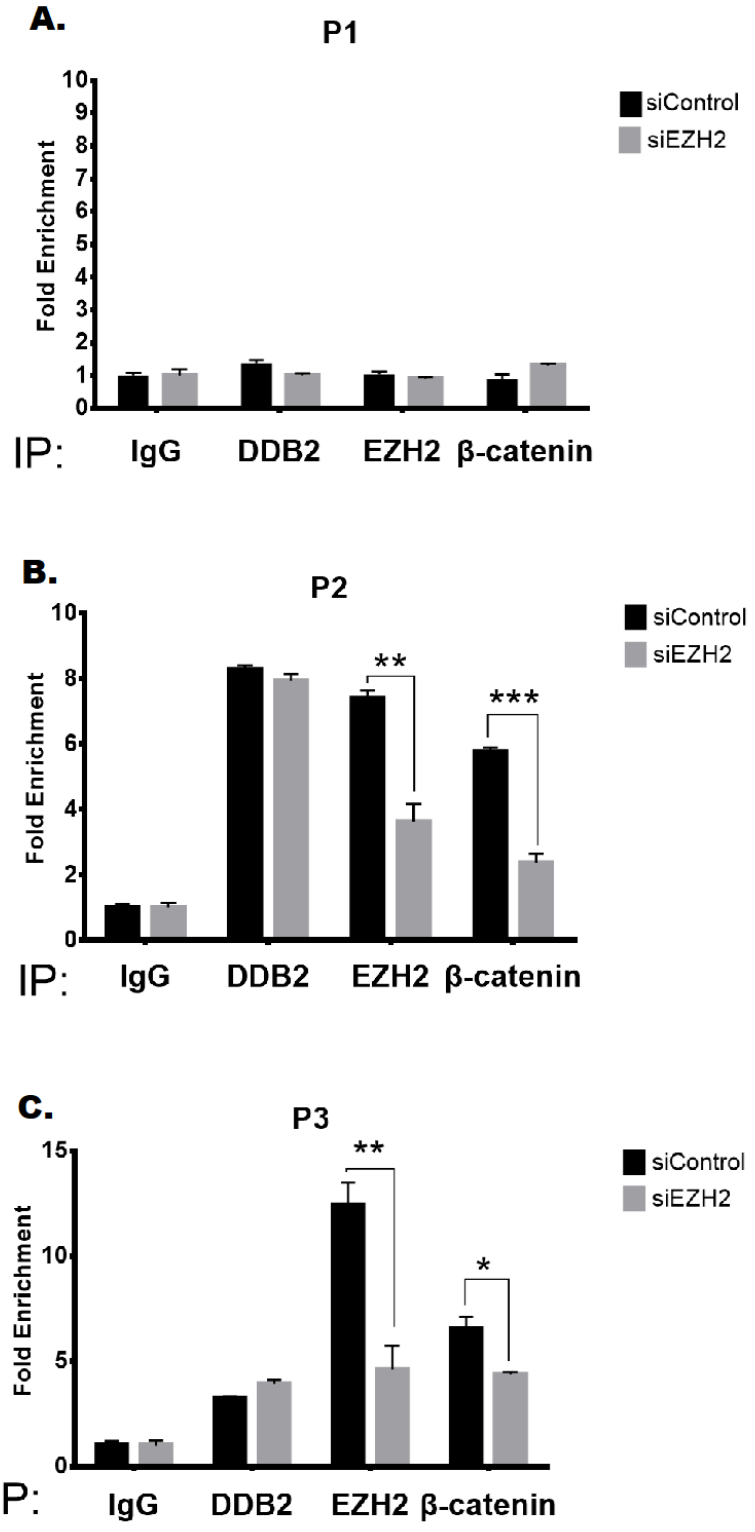
A.
P1
Fold Enrichment
siControl
siEZH2
IP:
IgG
DDB2
EZH2
β-catenin
B.
P2
**
***
C.
P3
*

Figure 20: EZH2 and PAF are required for *Rnf43* expression.

HCT 116 cells were transfected with siRNAs (siControl, siEZH2 or siPAF). mRNA level of EZH2 (A), PAF (B) and *Rnf43* (C) were measured and analyzed using qRT-PCR (Normalized by gapdh). N=3. All error bars indicate SD.

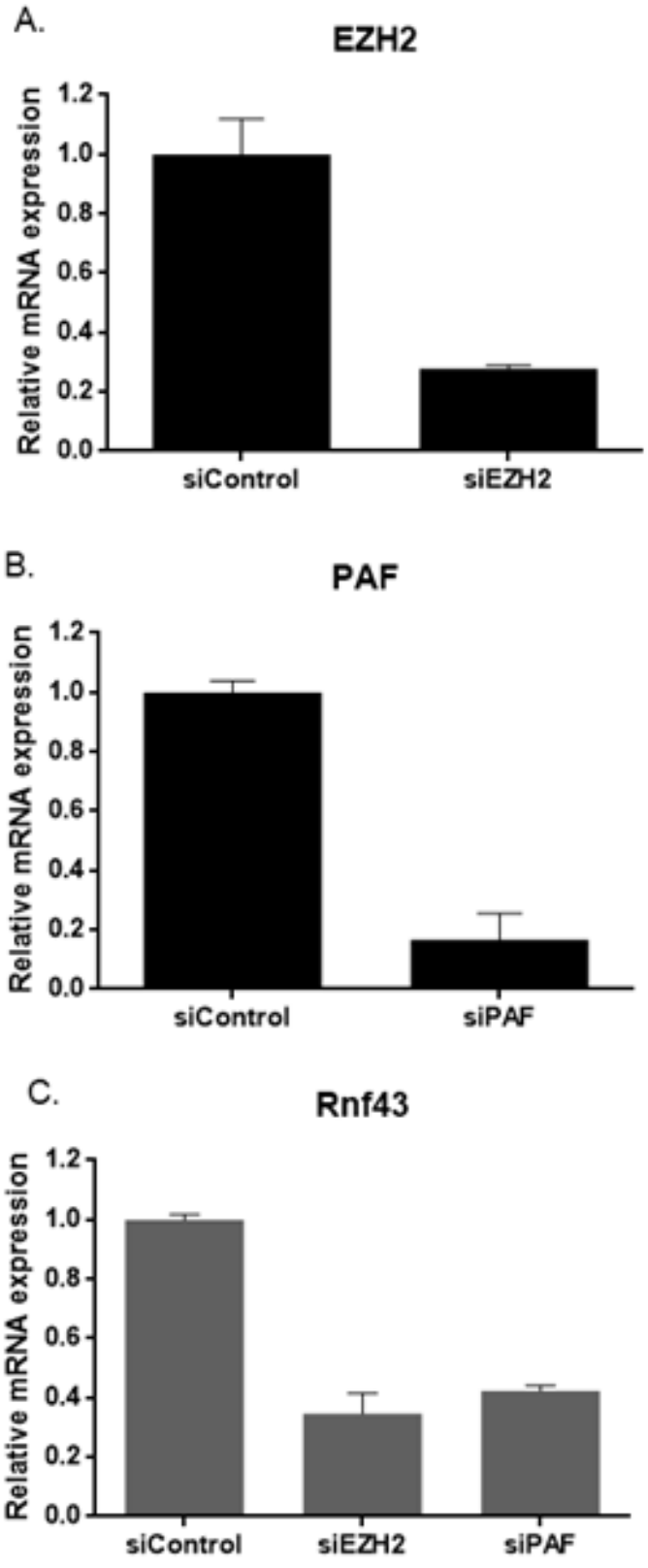
A.
EZH2
Relative mRNA expression
1.2
1.0
0.8
0.6
0.4
0.2
0.0
siControl
siEZH2
B.
PAF
Relative mRNA expression
1.2
1.0
0.8
0.6
0.4
0.2
0.0
siControl
siPAF
C.
Rnf43
Relative mRNA expression
1.2
1.0
0.8
0.6
0.4
0.2
0.0
siControl
siEZH2
siPAF

3.5 Evidence for interaction between the DDB2-binding and TCF4-binding chromatins in the *Rnf43* gene

Previous studies identified two TCF4/β-catenin binding sites within intron 2 of human *Rnf43* gene (Takahashi, Yamaguchi et al. 2014). As pointed out above, we confirmed binding of TCF4 and β-catenin at those two sites (Figure 14). We sought to investigate whether TCF4 is important for GSK3-inhibitor induced expression of *Rnf43*. A dominant-repressive form of TCF4 (dn-TCF4) was expressed in HCT116 cells.

Expression of dnTCF4 inhibited expression of *Rnf43* (Figure 21A), supporting the notion that TCF4 is required for expression of *Rnf43*. Also, we conducted ChIP assays in the presence or absence of dnTCF4 expression. As shown in Figure 21B, expression of dnTCF4 had very little impact on bindings of β-catenin and EZH2 onto the upstream P2/P3 region. The bindings of β-catenin as well as EZH2 in the intron2, on the other hand, were significantly inhibited by dnTCF4. Inhibition of *Rnf43* expression and inhibition of β-catenin binding by dn-TCF4 imply that the TCF4-sites in the introns are important for expression. Since the DDB2-binding is critical for expression of *Rnf43*, we considered the possibility of a functional interaction between the DDB2-binding chromatin and the TCF4-binding chromatin at intron 2 of the *Rnf43* gene. We carried out chromosome conformation capture (3C) assays to investigate an interaction between the two regions in *Rnf43* chromatin in the presence and absence of DDB2, following a strategy described before (Dekker, Marti-Renom et al. 2013). Briefly, HCT116 cells expressing Control-shRNA or DDB2-shRNA were crosslinked by formaldehyde to link the chromatin

segments that are in close spatial proximity. Chromatins were then digested with BglII, followed by ligation with DNA ligase. These steps link distal DNA sequences that are brought together because of chromatin interactions for analyses by PCR. The interactions were analyzed using 4 sets of PCR primers as depicted schematically in Figure 22A. In those experiments, we observed clear evidence for interactions with primer sets 1 and 2 (Figure 22B). Moreover, the interaction with the primer set 2 was dependent upon the presence of DDB2. These results demonstrate a DDB2-dependent interaction between the upstream chromatin region near DDB2-binding site and the intron region in *Rnf43* gene. To further investigate the involvement of the TCF-sites in the introns for the interaction, we carried out the 3C experiments with cells expressing dominant negative TCF4 (dnTCF4). Expression of dnTCF4 caused a significant reduction in the interaction observed with the primer set 2 (Figure 98C). These results confirm involvement of TCF-factors, bound to the TCF-elements in the intron, in chromatin interaction with DDB2 bound to the upstream P2/P3 region in the *Rnf43* gene.

Figure 21: TCF4 is required for *Rnf43* expression and mediates β-catenin/EZH2 interaction with intron 2 region of *Rnf43* gene.

(A) The expression of dominant negative TCF4 decreased Rnf43expression. HCT 116 cells stably expressing empty vector or dominant-negative TCF4 (dn-TCF4) were treated with DMSO or CHIR99021 (3.3μM, 16hrs). Relative mRNA levels of Rnf43and Axin2 were analyzed by qRT-PCR. N = 3, Error bars indicate SD. (B) Expression of dominant negative TCF4 reduced EZH2 and β-catenin interaction with TCF4 binding regions. The ChIP assay was performed in HCT 116 cells stably expressing empty vector or dn-TCF4. The enrichment of DDB2, EZH2 and β-catenin was analyzed at P2, P3 as well as at the TCF4 binding sites in the intron regions of Rnf43gene. The relative fold enrichment was quantified by normalization to input, and the fold enrichment of IgG is set as 1. N = 5, Error bars indicate SD. *: $P < 0.05$, **: $P < 0.01$.

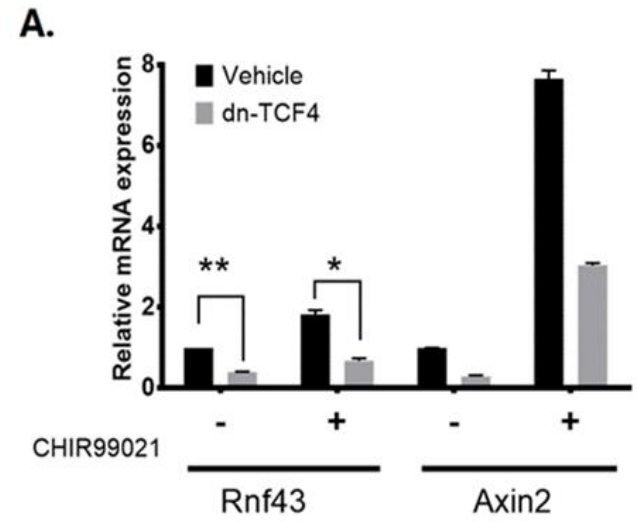
A.
Relative mRNA expression
Vehicle
dn-TCF4
**
*
CHIR99021
Rnf43
Axin2

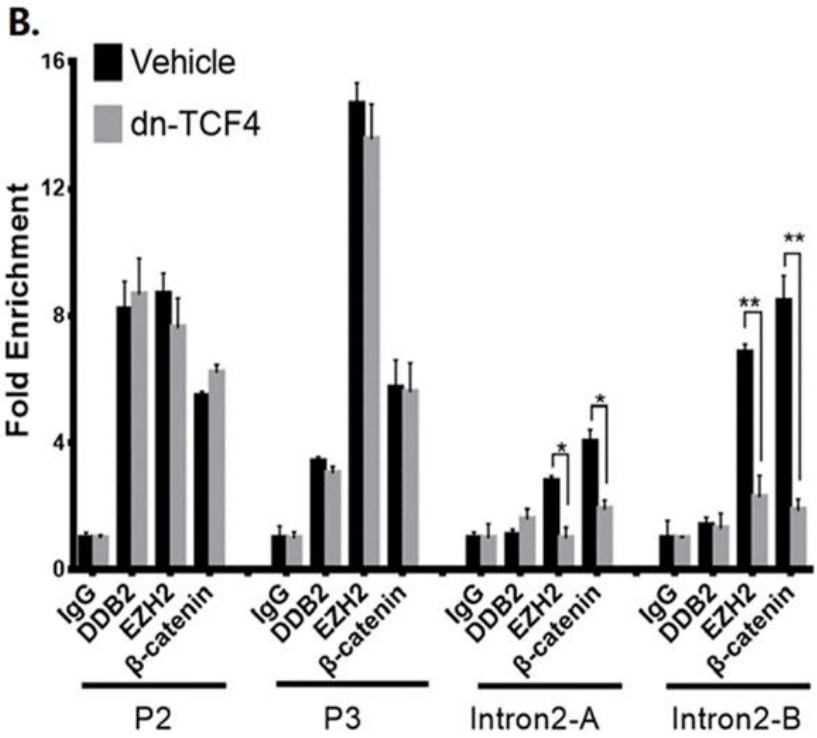
B.
Fold Enrichment
Vehicle
dn-TCF4
IgG
DDB2
EZH2
β-catenin
P2
P3
Intron2-A
Intron2-B

Figure 22: Chromatin looping structure between DDB2-binding and TCF4-binding regions in the *Rnf43* gene.

(A) A schematic diagram showing the location of primer and probe sets designed for the Chromatin Conformation Capture (3C) assay. The white rectangle indicates the putative DDB2 binding element at upstream regulatory region in the *Rnf43*gene. The black bars mark two binding sites of TCF4 in intron2 of the *Rnf43*gene. The black truncated lines across the *Rnf43*gene indicate the sites that are recognized by BglII restriction endonuclease. The arrows mark the primers for each of the primer sets. Four sets of primers are designed to detect physical interactions between restriction fragments. (B and C) Expression of DDB2-shRNA (B) or expression of a dominant negative mutant of TCF4 (C) decreases relative crosslinking frequency at Set2. The 3C assays were conducted in HCT 116 cells expressing shControl vs. shDDB2 (B); or control vector vs. dn-TCF expression vector (C). Four sets of primers and probes were analyzed using *Taqman* qPCR. A serial dilution of the control template was used for standard curve; and the relative crosslinking frequencies were normalized by *gapdh* loading control. N=4, Error bars indicate SD.

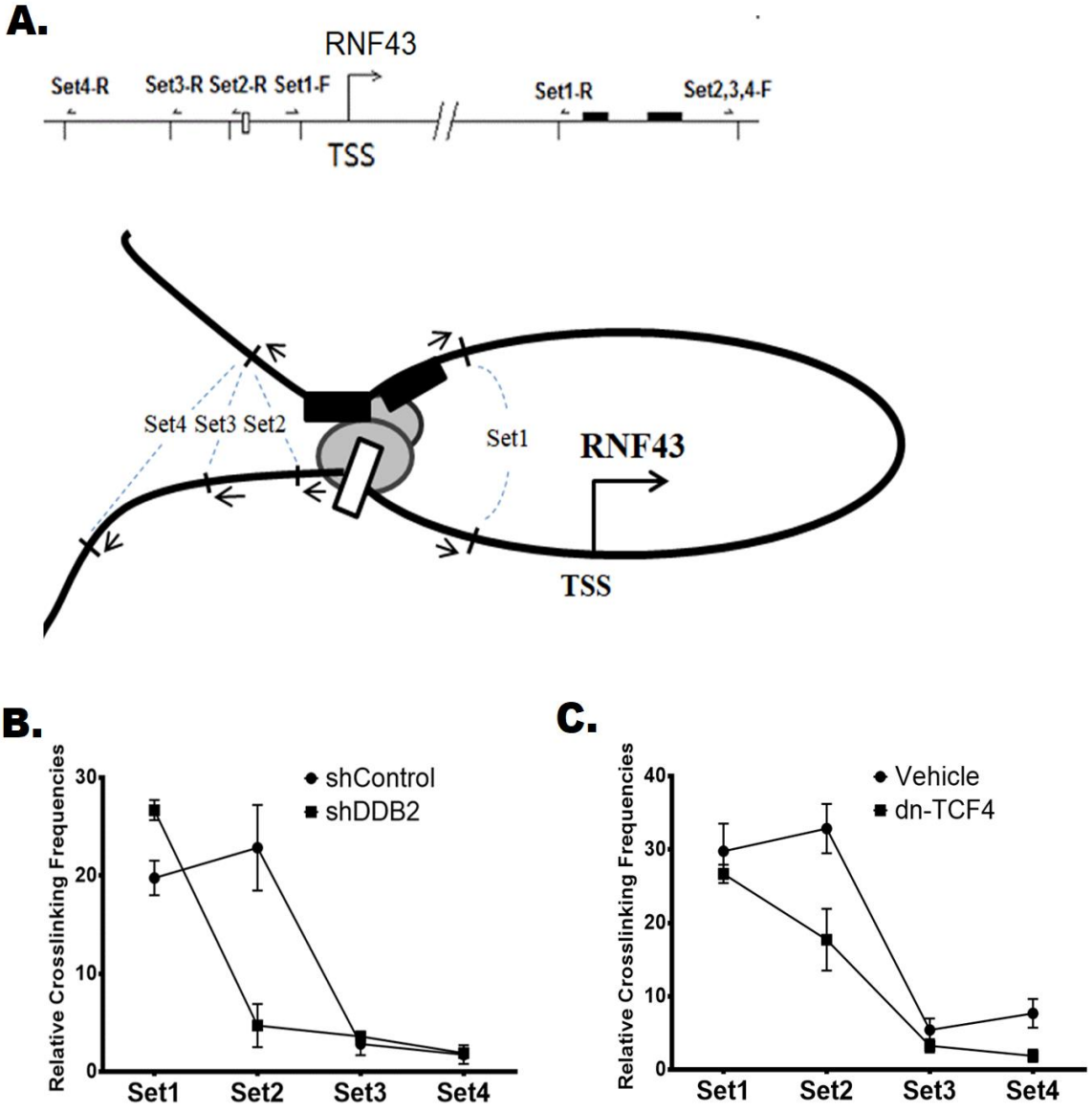
A.
RNF43
Set4-R
Set3-R
Set2-R
Set1-F
Set1-R
Set2,3,4-F
TSS
Set4
Set3
Set2
Set1
RNF43
TSS
B.
Relative Crosslinking Frequencies
shControl
shDDB2
Set1
Set2
Set3
Set4
C.
Relative Crosslinking Frequencies
Vehicle
dn-TCF4
Set1
Set2
Set3
Set4

3.6 DDB2 is required for RNF43-mediated ubiquitination of the Wnt-receptor FZD5

RNF43 is an E3 ubiquitin ligase for the Wnt receptor Frizzled and LRP5/6, and plays a negative regulatory role that attenuates Wnt-signaling(Koo, Spit et al. 2012). Since DDB2 is required for RNF43 expression, we investigated whether DDB2 deficiency leads to inhibition of Wnt-receptor ubiquitination. We analyzed ubiquitination of V5-tagged FZD5 (V5-FZD5) in HT-29 cells that co-express His-tagged Ub along with control-siRNA or DDB2-siRNA. His-tagged-ubiquitinated proteins were collected using Ni-agarose beads and the bound proteins were assayed for the presence of FZD5 using V5-ab. The HT-29 cells express RNF43 at high levels, and poly-ubiquitinated FZD5 can be detected easily. Interestingly, the DDB2-depleted cells exhibited a strong inhibition of the FZD5 poly-ubiquitination as well as an increased level of the mature form of V5-FZD5 (Figure 23A). Next, we compared the HT-29 cells with those harboring deletions in the *Rnf43* upstream region. Lack of DDB2 binding reduced protein expression of RNF43 in the deleted cells. Those cells also exhibited greatly reduced poly-ubiquitination of FZD5 compared to the parental HT-29 cells (Figure 23B). These results show that the interaction of DDB2 with the upstream region of *Rnf43* is critical for ubiquitination of the Wnt-receptors.

A recent study indicated that the RNF43 protein could sequester TCF4 in the nuclear periphery (Loregger, Grandl et al. 2015). We sought to investigate whether expression of DDB2 would induce perinuclear accumulation of TCF4. We expressed mVenus tagged DDB2 (green fluorescence) in SW620 cells and subjected the cells for immunostaining

Figure 23: DDB2 is required for RNF43-mediated FZD5 ubiquitination.

(A) DDB2 deficiency leads to inhibition of FZD5 ubiquitination. HT-29 cells were transfected with V5–FZD5, His-ubiquitin and siRNA-Control or siRNA-DDB2, as indicated. His-Ubiquitinated proteins were collected by nickel-nitrilotriacetic acid–agarose beads and the presence of ubiquitinated V5-FZD5 is detected by V5 antibody. (B) Lack of DDB2 bound region in *Rnf43*gene results in inhibition of FZD5 ubiquitination. HT-29 Parental, Short Del and Long Del cells were transfected with V5–FZD5 and His-ubiquitin. And the assay was performed as described above. IP, Immunopull-down; IB: Immunoblotting; Ub, ubiquitin. White triangles indicate mature, glycosylated V5-conjugated FZD5.

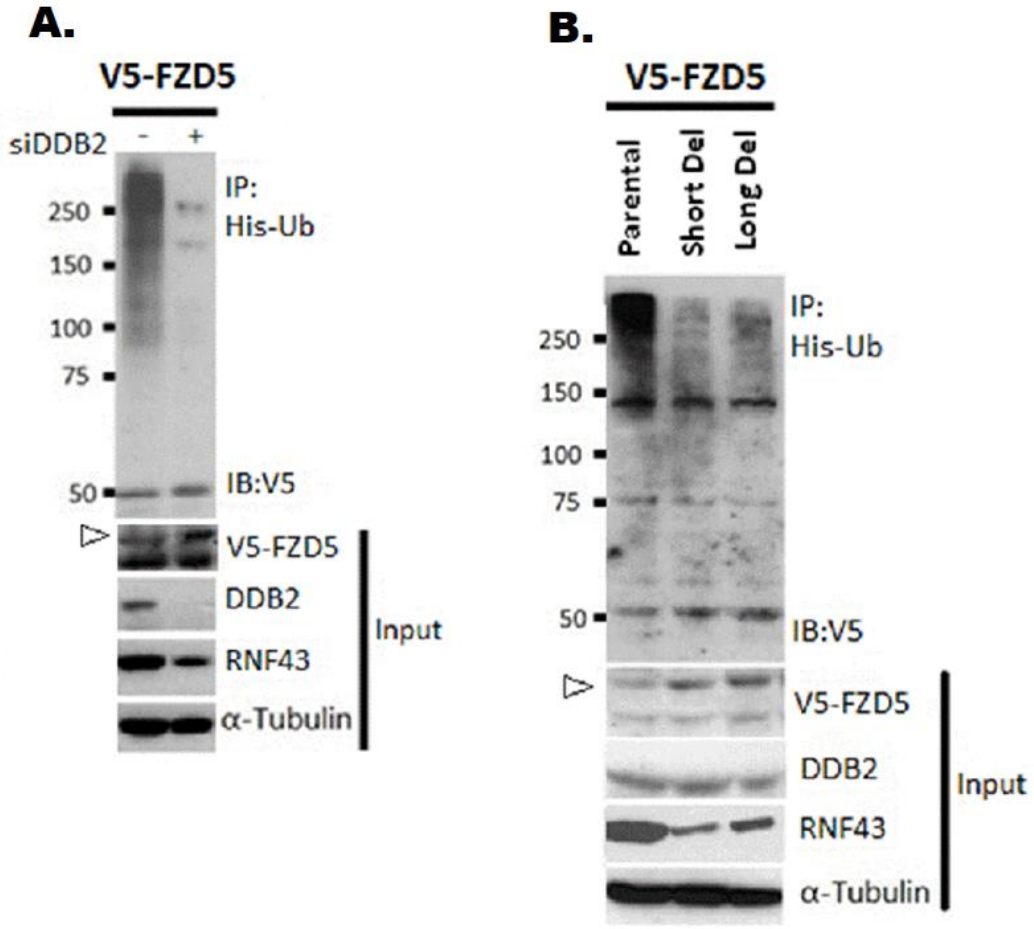
A.
V5-FZD5
siDDB2
-
+
250
150
100
75
50
IP:
His-Ub
IB:V5
V5-FZD5
DDB2
RNF43
α-Tubulin
Input
B.
V5-FZD5
Parental
Short Del
Long Del
250
150
100
75
50
IP:
His-Ub
IB:V5
V5-FZD5
DDB2
RNF43
α-Tubulin
Input

for TCF4 (red fluorescence). As shown in Figure 24, DDB2 expressing cells exhibited re-localization of TCF4. Moreover, when we compared HT-29 cells with HT-29 cells lacking the DDB2-site in the *Rnf43* promoter, there were cells in the parental line exhibiting perinuclear staining for TCF4, but that was absent in the DDB2-site deleted line (Figure 25).

Based on these, we predicted that cells lacking binding of DDB2 to the *Rnf43* regulatory region or cells with reduced expression of DDB2 would exhibit enhanced response to Wnt-ligands. To investigate that possibility, we compared HT-29 cells lacking DDB2-binding with the parental cells for response to exogenous Wnt3a. Following treatments with vehicle or Wnt3a, total RNA from the cells were assayed for expression of the Wnt response genes. In cells lacking DDB2-binding, Wnt3a had only a marginal effect on the expression of *Rnf43*. On the other hand, expression of Axin2 and c-Myc were greater in cells lacking DDB2-interaction when treated with Wnt3a (Figure 26). Similar observations were made in cells in which the level of DDB2 was diminished by siRNA expression. HT-29 cells expressing DDB2-siRNA exhibited a greater response to Wnt3a induced expression of the Wnt-target genes (Figure 27). These results confirm a role of DDB2 in the feed-back regulation of Wnt-signaling through RNF43.

Figure 24: DDB2 overexpression sequestered TCF4 to the nuclear membrane.

SW620 cells were transiently transfected with pCDNA4 or pCDNA4-DDB2-mVenus plasmids. Immunofluorescent staining was performed to determine localization of TCF4 (Scale bar= 10 μm).

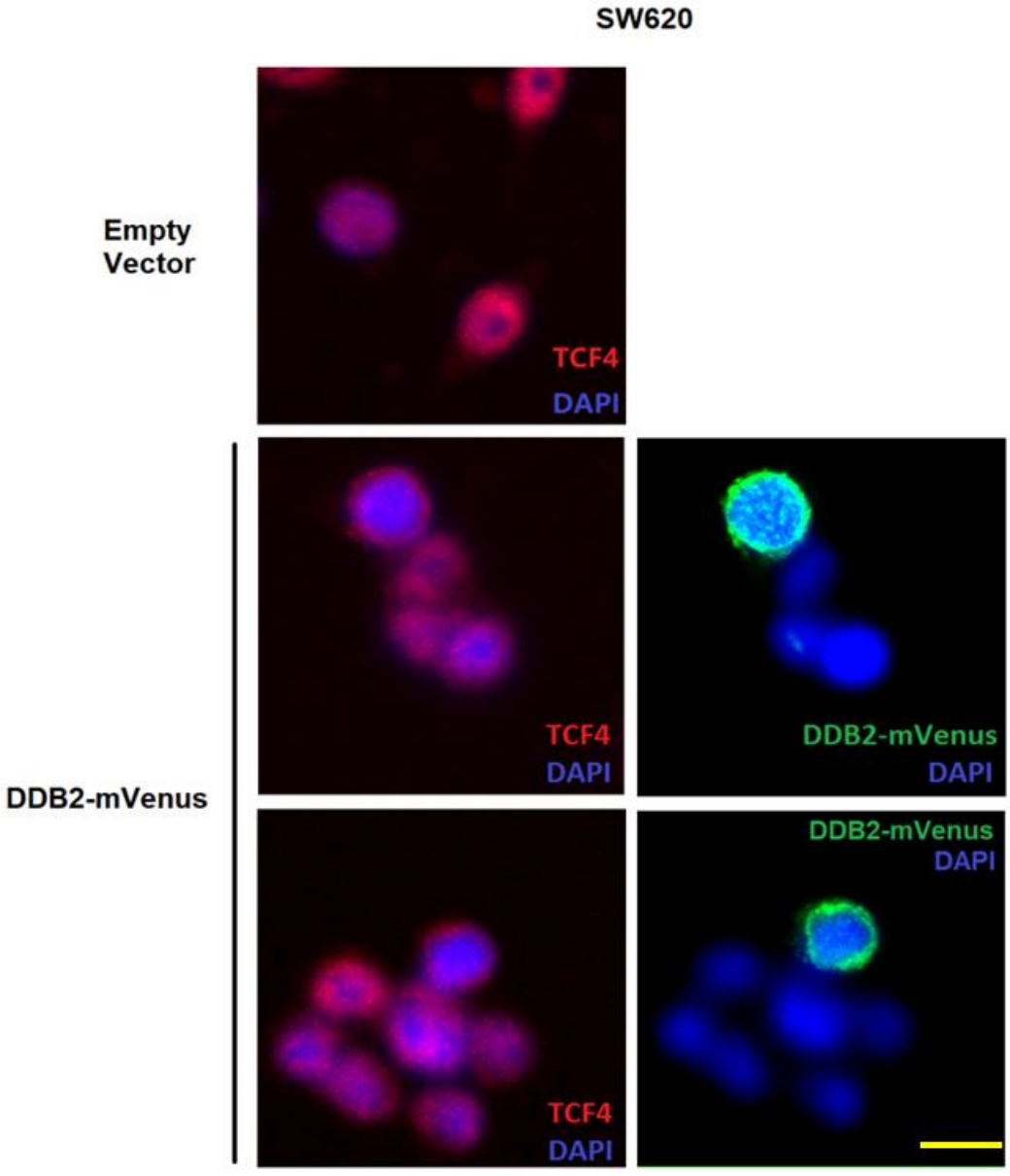
SW620
Empty Vector
TCF4
DAPI
DDB2-mVenus
TCF4
DAPI
DDB2-mVenus
DAPI
DDB2-mVenus
TCF4
DAPI
DDB2-mVenus
DAPI

Figure 25: DDB2 binding is required for the RNF43-mediated sequestration of TCF4 to the nuclear membrane.

HT-29 parental cells, Short del cells, Long del #1 and #2 cells were subjected to immunostaining for TCF4 followed by confocal microscopy (Scale bar= 10 μm).

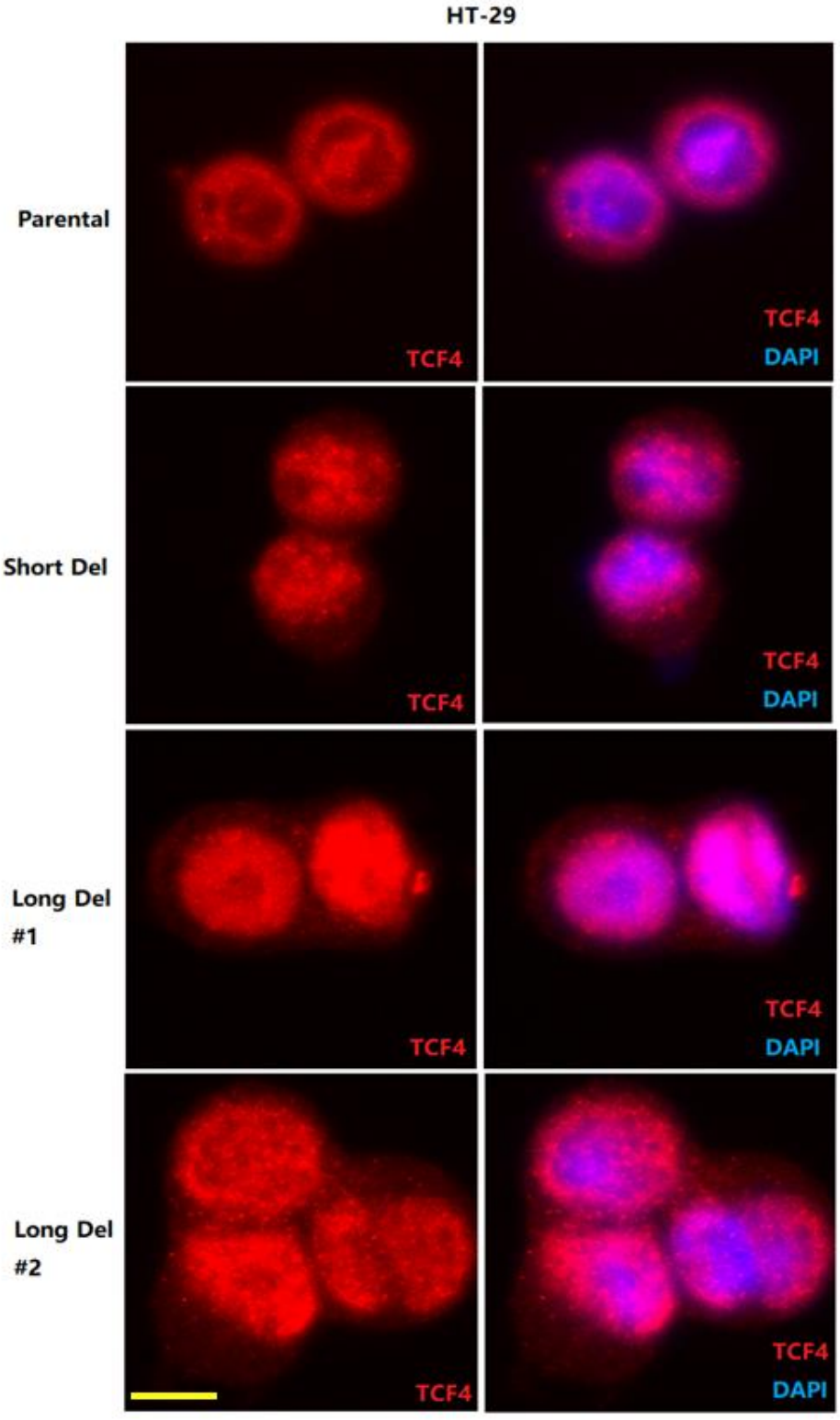
HT-29
Parental
TCF4
TCF4
DAPI
Short Del
TCF4
TCF4
DAPI
Long Del
#1
TCF4
TCF4
DAPI
Long Del
#2
TCF4
TCF4
DAPI

Figure 26: DDB2 regulates the expression Wnt target genes in colon cancer cells.

HT-29 cells transiently expressing siControl or siDDB2 were treated with vehicle or human recombinant Wnt3A protein (300ng/ml, 24hrs). Relative mRNA levels of DDB2, *Rnf43*, Axin2 and c-Myc were analyzed using qRT-PCR (Normalized by 18S rRNA). N=3. All error bars indicate SD.

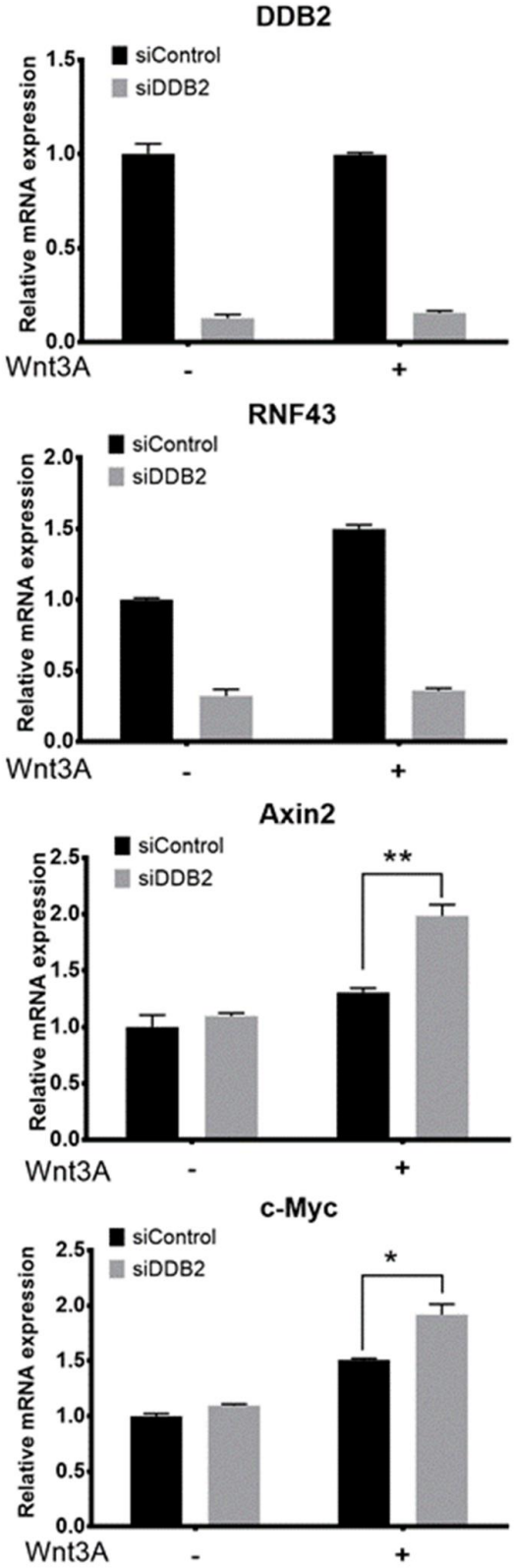
DDB2
siControl
siDDB2
Relative mRNA expression
1.5
1.0
0.5
0.0
Wnt3A
-
+
RNF43
siControl
siDDB2
Relative mRNA expression
2.0
1.5
1.0
0.5
0.0
Wnt3A
-
+
Axin2
siControl
siDDB2
**
Relative mRNA expression
2.5
2.0
1.5
1.0
0.5
0.0
Wnt3A
-
+
c-Myc
siControl
siDDB2
*
Relative mRNA expression
2.5
2.0
1.5
1.0
0.5
0.0
Wnt3A
-
+

Figure 27: DDB2 regulates the expression Wnt target genes through RNF43.

Lack of DDB2 binding region in *Rnf43*gene increases the expression of Wnt/β-catenin pathway target genes upon Wnt3a treatment. HT-29 Parental cells, Short Del cells and Long Del cells were treated with vehicle or human recombinant Wnt3A protein (300ng/ml, 24hrs). Relative mRNA levels of DDB2, *Rnf43*, Axin2 and c-Myc were analyzed using qRT-PCR (Normalized by 18S rRNA). N=3. All error bars indicate SD. *: $P < 0.05$, **: $P < 0.01$, ***: $P < 0.001$

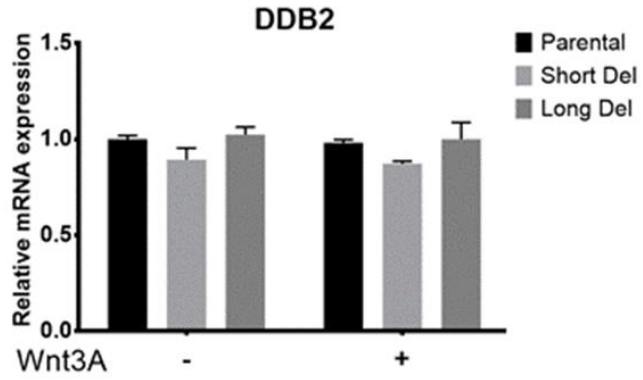
DDB2
Relative mRNA expression
1.5
1.0
0.5
0.0
Parental
Short Del
Long Del
Wnt3A
-
+

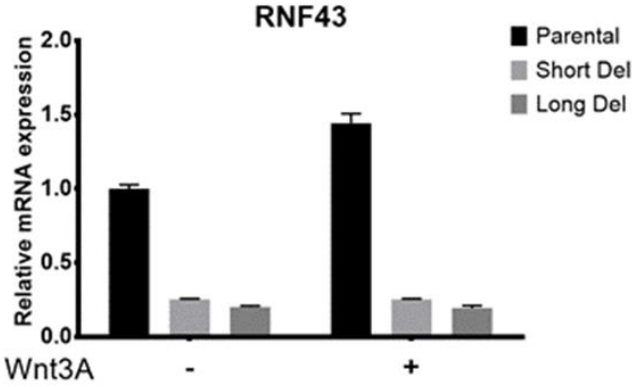
RNF43
Relative mRNA expression
2.0
1.5
1.0
0.5
0.0
Parental
Short Del
Long Del
Wnt3A
-
+

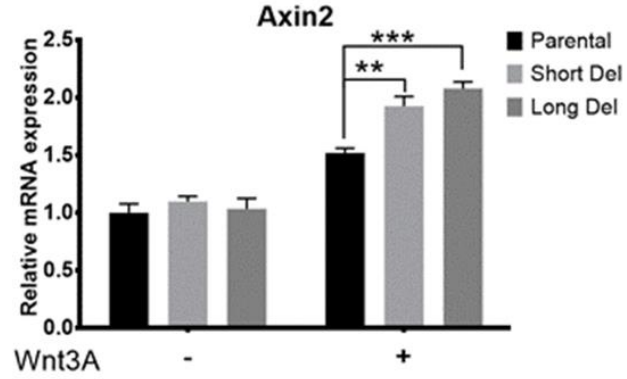
Axin2
***
**
Relative mRNA expression
2.5
2.0
1.5
1.0
0.5
0.0
Parental
Short Del
Long Del
Wnt3A
-
+

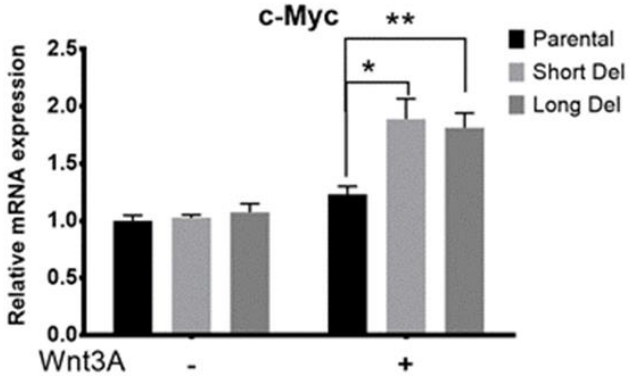
c-Myc
**
*
Relative mRNA expression
2.5
2.0
1.5
1.0
0.5
0.0
Parental
Short Del
Long Del
Wnt3A
-
+

3.7 DDB2 deficiency increases abundance of Wnt-receptors and enhances Wnt-pathway *in vivo* in a mouse model for colon cancer

Because Wnt-signaling is a major driver for colon cancer, we investigated whether DDB2 deficiency promotes colorectal tumor development. To investigate the effects of DDB2 on endogenous colorectal cancer, we subjected the male wild-type and DDB2 -/- mice to Azoxymethane (AOM)/Dextran Sulfate (DSS) chemical carcinogenesis protocol (Figure 28A). When compared 15 weeks after AOM injection, the DDB2-/- mice developed many more and much larger size tumors compared to the wild-type mice (Figure 28B and C). Whole-exome sequencing identified activating mutation in the *Ctnnb1* gene, which encodes β-catenin, in all tumor samples of both genotypes (Figure 30A).There was no significant difference in the profile of total variants between the wild-type samples and the DDB2-/- samples (Figure 29A and B). Also, there was no consistent mutation of the major mutational colon cancer driver genes, other than that of *Ctnnb1* (Figure 30B). The whole-exome sequencing results suggest that activating mutation in the *Ctnnb1* gene is the major driver of colon tumor development in AOM/DSS mouse model.

Next, we investigated whether the increased susceptibility of tumor development is related to deficiency in RNF43 and increased Wnt signaling. We performed immunohistochemical staining of the tumor tissue sections for RNF43, as well as for LRP5/6 that are co-receptors of Wnt ligands. As shown in Figure 31A and B, the tumor sections in the DDB2-/- mice are significantly deficient in RNF43. Consistent with that, compared to wild-type mice, the protein levels of LRP5/6 were significantly higher in the

Figure 28: DDB2 deficiency increases tumor incidence in mouse colon tumor model.

(A) Schematic of the AOM/DSS protocol. Mice were injected with AOM one week prior to beginning the 7-day treatment of DSS. AOM/DSS treated mice were sacrificed 15 weeks after AOM injection. (B) Representative images of mouse colorectum. At 15 weeks, male DDB2+/+ and DDB2-/- mice were sacrificed and the entire colorectal tissues were excised and whole mounts were examined from proximal to distal ends using light microscopy. Increased numbers of nodular and polyploid colonic tumors were observed in the colorectum of the DDB2-/- mice. (C) DDB2 -/- mice developed greater number of tumor nodules than wild-type mice. Quantification of total tumor nodules and the tumors larger than 2-mm diameter observed in 12 DDB2 +/+ mice and 14 DDB2-/- mice.

A.


AOM(10mg/Kg)
Sacrifice
DSS
W1 W2 W3 W4 W5 W6 W7 W8 W9 W10 W11 W12 W13 W14 W15 W16

B.

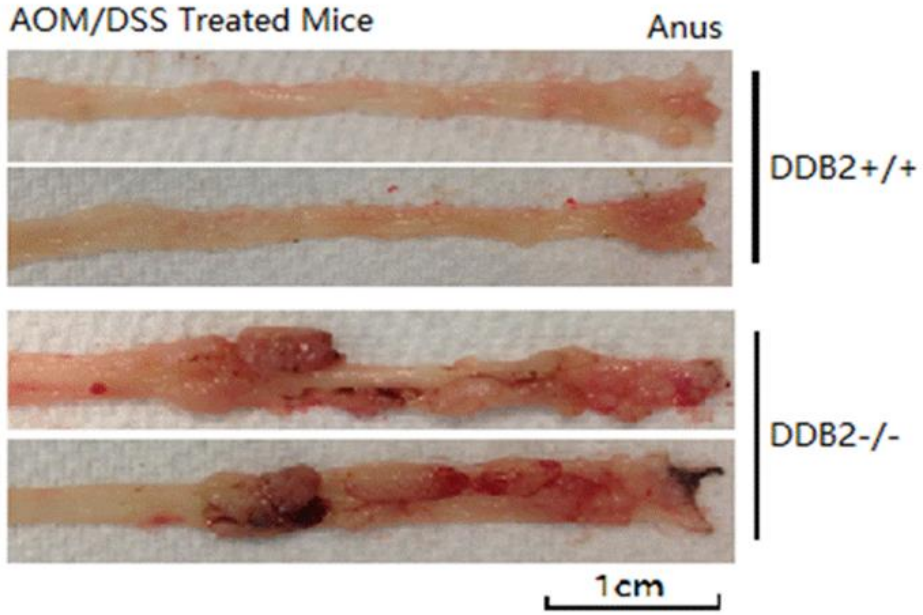
AOM/DSS Treated Mice
Anus
DDB2+/+
DDB2-/-
1cm

C.

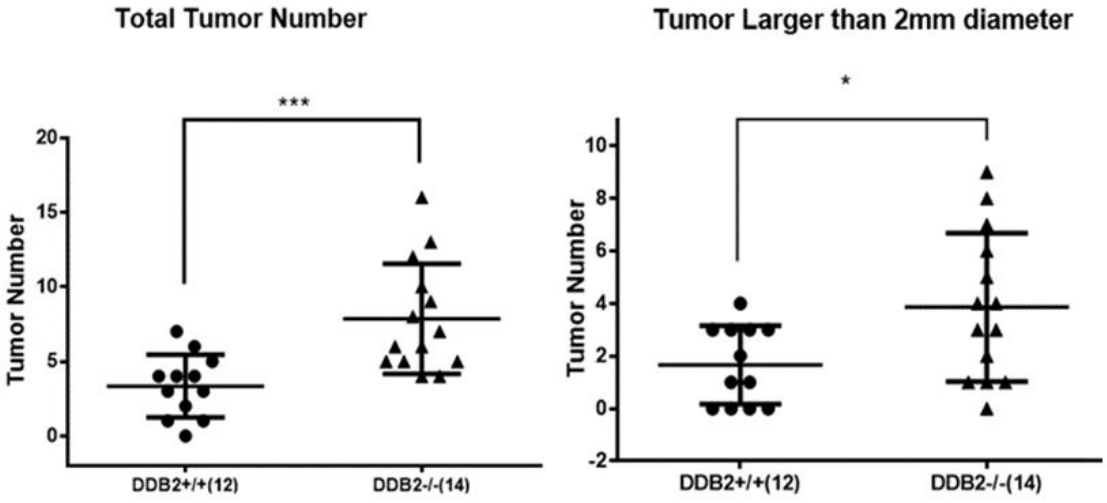
Total Tumor Number
***
Tumor Number
20
15
10
5
0
DDB2+/+(12)
DDB2-/-(14)
Tumor Larger than 2mm diameter
*
Tumor Number
10
8
6
4
2
0
-2
DDB2+/+(12)
DDB2-/-(14)

Figure 29: Whole exome sequencing showed similar mutation profile between the tumor samples from DDB2 +/+ and DDB2-/- mice.

(A) Total number of variants is plotted for all six samples. (B) The profile of total base alterations is plotted for all six samples.

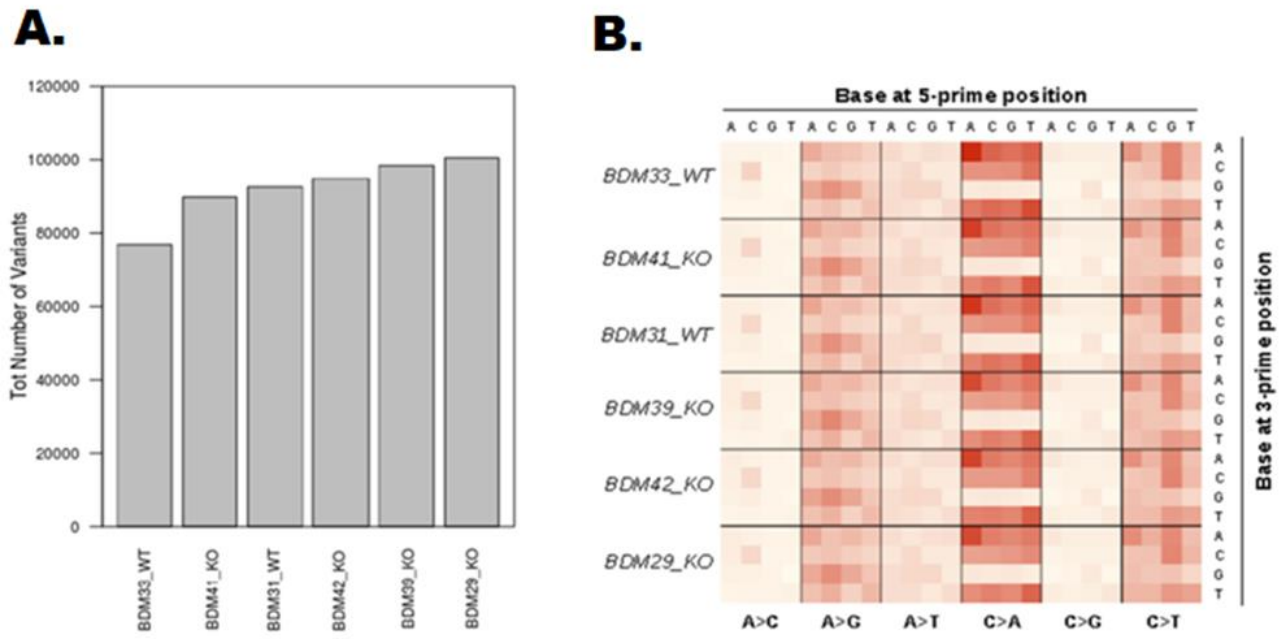
A.
120000
100000
80000
60000
40000
20000
0
Tot Number of Variants
BDM33_WT
BDM41_KO
BDM31_WT
BDM42_KO
BDM39_KO
BDM29_KO
B.
Base at 5-prime position
A C G T A C G T A C G T A C G T A C G T A C G T
BDM33_WT
BDM41_KO
BDM31_WT
BDM39_KO
BDM42_KO
BDM29_KO
A C G T A C G T A C G T A C G T A C G T A C G T
Base at 3-prime position
A>C
A>G
A>T
C>A
C>G
C>T

Figure 30: Whole exome sequencing showed missense mutation in *Ctnnb1* gene.

(A) A point mutation (101 G>A) in *Ctnnb*1 gene was found in all six samples. This mutation leads to the change of the 34th amino acid (34 G>E) in β-catenin protein, thus disrupts the E3 ligase β-TrCP binding motif on the N-terminus. Then β-TrCP fails to ubiquitinate β-catenin. This mutation prevents β-catenin from being degraded. (B) Major colorectal cancer driver gene alterations in six samples. 95 mutational cancer drivers were detected in 2 colorectal adenocarcinoma (COREAD) projects (Wood, Parsons et al. 2007, Cancer Genome Atlas 2012).Left panel: Mutation status for each gene and tumor sample (Missense, Nonsense, Frame-shift and Splice site. Gray box indicates that no mutations were detected). Right panel: Fraction of TCGA colorectal tumors with mutation by genes.

A.


β-TrCP binding motif
1
781
NH2
COOH
DSGIHS
33
37
E
β-catenin

B.

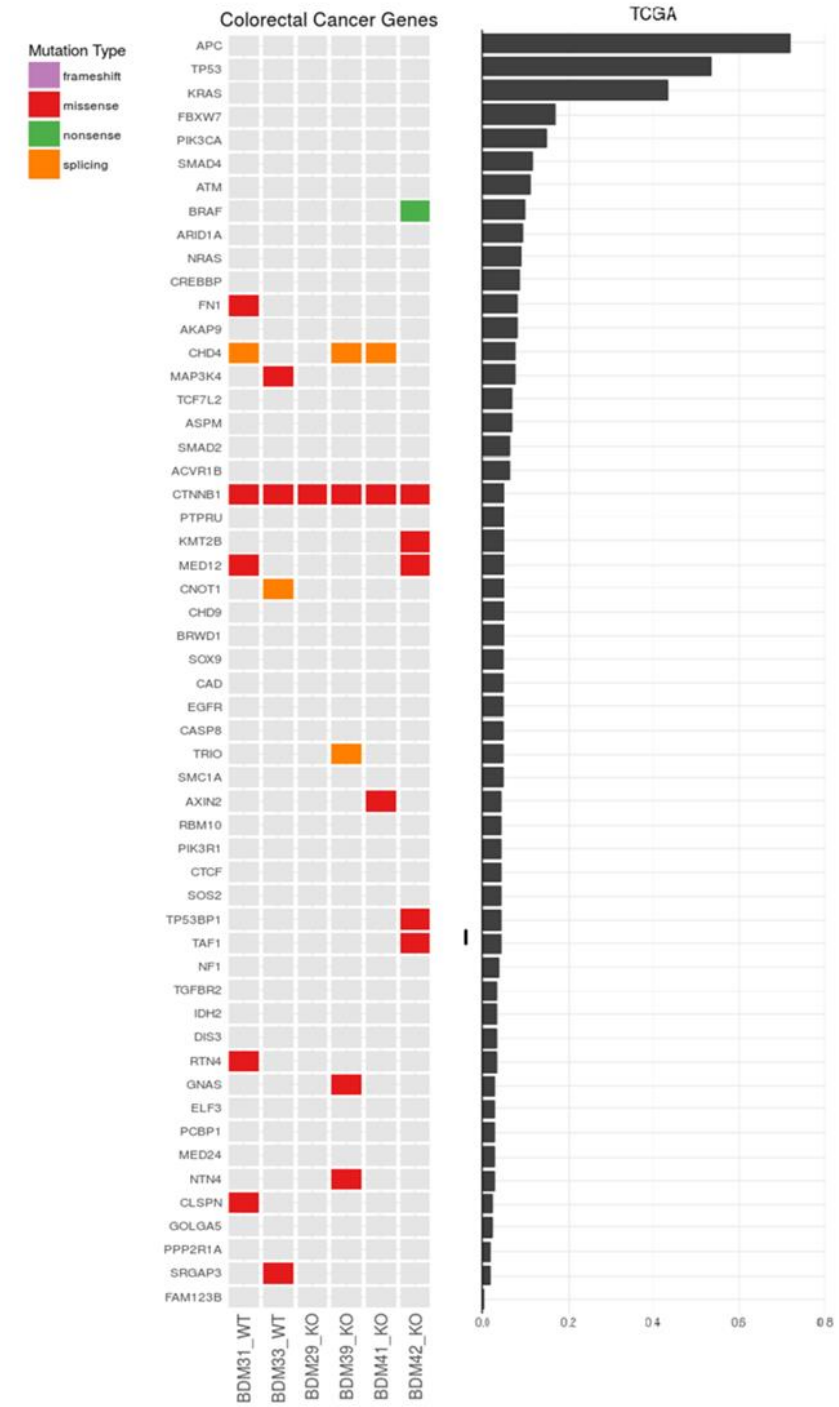
Colorectal Cancer Genes
TCGA
Mutation Type
frameshift
missense
nonsense
splicing
APC
TP53
KRAS
FBXW7
PIK3CA
SMAD4
ATM
BRAF
ARID1A
NRAS
CREBBP
FN1
AKAP9
CHD4
MAP3K4
TCF7L2
ASPM
SMAD2
ACVR1B
CTNNB1
PTPRU
KMT2B
MED12
CNOT1
CHD9
BRWD1
SOX9
CAD
EGFR
CASP8
TRIO
SMC1A
AXIN2
RBM10
PIK3R1
CTCF
SOS2
TP53BP1
TAF1
NF1
TGFBR2
IDH2
DIS3
RTN4
GNAS
ELF3
PCBP1
MED24
NTN4
CLSPN
GOLGA5
PPP2R1A
SRGAP3
FAM123B
BDM31_WT
BDM33_WT
BDM29_KO
BDM39_KO
BDM41_KO
BDM42_KO
0.0
0.2
0.4
0.6
0.8

tumor sections derived from the DDB2-/- mice (Figure 31A and B). We also examined the mRNA expression of Wnt target genes Axin2 and Cdx1 in these tumor samples. Both Axin2 and Cdx1 expression were increased in the tumor tissues derived from the DDB2-/- mice (Figure 32). These results suggest that DDB2 deficiency promotes colorectal tumor progression via hyper-activation of Wnt signaling.

Furthermore, we investigated if DDB2 deficiency regulates RNF43 and Wnt signaling in normal coloretum. Immunohistochemical staining was performed on normal colon tissue sections to examine the protein expression of RNF43 in the wild-type and DDB2-/- mice. RNF43 was barely detected in the colon crypts of DDB2-/- mice (Figure 33A and B). Additionally, there were increases in the mRNA level of Axin2 and Cdx1 in DDB2-/- mice colorectum (Figure 34A-C). Together, these data suggested that DDB2 is a key activator of RNF43, which negatively regulates Wnt/β-catenin signaling and suppresses colorectal tumor progression.

Figure 31: DDB2 deficiency in mouse colon tumors inhibits RNF43 expression and increases abundance of Wnt receptors.

(A) Colorectal tumors from DDB2-/- mice showed significantly decreased level of RNF43 expression and up-regulated level of LRP5/6. Immunohistochemical staining for DDB2, RNF43 and LRP5/6 were performed on the colorectal tissue sections from DDB2+/+ and DDB2-/- mice and images were taken under 40x objective. (Scale bar=50 μm). (B) Quantification of the percentage of RNF43 positive and LRP5/6 positive cells. N=15.

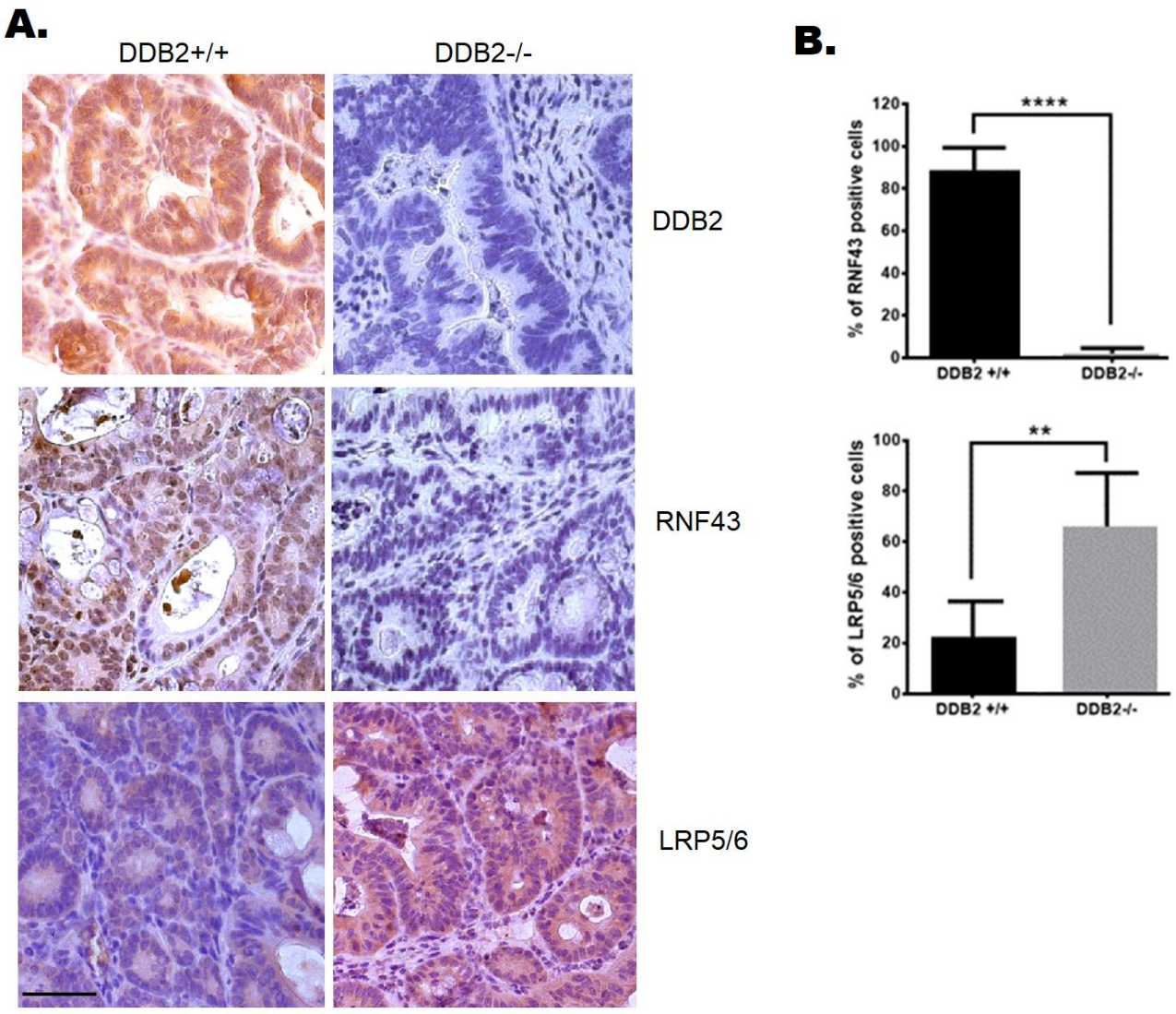
A.
DDB2+/+
DDB2-/-
DDB2
RNF43
LRP5/6
B.
% of RNF43 positive cells
120
100
80
60
40
20
0
****
DDB2 +/+
DDB2-/-
% of LRP5/6 positive cells
100
80
60
40
20
0
**
DDB2 +/+
DDB2-/-

Figure 32: Up-regulated expression of Wnt target genes in DDB2-/- tumors.

mRNA was extracted from colorectal tumors isolated from DDB2+/+ mice and DDB2-/- mice, and the relative mRNA levels of *Rnf43*, Axin2 and Cdx1 were examined by qPCR. N=5. All error bars indicate SD. *: P <0.05, **: P <0.01, ***: P <0.001

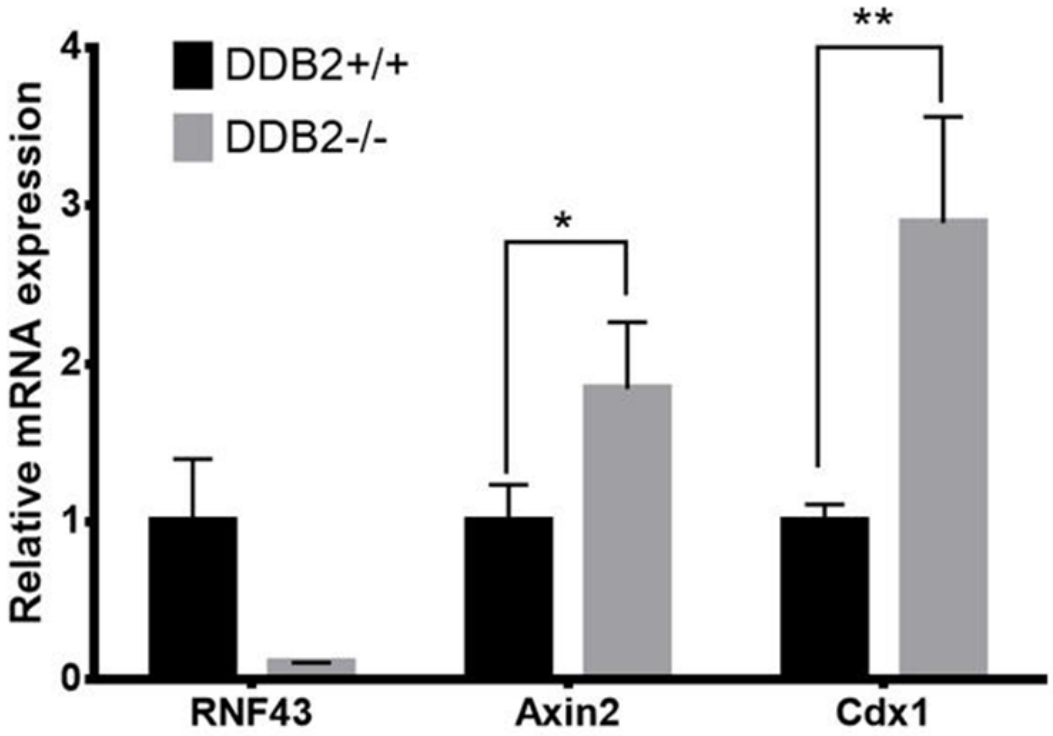
DDB2+/+
DDB2-/-
Relative mRNA expression
0
1
2
3
4
*
**
RNF43
Axin2
Cdx1

Figure 33: DDB2 regulates RNF43 expression in normal mouse colonic tissues.

(A) Immunohistochemical staining of mouse distal colon crypts shows dramatically reduced expression of RNF43 in DDB2-/- mouse (Scale bar=50 μm). (B) The quantification of RNF43 positive cells in mouse colon crypts. N=15. All error bars indicate SD. **: P <0.01.

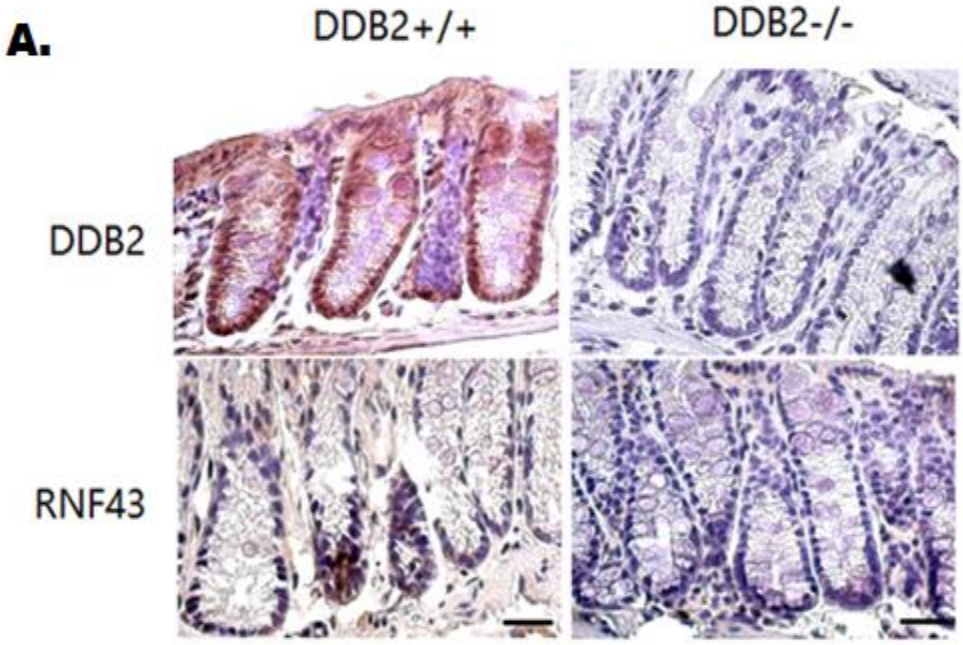
A.
DDB2+/+
DDB2-/-
DDB2
RNF43

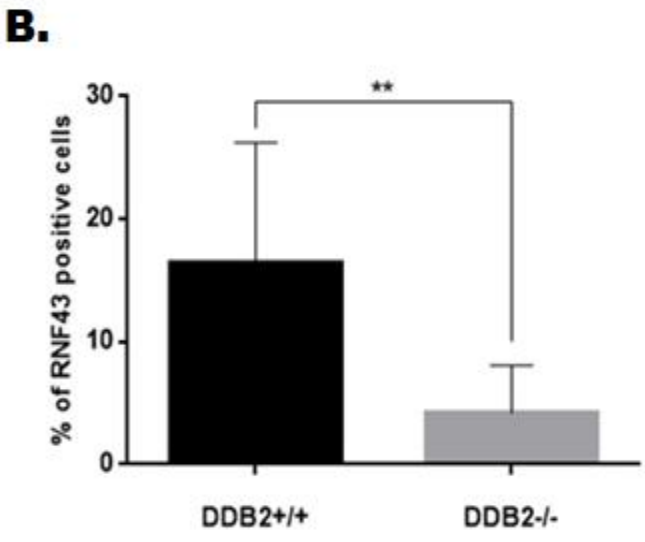
B.
**
% of RNF43 positive cells
30
20
10
0
DDB2+/+
DDB2-/-

Figure 34: DDB2 regulates Wnt target gene expression in normal mouse colonic tissues.

(A) The schematic of mouse colorectum. The entire colorectum is divided into three parts (Rectum, Distal Colon and Proximal Colon) and assayed separately. (B) The mRNA expression of Wnt target genes Axin2 and Cdx1 was assayed from rectum, distal colon and proximal colon respectively. N=5. All error bars indicate SD.

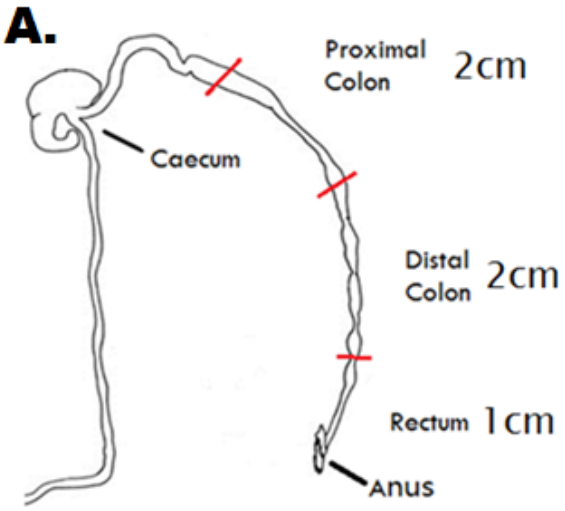
A.
Proximal Colon
2cm
Caecum
Distal Colon
2cm
Rectum
1cm
Anus

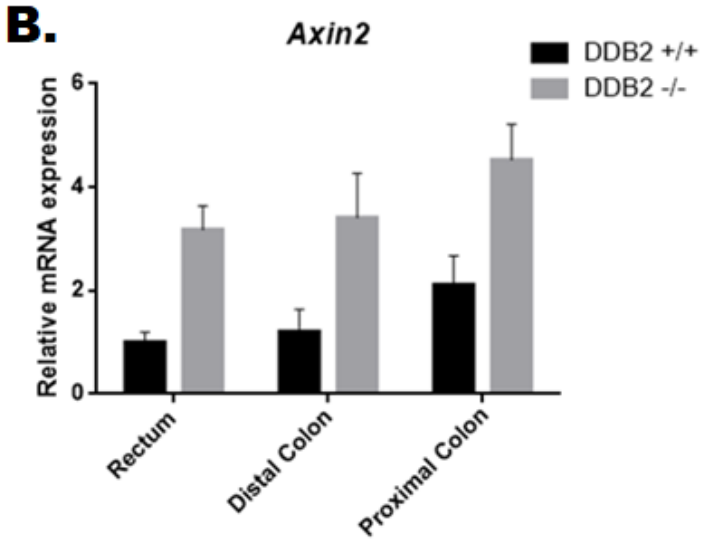
B.
Axin2
DDB2 +/+
DDB2 -/-
Relative mRNA expression
0
2
4
6
Rectum
Distal Colon
Proximal Colon

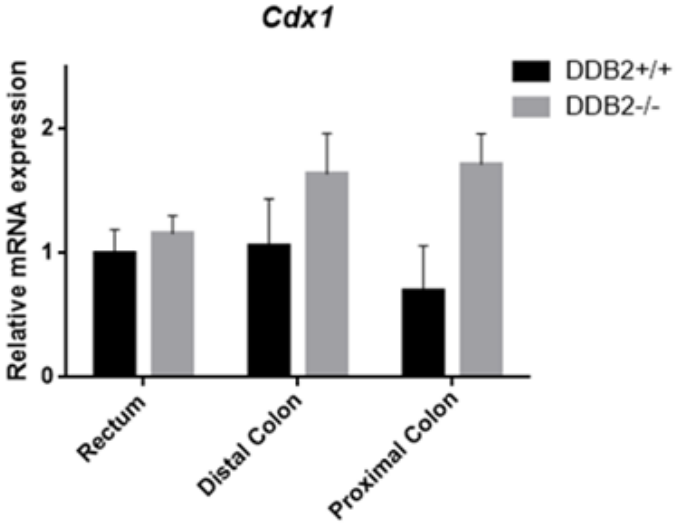
Cdx1
DDB2+/+
DDB2-/-
Relative mRNA expression
0
1
2
Rectum
Distal Colon
Proximal Colon

4. DISCUSSION

In my thesis work, I provide genetic evidence for a novel role of DDB2 in colon cancer development. The results are significant in several ways. First, I show that DDB2 is critical for expression of *Rnf43*, a regulator of Wnt/β-catenin signaling. It binds to an upstream regulatory region of *Rnf43* and recruits EZH2 as well as β-catenin. Moreover, DDB2 mediates an interaction of that upstream regulatory region with the previously identified TCF4-binding region (Takahashi, Yamaguchi et al. 2014) to activate expression of *Rnf43*. The observations also demonstrate a novel interplay between DDB2 and Wnt/β-catenin signaling in which DDB2 functions both as a partner as well as a regulator of Wnt/β-catenin signaling. Furthermore, I provided *in vivo* evidence linking DDB2-mediated activation of *Rnf43* to inhibition of colon cancer development.

In Wnt/β-catenin signaling, upon ligand-induced activation of the pathway, β-catenin is stabilized and accumulates in the nucleus to associate with the TCF/LEF family of transcription factors and activate expression of the TCF/LEF target genes (Korswagen and Clevers 1999, Cadigan and Waterman 2012). A study with over-expression of a dominant negative TCF4 indicated that all β-catenin/target gene interactions involve TCF/LEF factors (Schuijers, Mokry et al. 2014). It is noteworthy that the study with dominant negative TCF4 focused mainly on genes with ChIP signals between -2.5 to +2.5 kb (). DDB2-dependent recruitment of β-catenin at the -2.9 kb region of *Rnf43* in our study was not inhibited by dominant negative TCF4.

DDB2 recruits β-catenin through an interaction with EZH2, which was previously shown to associate with β-catenin and activate Wnt-target genes (Jung, Jun et al. 2013). That is different from the well-studied role of EZH2 in transcriptional repression. EZH2 is the functional enzymatic component of the Polycomb Repressive Complex 2 (PRC2). It participates in histone 3 tri-methylation and transcriptional repression (Margueron and Reinberg 2011). However, recently an unexpected model of EZH2 was revealed by Jung, HY and coworkers. They found that EZH2 is recruited by β-catenin through an interaction with PCNA-associated factor (PAF) - a component of translesion DNA synthesis (Jung, Jun et al. 2013). And this new PAF-EZH2- β-catenin transcriptional complex significantly enhances the activation of Wnt target genes. Therefore, in the setting of Wnt signaling activation, stabilized β-catenin sequesters PAF away from PCNA. PAF facilitates interaction between β-catenin and EZH2. EZH2 interaction with the mediator complex then recruits RNA Pol II-associated transcriptional machinery to TCF-binding elements and transactivates Wnt/β-catenin target genes (Jung, Jun et al. 2013). My study validates this novel PCR2 complex-independent role of EZH2 as a partner of downstream Wnt/β-catenin signaling and an activator of the Wnt target gene-*Rnf43*.

My results also show that TCF4 and DDB2 both are important for the expression of *Rnf43.* The TCF-binding elements are located in the second intron of *Rnf43* gene. Hatzis P and coworkers first carried out a genome-wide ChIP-seq analysis in colon cancer cells and found a pattern of TCF4 chromatin occupancy (Schuijers, Mokry et al. 2014). This data included a TCF4-binding peak in the intron 2 of *Rnf43* gene. Takahashi N. *et.al.*

later identified two TCF-binding elements in the intron 2 of *Rnf43* gene that associate with TCF4 and β-catenin in colon cancer cells (Takahashi, Yamaguchi et al. 2014). Data from luciferase assay also showed that these two TCF4 binding sites are able to activate Wnt reporter genes (Takahashi, Yamaguchi et al. 2014). I first validated that TCF4 and β-catenin associate with the identified elements in the intron 2 of *Rnf43* gene. And I also found EZH2 enrichment on the same elements, which is TCF4 and β-catenin dependent. Furthermore, the chromosome conformation capture (3C) analysis suggested a functional interaction exists between the DDB2-binding and TCF4-binding fragments in the *Rnf43* gene in colon cancer cells. I was able to detect high cross-linking frequencies right next to the putative interaction sites which indicated the high possibility of the interaction between DDB2-binding motif and TCF4-binding elements in *Rnf43* gene. Besides, the high cross-linking frequencies were abolished in both DDB2 deficient cells and the cells expressing dominant negative TCF4, suggesting that the interaction is both DDB2 and TCF4 dependent. Based on the above analysis, it is possible that the TCF4 bound β-catenin and the DDB2 bound EZH2 mediate a chromatin looping structure that is critical for the expression of *Rnf43*.

The observation that DDB2 is critical for the Wnt/β-catenin pathway activation of *Rnf43* is significant because *Rnf43* is a tumor suppressor that regulates Wnt/β-catenin by regulating the Wnt-receptors through poly-ubiquitnation (Koo, Spit et al. 2012), as well as by sequestering TCF4 to nuclear membrane (Loregger, Grandl et al. 2015). Colon cancer cells secrete high-levels of Wnt ligands, which bind to the Wnt-receptors to enhance the signaling pathway even in the presence of inactivating mutations in the APC

gene or activating mutation in *ctnnb1* gene (Voloshanenko, Erdmann et al. 2013). Inhibition of that pathway through inhibition of Wnt-ligand secretion reduces expression of the Wnt-target genes, resulting in a loss of tumorigenicity in colon cancer cells harboring activating mutations in the Wnt/β-catenin pathway (Voloshanenko, Erdmann et al. 2013). That is consistent also with our studies comparing colon tumor development in DDB2-/- and DDB2+/+ mice. In my mouse model studies, I compared DDB2 knockout mice with wild-type mice in the AOM/DSS inducing colon tumor model. It was shown that, in rat model, AOM induces mutations in *K-ras* and β-catenin that alters both Ras pathway and Wnt pathway (Takahashi and Wakabayashi 2004). However, in our C57BL/6 mouse background, AOM/DSS carcinogenesis protocol only generated activating mutations in the *ctnnb1* gene in tumors derived from both strains (Figure 35A and B). The missense mutation in *ctnnb1* gene leads to the change of the 34th amino acid (34 G>E) in β-catenin protein (Figure 66A), thus disrupts the E3 ligase β-TrCP binding motif on the N-terminus. β-TrCP then fails to ubiquitinate β-catenin. This mutation prevents β-catenin from being degraded in the AOM/DSS mouse model, and it is also found in human colon cancer cases (Brannon, Vakiani et al. 2014). The pathway analysis also indicates that only Wnt/β-catenin pathway is altered in our AOM/DSS mouse model, which makes it a perfect model to study the regulation of Wnt/β-catenin pathway in colon tumors. In that regard it is interesting that the DDB2-/- mice developed greater number and larger size tumors compared to the DDB2+/+ mice. Also, I observed increased abundance of Wnt co-recepter LRP5 and LRP6 in mouse tumor samples in DDB2-/- background, coinciding with completely abolished RNF43 expression. Moreover, the Wnt target genes were expressed at higher levels in the DDB2-/- tumors. These results

Figure 35: Whole exome sequencing showed only Wnt/β-catenin pathway is altered in mouse AOM/DSS model.

(A). Mutation status for Wnt pathway related genes and tumor samples (GO: 0016055). Genes on the y-axis are ranked based on mutation frequency in TCGA. (B) Mutation status for Ras pathway related genes and tumor samples (GO: 0007265). Genes on the y-axis are ranked based on mutation frequency in TCGA.


A.
Mutations in GO:0016055
APC
MACF1
CTNNB1
RNF43
AXIN2
TLE4
FBXW11
GSK3B
APCDD1
LEF1
WNT10B
WNT3
CTNND1
CCNE1
TLE3
WNT11
WNT2B
FBXW4
XIAP
AXIN1
WNT8A
TLE2
WNT9B
WNT5A
WNT7A
WNT7B
CCNY
RNF146
WNT16
WNT9A
GSK3A
TLE1
WNT1
WNT2
WNT3A
WNT4
WNT6
RNF138
CTNNBIP1
CCND1
DDIT3
MYC
WNT10A
WNT5B
WNT8B
BDM31_WT
BDM33_WT
BDM29_KO
BDM39_KO
BDM41_KO
BDM42_KO
Mutation Type
frameshift
missense
nonsense
splicing
B.
Mutations in GO:0007265
KRAS
NRAS
IQGAP3
NF1
SOS1
PLCE1
RASGRP3
NTN1
RASGRP1
PLK2
SHTN1
CNKSR1
SYNGAP1
GRB2
BRAP
USP8
DOK1
RIT1
HRASLS
RRAS2
DHCR24
DOK2
LAT
MAPKAPK5
SDCBP
RALA
RALB
HRAS
RFXANK
RSU1
ULK1
DOK3
RASSF1
ARL6
BDM31_WT
BDM33_WT
BDM29_KO
BDM39_KO
BDM41_KO
BDM42_KO
Mutation Type
frameshift
missense
nonsense
splicing

are consistent with my studies with human colon cancer cells in which I observed that cells lacking DDB2 expression or cells lacking DDB2-binding motif in the *Rnf43* gene are also deficient in poly-ubiquitination of the Wnt-receptor FZD5, and that those cells exhibit greater response to exogenous Wnt-ligand.

In addition, consistent with previous study (Loregger, Grandl et al. 2015), I also observed that endogenous RNF43 exhibits nuclear localization in colonic crypt and cancer cells. Moreover, immune-fluorescent staining shows that DDB2 overexpression in SW 620 cells induces endogenous TCF4 to re-localize to the nuclear periphery. The effects of DDB2 on re-localization of TCF4 were also observed in HT-29 cells harboring deletion of DDB2-binding motif in the *Rnf43* upstream regulatory region. Those cells, unlike the parental HT-29 cells, failed to exhibit the RNF43-mediated sequestration of TCF4 in the nuclear periphery, and exhibit abundant localization in the nucleoplasm. Despite the fact that I noticed DDB2 regulates RNF43-mediated TCF4 translocation in nucleus, without Wnt ligands treatment I did not observe a significant increase of basal level Wnt target genes expression in HT-29 cells. That was true also with DDB2 deficient cells and with cells harboring deletion of DDB-binding motif in RNF43 gene.

Furthermore, we observed a strong correlation between the expression of RNF43 and DDB2 in human colonic tissues. Previous studies have shown a decreasing pattern of DDB2 expression in human colon cancer samples, along with increased grades (Roy, Bommi et al. 2013). Expectedly, I analyzed the mRNA expression data from Oncomine

database and the limited dataset allowed me to find a reduced mRNA expression of *Rnf43* from grade 2 to grade 3 in colon cancer patient samples, which correlates with the DDB2 protein expression pattern. Furthermore, I analyzed the progression tissue micro-array (TMA) from colon cancer patients, which contains not only the adenocarcinomas but also the adjacent normal tissue, hyperplastic tissue and dysplastic tissue from the same patient. I analyzed 24 patients and as expected, based the immune-staining results DDB2 and RNF43 expression are highly correlated with each other, particularly the expression of both proteins exhibits a decreasing pattern from adjacent normal tissue to hyperplasia, but an increasing pattern from hyperplasia to dysplasia and adenocarcinomas. This observation is interesting because hyperplastic stage is believed as the earliest event when Wnt/β-catenin pathway has been altered. And the data from human samples strongly suggest a role of DDB2/RNF43 axis in the early steps involved in the pathogenesis of colon cancer, though how DDB2 is regulated in the early hyperplasia is still unknown.

The observations that DDB2 is required for Wnt-activated expression of *Rnf43* identify DDB2 as a new component in the Wnt/β-catenin signaling pathway in colon cancer cells (Figure 36). And the critical role of DDB2 in *Rnf43* activation also identifies DDB2 as a negative regulator of the Wnt/β-catenin signaling pathway. Although it has been studied for more than three decades, the deregulation of the Wnt/β-catenin pathway in colon cancer is still poorly understood because, in addition to activating pro-cancer genes, this pathway also activates expression of several tumor suppressor genes, including *Rnf43*. The observations that DDB2 is required for expression of *Rnf43* and that the expression of both DDB2 and RNF43 diminished at the very early stage of hyperplasia offer new

insights into the mechanisms of Wnt/β-catenin pathway deregulation that drive early development of colon cancer. Also, the observations that DDB2 interacts with β-catenin to activate *Rnf43* expression suggest that there might be other Wnt target tumor suppressor genes that are activated in a manner similar to *Rnf43*.

Figure 36: Model of how DDB2 regulates Wnt/β-catenin pathway and colon cancer development through RNF43.

DDB2 is required for the activation of *Rnf43* expression. Therefore, DDB2 indirectly impacts the RNF43-mediated down regulation of the Wnt/β-catenin pathway. DDB2 suppresses colon cancer development by inhibiting Wnt/β-catenin signaling in colon cancer cells.

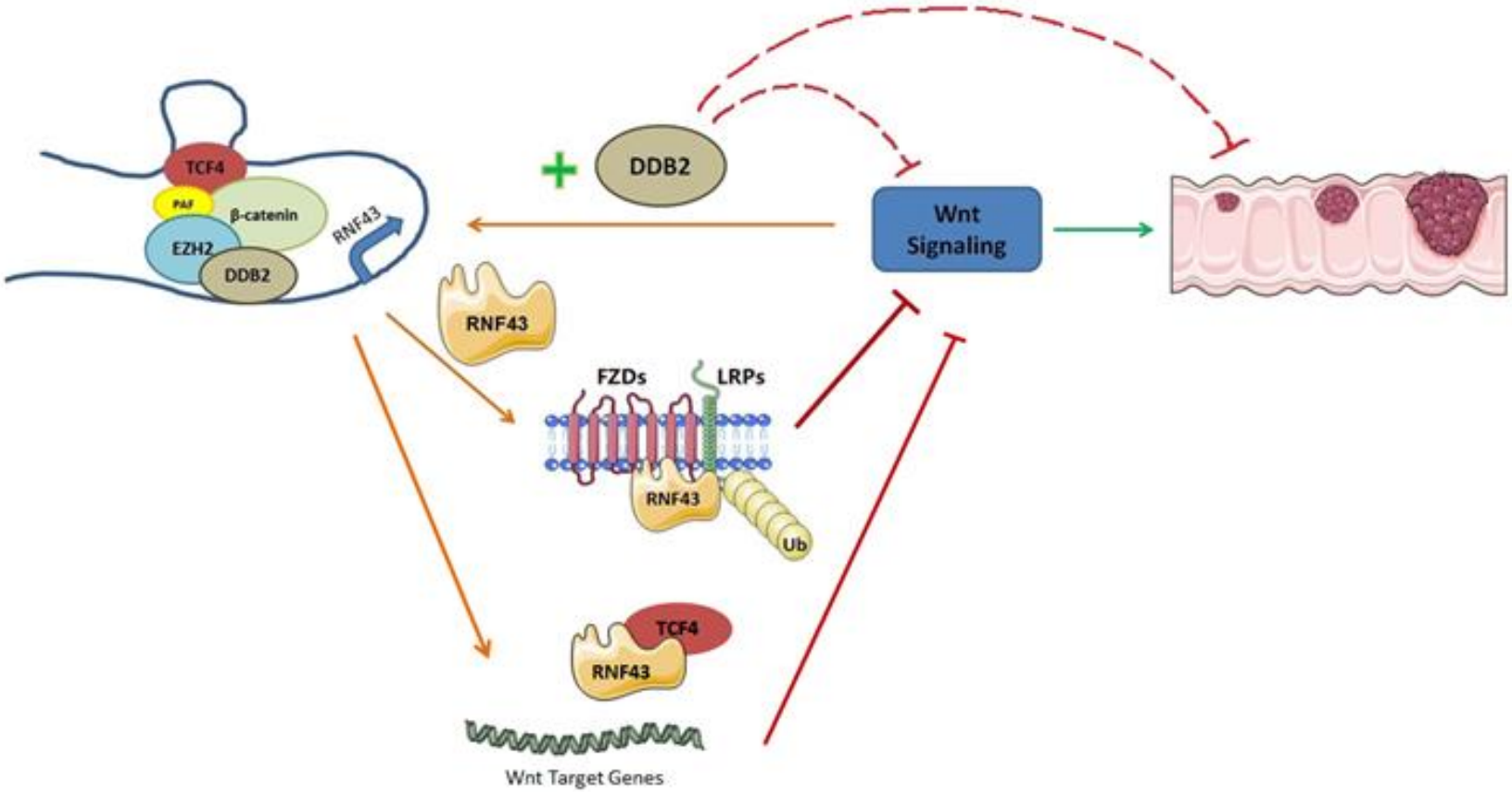
TCF4
PAF
β-catenin
EZH2
DDB2
RNF43
DDB2
Wnt
Signaling
RNF43
FZDs
LRPs
RNF43
Ub
TCF4
RNF43
Wnt Target Genes

6. CITED LITERATURE

Bond, C. E., D. M. McKeone, M. Kalimutho, M. L. Bettington, S. A. Pearson, T. D. Dumenil, L. F. Wockner, M. Burge, B. A. Leggett and V. L. Whitehall (2016). "RNF43 and ZNRF3 are commonly altered in serrated pathway colorectal tumorigenesis." Oncotarget **7**(43): 70589-70600.

Brannon, A. R., E. Vakiani, B. E. Sylvester, S. N. Scott, G. McDermott, R. H. Shah, K. Kania, A. Viale, D. M. Oschwald, V. Vacic, A. K. Emde, A. Cercek, R. Yaeger, N. E. Kemeny, L. B. Saltz, J. Shia, M. I. D'Angelica, M. R. Weiser, D. B. Solit and M. F. Berger (2014). "Comparative sequencing analysis reveals high genomic concordance between matched primary and metastatic colorectal cancer lesions." Genome Biol **15**(8): 454.

Cadigan, K. M. and M. L. Waterman (2012). "TCF/LEFs and Wnt signaling in the nucleus." Cold Spring Harb Perspect Biol **4**(11).

Cancer Genome Atlas, N. (2012). "Comprehensive molecular characterization of human colon and rectal cancer." Nature **487**(7407): 330-337.

Carmon, K. S., X. Gong, Q. Lin, A. Thomas and Q. Liu (2011). "R-spondins function as ligands of the orphan receptors LGR4 and LGR5 to regulate Wnt/beta-catenin signaling." Proc Natl Acad Sci U S A **108**(28): 11452-11457.

Carmon, K. S., X. Gong, J. Yi, A. Thomas and Q. Liu (2014). "RSPO-LGR4 functions via IQGAP1 to potentiate Wnt signaling." Proc Natl Acad Sci U S A **111**(13): E1221-1229.

Chai, R., A. Xia, T. Wang, T. A. Jan, T. Hayashi, O. Bermingham-McDonogh and A. G. Cheng (2011). "Dynamic expression of Lgr5, a Wnt target gene, in the developing and mature mouse cochlea." J Assoc Res Otolaryngol **12**(4): 455-469.

Chen, P. H., X. Chen, Z. Lin, D. Fang and X. He (2013). "The structural basis of R-spondin recognition by LGR5 and RNF43." Genes Dev **27**(12): 1345-1350.

Clevers, H. (2004). "Wnt breakers in colon cancer." Cancer Cell **5**(1): 5-6.

Clevers, H. (2006). "Wnt/beta-catenin signaling in development and disease." Cell **127**(3): 469-480.

Clevers, H. and R. Nusse (2012). "Wnt/beta-catenin signaling and disease." Cell **149**(6): 1192-1205.

de Lau, W., W. C. Peng, P. Gros and H. Clevers (2014). "The R-spondin/Lgr5/*Rnf43* module: regulator of Wnt signal strength." Genes Dev **28**(4): 305-316.

Dekker, J., M. A. Marti-Renom and L. A. Mirny (2013). "Exploring the three-dimensional organization of genomes: interpreting chromatin interaction data." Nature Reviews Genetics **14**(6): 390-403.

Dekker, J., M. A. Marti-Renom and L. A. Mirny (2013). "Exploring the three-dimensional organization of genomes: interpreting chromatin interaction data." Nat Rev Genet **14**(6): 390-403.

Dienstmann, R. and J. Tabernero (2016). "Spectrum of Gene Mutations in Colorectal Cancer: Implications for Treatment." Cancer J **22**(3): 149-155.

Dijk, M., D. Typas, L. Mullenders and A. Pines (2014). "Insight in the multilevel regulation of NER." Exp Cell Res **329**(1): 116-123.

Drost, J., R. H. van Jaarsveld, B. Ponsioen, C. Zimberlin, R. van Boxtel, A. Buijs, N. Sachs, R. M. Overmeer, G. J. Offerhaus, H. Begthel, J. Korving, M. van de Wetering, G. Schwank, M. Logtenberg, E. Cuppen, H. J. Snippert, J. P. Medema, G. J. Kops and H. Clevers (2015). "Sequential cancer mutations in cultured human intestinal stem cells." Nature **521**(7550): 43-47.

Dualan, R., T. Brody, S. Keeney, A. F. Nichols, A. Admon and S. Linn (1995). "Chromosomal localization and cDNA cloning of the genes (DDB1 and DDB2) for the p127 and p48 subunits of a human damage-specific DNA binding protein." Genomics **29**(1): 62-69.

El-Mahdy, M. A., Q. Zhu, Q. E. Wang, G. Wani, M. Praetorius-Ibba and A. A. Wani (2006). "Cullin 4A-mediated proteolysis of DDB2 protein at DNA damage sites regulates in vivo lesion recognition by XPC." J Biol Chem **281**(19): 13404-13411.

Ennen, M., R. Klotz, N. Touche, S. Pinel, C. Barbieux, V. Besancenot, E. Brunner, D. Thiebaut, A. C. Jung, S. Ledrappier, L. Domenjoud, J. Abecassis, F. Plenat, S. Grandemange and P. Becuwe (2013). "DDB2: a novel regulator of NF-kappaB and breast tumor invasion." Cancer Res **73**(16): 5040-5052.

Erwin, C. R., M. D. Jarboe, M. A. Sartor, M. Medvedovic, K. F. Stringer, B. W. Warner and M. D. Bates (2006). "Developmental characteristics of adapting mouse small intestine crypt cells." Gastroenterology **130**(4): 1324-1332.

Fantini, D., S. Huang, J. M. Asara, S. Bagchi and P. Raychaudhuri (2017). "Chromatin association of XRCC5/6 in the absence of DNA damage depends on the XPE gene product DDB2." Mol Biol Cell **28**(1): 192-200.

Farin, H. F., I. Jordens, M. H. Mosa, O. Basak, J. Korving, D. V. Tauriello, K. de Punder, S. Angers, P. J. Peters, M. M. Maurice and H. Clevers (2016). "Visualization of a short-range Wnt gradient in the intestinal stem-cell niche." Nature **530**(7590): 340-343.

Fearon, E. R. (2011). "Molecular genetics of colorectal cancer." Annu Rev Pathol **6**: 479-507.

Featherstone, C. and S. P. Jackson (1999). "Ku, a DNA repair protein with multiple cellular functions?" Mutat Res **434**(1): 3-15.

Fisher, T. S. and V. A. Zakian (2005). "Ku: a multifunctional protein involved in telomere maintenance." DNA Repair (Amst) **4**(11): 1215-1226.

Fitch, M. E., I. V. Cross, S. J. Turner, S. Adimoolam, C. X. Lin, K. G. Williams and J. M. Ford (2003). "The DDB2 nucleotide excision repair gene product p48 enhances global genomic repair in p53 deficient human fibroblasts." DNA Repair (Amst) **2**(7): 819-826.

Fitch, M. E., S. Nakajima, A. Yasui and J. M. Ford (2003). "In vivo recruitment of XPC to UV-induced cyclobutane pyrimidine dimers by the DDB2 gene product." J Biol Chem **278**(47): 46906-46910.

Fujii, M. and T. Sato (2014). "Culturing intestinal stem cells: applications for colorectal cancer research." Front Genet **5**: 169.

Giannakis, M., E. Hodis, X. Jasmine Mu, M. Yamauchi, J. Rosenbluh, K. Cibulskis, G. Saksena, M. S. Lawrence, Z. R. Qian, R. Nishihara, E. M. Van Allen, W. C. Hahn, S. B.

Gabriel, E. S. Lander, G. Getz, S. Ogino, C. S. Fuchs and L. A. Garraway (2014). "RNF43 is frequently mutated in colorectal and endometrial cancers." Nat Genet **46**(12): 1264-1266.

Gong, X., K. S. Carmon, Q. Lin, A. Thomas, J. Yi and Q. Liu (2012). "LGR6 is a high affinity receptor of R-spondins and potentially functions as a tumor suppressor." PLoS One **7**(5): e37137.

Haegebarth, A. and H. Clevers (2009). "Wnt signaling, lgr5, and stem cells in the intestine and skin." Am J Pathol **174**(3): 715-721.

Han, C., R. Zhao, X. Liu, A. Srivastava, L. Gong, H. Mao, M. Qu, W. Zhao, J. Yu and Q. E. Wang (2014). "DDB2 suppresses tumorigenicity by limiting the cancer stem cell population in ovarian cancer." Mol Cancer Res **12**(5): 784-794.

Hao, H. X., X. Jiang and F. Cong (2016). "Control of Wnt Receptor Turnover by R-spondin-ZNRF3/RNF43 Signaling Module and Its Dysregulation in Cancer." Cancers (Basel) **8**(6).

Hao, H. X., Y. Xie, Y. Zhang, O. Charlat, E. Oster, M. Avello, H. Lei, C. Mickanin, D. Liu, H. Ruffner, X. Mao, Q. Ma, R. Zamponi, T. Bouwmeester, P. M. Finan, M. W. Kirschner, J. A. Porter, F. C. Serluca and F. Cong (2012). "ZNRF3 promotes Wnt receptor turnover in an R-spondin-sensitive manner." Nature **485**(7397): 195-200.

Hayes, S., P. Shiyanov, X. Chen and P. Raychaudhuri (1998). "DDB, a putative DNA repair protein, can function as a transcriptional partner of E2F1." Mol Cell Biol **18**(1): 240-249.

Hwang, B. J., J. M. Ford, P. C. Hanawalt and G. Chu (1999). "Expression of the p48 xeroderma pigmentosum gene is p53-dependent and is involved in global genomic repair." Proc Natl Acad Sci U S A **96**(2): 424-428.

Ilyas, M., I. P. Tomlinson, A. Rowan, M. Pignatelli and W. F. Bodmer (1997). "Beta-catenin mutations in cell lines established from human colorectal cancers." Proc Natl Acad Sci U S A **94**(19): 10330-10334.

Itoh, T., D. Cado, R. Kamide and S. Linn (2004). "DDB2 gene disruption leads to skin tumors and resistance to apoptosis after exposure to ultraviolet light but not a chemical carcinogen." Proc Natl Acad Sci U S A **101**(7): 2052-2057.

Itoh, T., S. Iwashita, M. B. Cohen, D. K. Meyerholz and S. Linn (2007). "Ddb2 is a haploinsufficient tumor suppressor and controls spontaneous germ cell apoptosis." Hum Mol Genet **16**(13): 1578-1586.

Itoh, T., T. Mori, H. Ohkubo and M. Yamaizumi (1999). "A newly identified patient with clinical xeroderma pigmentosum phenotype has a non-sense mutation in the DDB2 gene and incomplete repair in (6-4) photoproducts." J Invest Dermatol **113**(2): 251-257.

Itoh, T., A. Nichols and S. Linn (2001). "Abnormal regulation of DDB2 gene expression in xeroderma pigmentosum group E strains." Oncogene **20**(48): 7041-7050.

Jiang, X., O. Charlat, R. Zamponi, Y. Yang and F. Cong (2015). "Dishevelled promotes Wnt receptor degradation through recruitment of ZNRF3/RNF43 E3 ubiquitin ligases." Mol Cell **58**(3): 522-533.

Jin, Y. R. and J. K. Yoon (2012). "The R-spondin family of proteins: emerging regulators of WNT signaling." Int J Biochem Cell Biol **44**(12): 2278-2287.

Jung, H. Y., S. Jun, M. Lee, H. C. Kim, X. Wang, H. Ji, P. D. McCrea and J. I. Park (2013). "PAF and EZH2 induce Wnt/beta-catenin signaling hyperactivation." Mol Cell **52**(2): 193-205.

Jung, Y. S., S. Jun, S. H. Lee, A. Sharma and J. I. Park (2015). "Wnt2 complements Wnt/beta-catenin signaling in colorectal cancer." Oncotarget **6**(35): 37257-37268.

Koo, B. K., M. Spit, I. Jordens, T. Y. Low, D. E. Stange, M. van de Wetering, J. H. van Es, S. Mohammed, A. J. Heck, M. M. Maurice and H. Clevers (2012). "Tumour suppressor RNF43 is a stem-cell E3 ligase that induces endocytosis of Wnt receptors." Nature **488**(7413): 665-669.

Korswagen, H. C. and H. C. Clevers (1999). "Activation and repression of wingless/Wnt target genes by the TCF/LEF-1 family of transcription factors." Cold Spring Harb Symp Quant Biol **64**: 141-147.

Krausova, M. and V. Korinek (2014). "Wnt signaling in adult intestinal stem cells and cancer." Cell Signal **26**(3): 570-579.

Leushacke, M. and N. Barker (2012). "Lgr5 and Lgr6 as markers to study adult stem cell roles in self-renewal and cancer." Oncogene **31**(25): 3009-3022.

Li, J., Q. E. Wang, Q. Zhu, M. A. El-Mahdy, G. Wani, M. Praetorius-Ibba and A. A. Wani (2006). "DNA damage binding protein component DDB1 participates in nucleotide excision repair through DDB2 DNA-binding and cullin 4A ubiquitin ligase activity." Cancer Res **66**(17): 8590-8597.

Lin, Y. C. and J. D. Gralla (2005). "Stimulation of the XPB ATP-dependent helicase by the beta subunit of TFIIE." Nucleic Acids Res **33**(9): 3072-3081.

Loregger, A., M. Grandl, R. Mejias-Luque, M. Allgauer, K. Degenhart, V. Haselmann, C. Oikonomou, P. Hatzis, K. P. Janssen, U. Nitsche, D. Gradl, O. van den Broek, O. Destree, K. Ulm, M. Neumaier, B. Kalali, A. Jung, I. Varela, R. M. Schmid, R. Rad, D. H. Busch and M. Gerhard (2015). "The E3 ligase RNF43 inhibits Wnt signaling downstream of mutated beta-catenin by sequestering TCF4 to the nuclear membrane." Sci Signal **8**(393): ra90.

Madan, B., Z. Ke, N. Harmston, S. Y. Ho, A. O. Frois, J. Alam, D. A. Jeyaraj, V. Pendharkar, K. Ghosh, I. H. Virshup, V. Manoharan, E. H. Ong, K. Sangthongpitag, J. Hill, E. Petretto, T. H. Keller, M. A. Lee, A. Matter and D. M. Virshup (2016). "Wnt addiction of genetically defined cancers reversed by PORCN inhibition." Oncogene **35**(17): 2197-2207.

Malinauskas, T. and E. Y. Jones (2014). "Extracellular modulators of Wnt signalling." Curr Opin Struct Biol **29**: 77-84.

Margueron, R. and D. Reinberg (2011). "The Polycomb complex PRC2 and its mark in life." Nature **469**(7330): 343-349.

Markowitz, S. D., D. M. Dawson, J. Willis and J. K. Willson (2002). "Focus on colon cancer." Cancer Cell **1**(3): 233-236.

Matakidou, A., T. Eisen, C. Fleischmann, H. Bridle, R. S. Houlston and G. Consortium (2006). "Evaluation of xeroderma pigmentosum XPA, XPC, XPD, XPF, XPB, XPG and DDB2 genes in familial early-onset lung cancer predisposition." Int J Cancer **119**(4): 964-967.

Matsushita, N., S. Yamamoto, Y. Inoue, A. Aruga and M. Yamamoto (2017). "RT-qPCR analysis of the tumor antigens TOMM34 and RNF43 in samples extracted from paraffin-embedded specimens of colorectal cancer." Oncol Lett **14**(2): 2281-2287.

Medema, J. P. and L. Vermeulen (2011). "Microenvironmental regulation of stem cells in intestinal homeostasis and cancer." Nature **474**(7351): 318-326.

Min, B. H., J. Hwang, N. K. Kim, G. Park, S. Y. Kang, S. Ahn, S. Ahn, S. Y. Ha, Y. K. Lee, R. Kushima, M. Van Vrancken, M. J. Kim, C. Park, H. Y. Park, J. Chae, S. S. Jang, S. J. Kim, Y. H. Kim, J. I. Kim and K. M. Kim (2016). "Dysregulated Wnt signalling and recurrent mutations of the tumour suppressor RNF43 in early gastric carcinogenesis." J Pathol **240**(3): 304-314.

Minig, V., Z. Kattan, J. van Beeumen, E. Brunner and P. Becuwe (2009). "Identification of DDB2 protein as a transcriptional regulator of constitutive SOD2 gene expression in human breast cancer cells." J Biol Chem **284**(21): 14165-14176.

Miyamoto, K., H. Sakurai and T. Sugiura (2008). "Proteomic identification of a PSF/p54nrb heterodimer as RNF43 oncoprotein-interacting proteins." Proteomics **8**(14): 2907-2910.

Nag, A., T. Bondar, S. Shiv and P. Raychaudhuri (2001). "The xeroderma pigmentosum group E gene product DDB2 is a specific target of cullin 4A in mammalian cells." Mol Cell Biol **21**(20): 6738-6747.

Niu, L., H. Z. Qin, H. Q. Xi, B. Wei, S. Y. Xia and L. Chen (2015). "RNF43 Inhibits Cancer Cell Proliferation and Could be a Potential Prognostic Factor for Human Gastric Carcinoma." Cell Physiol Biochem **36**(5): 1835-1846.

Nusse, R. (2005). "Wnt signaling in disease and in development." Cell Res **15**(1): 28-32.

Nusse, R. and H. Varmus (2012). "Three decades of Wnts: a personal perspective on how a scientific field developed." EMBO J **31**(12): 2670-2684.

Pai, R., A. S. Tarnawski and T. Tran (2004). "Deoxycholic acid activates beta-catenin signaling pathway and increases colon cell cancer growth and invasiveness." Mol Biol Cell **15**(5): 2156-2163.

Planas-Paz, L., V. Orsini, L. Boulter, D. Calabrese, M. Pikiolek, F. Nigsch, Y. Xie, G. Roma, A. Donovan, P. Marti, N. Beckmann, M. T. Dill, W. Carbone, S. Bergling, A. Isken, M. Mueller, B. Kinzel, Y. Yang, X. Mao, T. B. Nicholson, R. Zamponi, P. Capodieci, R. Valdez, D. Rivera, A. Loew, C. Ukomadu, L. M. Terracciano, T. Bouwmeester, F. Cong, M. H. Heim, S. J. Forbes, H. Ruffner and J. S. Tchorz (2016).

"The RSPO-LGR4/5-ZNRF3/RNF43 module controls liver zonation and size." Nat Cell Biol **18**(5): 467-479.

Qiao, S., W. Guo, L. Liao, L. Wang, Z. Wang, R. Zhang, D. Xu, Y. Zhang, Y. Pan, Z. Wang and Y. Chen (2015). "DDB2 is involved in ubiquitination and degradation of PAQR3 and regulates tumorigenesis of gastric cancer cells." Biochem J **469**(3): 469-480.

Roy, N., P. V. Bommi, U. G. Bhat, S. Bhattacharjee, I. Elangovan, J. Li, K. C. Patra, D. Kopanja, A. Blunier, R. Benya, S. Bagchi and P. Raychaudhuri (2013). "DDB2 suppresses epithelial-to-mesenchymal transition in colon cancer." Cancer Res **73**(12): 3771-3782.

Roy, N., I. Elangovan, D. Kopanja, S. Bagchi and P. Raychaudhuri (2013). "Tumor regression by phenethyl isothiocyanate involves DDB2." Cancer Biol Ther **14**(2): 108-116.

Ryland, G. L., S. M. Hunter, M. A. Doyle, S. M. Rowley, M. Christie, P. E. Allan, D. D. Bowtell, G. Australian Ovarian Cancer Study, K. L. Gorringe and I. G. Campbell (2013). "RNF43 is a tumour suppressor gene mutated in mucinous tumours of the ovary." J Pathol **229**(3): 469-476.

Schuijers, J., M. Mokry, P. Hatzis, E. Cuppen and H. Clevers (2014). "Wnt-induced transcriptional activation is exclusively mediated by TCF/LEF." EMBO J **33**(2): 146-156.

Sekine, S., S. Yamashita, T. Tanabe, T. Hashimoto, H. Yoshida, H. Taniguchi, M. Kojima, K. Shinmura, Y. Saito, N. Hiraoka, T. Ushijima and A. Ochiai (2016). "Frequent PTPRK-RSPO3 fusions and RNF43 mutations in colorectal traditional serrated adenoma." J Pathol **239**(2): 133-138.

Seshagiri, S., E. W. Stawiski, S. Durinck, Z. Modrusan, E. E. Storm, C. B. Conboy, S. Chaudhuri, Y. Guan, V. Janakiraman, B. S. Jaiswal, J. Guillory, C. Ha, G. J. Dijkgraaf, J. Stinson, F. Gnad, M. A. Huntley, J. D. Degenhardt, P. M. Haverty, R. Bourgon, W. Wang, H. Koeppen, R. Gentleman, T. K. Starr, Z. Zhang, D. A. Largaespada, T. D. Wu and F. J. de Sauvage (2012). "Recurrent R-spondin fusions in colon cancer." Nature **488**(7413): 660-664.

Seshagiri, S., E. W. Stawiski, S. Durinck, Z. Modrusan, E. E. Storm, C. B. Conboy, S. Chaudhuri, Y. H. Guan, V. Janakiraman, B. S. Jaiswal, J. Guillory, C. Ha, G. J. P. Dijkgraaf, J. Stinson, F. Gnad, M. A. Huntley, J. D. Degenhardt, P. M. Haverty, R.

Bourgon, W. R. Wang, H. Koeppen, R. Gentleman, T. K. Starr, Z. M. Zhang, D. A. Largaespada, T. D. Wu and F. J. de Sauvage (2012). "Recurrent R-spondin fusions in colon cancer." Nature **488**(7413): 660-+.

Shinada, K., T. Tsukiyama, T. Sho, F. Okumura, M. Asaka and S. Hatakeyama (2011). "RNF43 interacts with NEDL1 and regulates p53-mediated transcription." Biochem Biophys Res Commun **404**(1): 143-147.

Siegel, R. L., K. D. Miller, S. A. Fedewa, D. J. Ahnen, R. G. S. Meester, A. Barzi and A. Jemal (2017). "Colorectal cancer statistics, 2017." CA Cancer J Clin **67**(3): 177-193.

Steinhart, Z., Z. Pavlovic, M. Chandrashekhar, T. Hart, X. Wang, X. Zhang, M. Robitaille, K. R. Brown, S. Jaksani, R. Overmeer, S. F. Boj, J. Adams, J. Pan, H. Clevers, S. Sidhu, J. Moffat and S. Angers (2017). "Genome-wide CRISPR screens reveal a Wnt-FZD5 signaling circuit as a druggable vulnerability of RNF43-mutant pancreatic tumors." Nat Med **23**(1): 60-68.

Sugasawa, K. (2016). "Molecular mechanisms of DNA damage recognition for mammalian nucleotide excision repair." DNA Repair (Amst) **44**: 110-117.

Sugiura, T., A. Yamaguchi and K. Miyamoto (2008). "A cancer-associated RING finger protein, RNF43, is a ubiquitin ligase that interacts with a nuclear protein, HAP95." Exp Cell Res **314**(7): 1519-1528.

Taipale, J. and P. A. Beachy (2001). "The Hedgehog and Wnt signalling pathways in cancer." Nature **411**(6835): 349-354.

Takahashi, M. and K. Wakabayashi (2004). "Gene mutations and altered gene expression in azoxymethane-induced colon carcinogenesis in rodents." Cancer Sci **95**(6): 475-480.

Takahashi, N., K. Yamaguchi, T. Ikenoue, T. Fujii and Y. Furukawa (2014). "Identification of two Wnt-responsive elements in the intron of RING finger protein 43 (RNF43) gene." PLoS One **9**(1): e86582.

Takeda, K., I. Kinoshita, Y. Shimizu, Y. Matsuno, T. Shichinohe and H. Dosaka-Akita (2011). "Expression of LGR5, an intestinal stem cell marker, during each stage of colorectal tumorigenesis." Anticancer Res **31**(1): 263-270.

Taketo, M. M. and W. Edelmann (2009). "Mouse models of colon cancer." Gastroenterology **136**(3): 780-798.

Tan, T. and G. Chu (2002). "p53 Binds and activates the xeroderma pigmentosum DDB2 gene in humans but not mice." Mol Cell Biol **22**(10): 3247-3254.

Tuteja, R. and N. Tuteja (2000). "Ku autoantigen: a multifunctional DNA-binding protein." Crit Rev Biochem Mol Biol **35**(1): 1-33.

van den Brink, G. R. and G. J. Offerhaus (2007). "The morphogenetic code and colon cancer development." Cancer Cell **11**(2): 109-117.

Voloshanenko, O., G. Erdmann, T. D. Dubash, I. Augustin, M. Metzig, G. Moffa, C. Hundsrucker, G. Kerr, T. Sandmann, B. Anchang, K. Demir, C. Boehm, S. Leible, C. R. Ball, H. Glimm, R. Spang and M. Boutros (2013). "Wnt secretion is required to maintain high levels of Wnt activity in colon cancer cells." Nat Commun **4**: 2610.

Wang, G., Y. Fu, X. Yang, X. Luo, J. Wang, J. Gong and J. Hu (2017). "Brg-1 targeting of novel miR550a-5p/RNF43/Wnt signaling axis regulates colorectal cancer metastasis." Oncogene.

Wang, Q. E., Q. Zhu, G. Wani, J. Chen and A. A. Wani (2004). "UV radiation-induced XPC translocation within chromatin is mediated by damaged-DNA binding protein, DDB2." Carcinogenesis **25**(6): 1033-1043.

Waters, R., P. van Eijk and S. Reed (2015). "Histone modification and chromatin remodeling during NER." DNA Repair (Amst) **36**: 105-113.

Weeda, G., M. Rossignol, R. A. Fraser, G. S. Winkler, W. Vermeulen, L. J. van 't Veer, L. Ma, J. H. Hoeijmakers and J. M. Egly (1997). "The XPB subunit of repair/transcription factor TFIIH directly interacts with SUG1, a subunit of the 26S proteasome and putative transcription factor." Nucleic Acids Res **25**(12): 2274-2283.

Wolpin, B. M. and R. J. Mayer (2008). "Systemic treatment of colorectal cancer." Gastroenterology **134**(5): 1296-1310.

Wood, L. D., D. W. Parsons, S. Jones, J. Lin, T. Sjoblom, R. J. Leary, D. Shen, S. M. Boca, T. Barber, J. Ptak, N. Silliman, S. Szabo, Z. Dezso, V. Ustyanksky, T. Nikolskaya, Y. Nikolsky, R. Karchin, P. A. Wilson, J. S. Kaminker, Z. Zhang, R. Croshaw, J. Willis,

D. Dawson, M. Shipitsin, J. K. Willson, S. Sukumar, K. Polyak, B. H. Park, C. L. Pethiyagoda, P. V. Pant, D. G. Ballinger, A. B. Sparks, J. Hartigan, D. R. Smith, E. Suh, N. Papadopoulos, P. Buckhaults, S. D. Markowitz, G. Parmigiani, K. W. Kinzler, V. E. Velculescu and B. Vogelstein (2007). "The genomic landscapes of human breast and colorectal cancers." Science **318**(5853): 1108-1113.

Xie, H., C. Xing, G. Cao, B. Wei, X. Xu, P. Song, L. Chen, H. Chen, S. Yin, L. Zhou and S. Zheng (2015). "Association of RNF43 with cell cycle proteins involved in p53 pathway." Int J Clin Exp Pathol **8**(11): 14995-15000.

Yagyu, R., Y. Furukawa, Y. M. Lin, T. Shimokawa, T. Yamamura and Y. Nakamura (2004). "A novel oncoprotein RNF43 functions in an autocrine manner in colorectal cancer." Int J Oncol **25**(5): 1343-1348.

Yoon, T., A. Chakrabortty, R. Franks, T. Valli, H. Kiyokawa and P. Raychaudhuri (2005). "Tumor-prone phenotype of the DDB2-deficient mice." Oncogene **24**(3): 469-478.

Zebisch, M. and E. Y. Jones (2015). "ZNRF3/RNF43--A direct linkage of extracellular recognition and E3 ligase activity to modulate cell surface signalling." Prog Biophys Mol Biol **118**(3): 112-118.

Zebisch, M., Y. Xu, C. Krastev, B. T. MacDonald, M. Chen, R. J. Gilbert, X. He and E. Y. Jones (2013). "Structural and molecular basis of ZNRF3/RNF43 transmembrane ubiquitin ligase inhibition by the Wnt agonist R-spondin." Nat Commun **4**: 2787.

Zhao, R., T. Cui, C. Han, X. Zhang, J. He, A. K. Srivastava, J. Yu, A. A. Wani and Q. E. Wang (2015). "DDB2 modulates TGF-beta signal transduction in human ovarian cancer cells by downregulating NEDD4L." Nucleic Acids Res **43**(16): 7838-7849.

Zolezzi, F. and S. Linn (2000). "Studies of the murine DDB1 and DDB2 genes." Gene **245**(1): 151-159.

VITA

NAME: Shuo Huang

EDUCATION: B.A., Biomedical Engineering, Zhejiang University, Hangzhou, China, 2010

AWARDS: Best Poster Award **2017 Annual BMG Departmental Retreat**

ABSTRACTS: **Huang S**, Fantini D, Merrill BJ, Bagchi S, Raychaudhuri P. DDB2 Transactivates RNF43 E3 Ubiquitin Ligase and Regulates Wnt/β-catenin Signaling in Colon Cancer Cells **Annual GEMS Research Symposium.** September 16, 2016

Huang S, Fantini D, Merrill BJ, Bagchi S, Raychaudhuri P. DDB2 Transactivates RNF43 E3 Ubiquitin Ligase and Regulates Wnt/β-catenin Signaling in Colon Cancer Cells **UI Cancer Center Caner Research Forum**. October 18, 2016

Huang S, Fantini D, Merrill BJ, Bagchi S, Raychaudhuri P. DDB2 Activates Rnf43 and Regulates Wnt/β-catenin Signaling in Colon Cancer Cells. **EXPERIMENTAL BIOLOGY 2017.** April 22 -26, 2017

Huang S, Fantini D, Merrill BJ, Bagchi S, Guzman G, Raychaudhuri P. DDB2, a Novel Partner and Regulator of Wnt Signaling in Colon Cancer **Gordon Research Conferences: Wnt Signaling.** August 6-11, 2017

PUBLICATIONS: **Huang S**, Fantini D, Merrill BJ, Bagchi S, Guzman G, Raychaudhuri P. DDB2 is a Novel Regulator of Wnt-Signaling in Colon Cancer. *Cancer Research*. (In press)

Fantini D, **Huang S**, Asara JM, Bagchi S, Raychaudhuri P. Chromatin association of XRCC5/6 in the absence of DNA damage depends on the XPE gene product DDB2. *Mol Biol Cell*. 2017 Jan 1;**28** (1):192-200.